The role of the N-capping box in the α1 helix on the structure and stability of CLIC1

Fidan Karatas

A dissertation submitted to the Faculty of Science, University of the Witwatersrand, Johannesburg, in fulfillment of the requirements for the degree of Master of Science.

Johannesburg, 2011

Declaration

I declare that this dissertation is my own, unaided work. It is being submitted for the degree of Master of Science in the University of the Witwatersrand, Johannesburg. It has not been submitted for any other degree or examination at any other University.

Fidan Karatas

_____ day of_____, 2011

ABSTRACT

CLIC1 is an intracellular channel protein that either exists in a soluble state in the cytoplasm or is bound to the membrane. The mechanism by which CLIC1 traverses the membrane is not currently known although it is likely to depend on oxidation and pH. The α1 helix of CLIC1, located in the putative transmembrane region, is proposed to span the membrane with the N-terminal end protruding into the extracellular matrix. Recent studies show that this helix contains an N-capping box residue (Ser27), which will act as a lock on the α1 helix (Stoychev *et al*., 2009). In order to find out the contribution of this residue to the stability of the protein, Ser27 was replaced with proline, a helix breaker. A comparative study was conducted that focused on the characterisation of the mutant in terms of secondary and tertiary structure and determination of its conformational stability at equilibrium in comparison with the wild-type. The study was performed at both pH7 and 5.5 which takes into account the environment in the cytoplasm (pH7) and at the membrane surface (pH5.5), respectively. The secondary structure of the mutant was found to be less helical as compared to the wild-type. In terms of tertiary structure, the unique tryptophan residue, Trp35 was found to be more buried in the mutant compared to the wild-type. The wild-type does not have exposed hydrophobic patches and does not bind to 8-anilino-1-naphthalene sulfonic acid (ANS) in the native state at pH7 and pH5.5. However, ANS binds to the mutant in the native state indicating that more hydrophobic patches in the protein are exposed to the solvent. At both values, the mutant displays much lower stability at both pH7 and 5.5 as compared to the wild-type. As a conclusion, it was found that the N-capping box residue, Ser27, plays a significant role as a good helix initiating residue. Moreover, this residue has a significant effect in stabilising the α1 helix and may play a role in the cooperativity between the N- and C-domains and thus in stabilising the whole protein.

This work is dedicated to:

My Dad and Mom,

without whom none of this would have been possible

To my dearest husband, Gursoy, who was the great and positive support throughout and to my dearest children Ahmet Vedat and Elif Bahar who are the origin of my happiness.

Acknowledgements

I acknowledge my supervisor, Dr Sylvia Fanucchi to whom I am always thankful for supporting and inspiring me and who always had time for my endless questions. I am grateful to her for discussing my research, and leading me on many aspects of CLIC1 throughout my project. I also acknowledge my co-supervisor, Professor Heini Dirr who always had a positive approach to my study and encouraged me. I would like to thank them for the guidance and support they provided. Special thanks are due to Dr Yasien Sayed for giving of his time to help me with my questions. I thank my colleagues in the Protein Structure-Function Research Unit for the team spirit. Grateful thanks are extended to Roslin Adamson for sharing her experiences with me and always giving me positive energy.

I acknowledge the National Research Foundation for financial support.

Table of Contents

List of abbreviations

A_{260}	absorbance at 260 nm
A_{280}	absorbance at 280 nm
Å	angström
amp	ampicillin
amp_r	ampicillin resistance
ANS	8-anilino-1-naphthalene sulfonic acid
ATP	adenosine triphosphate
bp	base pairs
CD	circular dichroism
CFTR	cystic fibrosis transmembrane conductance regulator
CLIC	chloride intracellular channel
CLIC1-WT	CLIC1-wild-type
C_m	the denaturant concentration at the midpoint of the unfolding curve
D	dielectric constant
kDa	kiloDaltons
DEAE	diethylaminoethyl

ΔG	the change in Gibbs free energy
$\Delta G_{(H2O)}$	change in Gibbs free energy of unfolding in the absence of denaturant
dH_2O	distilled water
DNA	deoxyribonucleic acid
DNase	deoxyribonuclease
DT	diphtheria toxin
DTT	dithiothreitol
E_{222}	ellipticity at 222 nm
EDTA	ethylenediaminetetra-acetic acid
ε	extinction coefficient
Ex.280	excitation at 280 nm
Ex.295	excitation at 295 nm
ExPASy	expert protein analysis system
F_0	fluorescence intensity in the absence of quencher
F	fluorescence intensity
F310	fluorescence emission intensity at 310 nm
F320	fluorescence emission intensity at 320 nm

F345	fluorescence emission intensity at 345 nm
F460	fluorescence emission intensity at 460 nm
Far-UV CD	far-ultraviolet circular dichroism
GABA	γ-amino-n-butyric acid
GSH	reduced glutathione
GSSG	oxidised glutathione
GST	glutathione *S*-transferase
hGST O1-1	human omega class glutathione *S*-transferase
hGH	human growth hormone
I	intermediate species
IAEW	intensity averaged emission wavelenegth
IPTG	isopropyl-1-thio-β-D-galactopyranoside
K_{SV}	Stern-Volmer quenching constant
K_d	dissociation constant
K_{eq}	equilibrium constant
ℓ	litre
LB	lysogeny-Bertani

$\lambda_{em\ max}$	fluorescence emission wavelength maximum
mdeg	millidegrees
m-value	the dependence of the free energy of unfolding on denaturant concentration
N	native
OD	optical density
ORF	open reading frame
PAGE	polyacrylamide gel electrophoresis
PDB	protein data bank
PFT	pore-forming toxin
p*I*	isoelectric point
PTM	putative transmembrane region
Q	quencher
RNase	ribonuclease
× g	revolutions per minute
RyR	ryanodine receptors
SDS	sodium dodecyl sulfate
*Sj*GST	*Schistosoma japonicum* glutathione *S*-transferase

TEMED	*N*, *N*, *N*', *N*'-tetramethylethylenediamine
[Θ]	mean residual ellipticity
TM	transmembrane
U	unfolded
UV	ultraviolet
YT	yeast tryptone

The IUPAC-IUBMB one and three letter codes for naming amino acids were used throughout.

List of figures

List of tables

CHAPTER 1: INTRODUCTION

1.1. α-Helices and capping boxes

The α-helix is one of the basic conformational motifs in the secondary structure of globular proteins (Pauling *et al*., 1951). It is a sequential structure composed of at least seven amino acid residues twisting around each Cα atom (Harper and Rose, 1993). The backbone conformation of proteins can be defined as being in a helical state when the torsion angles or dihedral angles are limited to the values of Φ= 64˚ ±7˚, Ψ= 41˚± 7˚ (Richardson, 1981). When the backbone amino acids assume these angles, the polar groups in the backbone will form hydrogen bonds with each other. The formation of these backbone hydrogen bonds stabilises the helix (Presta and Rose, 1988) (Figure 1). The hydrogen bond pattern is formulated as n-(n+4) and can be formed by no less than 3 residues available in sequence (Presta and Rose, 1988). Although the helix is stabilised by backbone hydrogen bonds, the hydrogen bonds that occur with the side-chains also confer stability to the helix and have the additional function of signalling for the initiation and/or termination of folding of α–helices (elMasry and Fersht, 1994; Lyu *et al*., 1993; Zhou *et al*., 1994; Zuhovsky *et al*., 1994). This mechanism was initially described as capping (Richardson and Richardson, 1988; Harper and Rose, 1993; Zhou *et al*, 1993) and later on as a capping box (Harper and Rose, 1993; Dasgupta and Bell, 1993; Aurora *et al.*, 1994; Seale *et al.*, 1994; Munoz *et al.*, 1995) and can be present at both the N-terminal (N-cap) and the C-terminal (C-cap) ends of a helix. The most favourable N-cap residues are serine, threonine, asparagine and aspartate (Harper and Rose, 1993; Richardson and Richardson, 1988).

The nomenclature of helices with their flanking residues can be labelled as follows:

N′′–N′–**N-cap**–N1–N2–N3–...–C3–C2–C1–**C-cap**–C′–C′′

The amino acids at the N- and C-caps are positioned at the starting and the ending parts of the helix respectively, connecting the helix to the adjacent helix or strand (Figure 1).

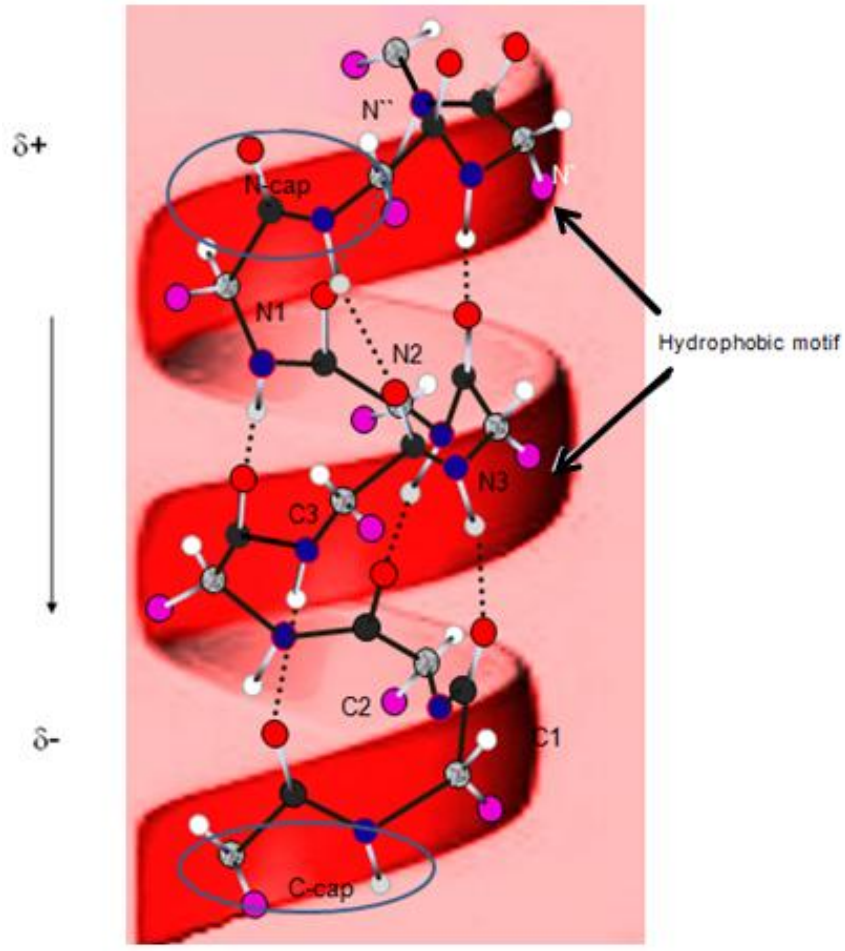

Figure 1: Schematic diagram of a typical α-helix showing the N- and C-capping motifs in α-helices. The capping boxes are the starting and the ending points of the helix. The backbone hydrogen bonds are formed between residues following the pattern formulated as n-(n+4). Thus, hydrogen bonds are formed between the residues N`` and N1, N` and N2, N2 and C2, N3... C1, C3 and C-cap during the helix formation. The symbols, δ- and δ+, show the partial negative and partial positive charges of the helix dipole, respectively. The direction of the N-Cα peptide bonds is shown by the arrow. Hydrogen bonds are shown by dotted lines.

The residues N1, N2, N3...C3, C2, and C1 are located within the helix. The residues N´´, N´, C´, and C´´ are named as ‘‘preceding or succeeding” and do not form part of the helix angles (Presta and Rose, 1988). The formation of an α-helix is initiated from the direction of the partial positive charge to the partial negative charge of the helix dipole (Figure 1).

A hydrophobic staple motif is also formed in some helices as a stabilising motif by the side chain of a hydrophobic residue at the N` position immediately preceding the N-cap that interacts with another hydrophobic residue at the N4 position within the helix (Jimenez *et al*., 1994; Seale *et al*., 1994; Munoz *et al*., 1995) (Figure 1).

1.2. Factors stabilising α-helices

1.2.1. The principle forces stabilising α-helices and proteins

α-helices are secondary structural components of proteins and thus there is a correlation between the stability of α-helices and the stability of entire proteins. The essential factors affecting the stability of α-helices and consequently protein folding are van der Waals forces, hydrophobic interactions, hydrogen bonds, pH, conformational entropy, electrostatic interactions, and the dielectric constant of the environment.

Van der Waals forces are non-covalent interactions that hold the electrically neutral dipolar residues together in the secondary structure of proteins. Under standard conditions these interactions are disrupted easily. The van der Waals forces along with London dispersion forces, a type of weak van der Waals forces, are formed by the groups tightly packed in the interior parts of folded proteins and have a significant impact on the stability of the folded state of a protein (Chakravarty *et al*., 2002; Chen and Stites, 2001; Ericksson *et al.,* 1992; Loladze *et al*., 2002; Ratnaparkhi and Varadarajan, 2000).

The hydrophobic effect is one of the driving factors in helix formation and protein folding during which the hydrophobic residues tend to isolate themselves from water and any other polar solvents.

During the process, the polar and charged residues reside on the surface while the hydrophobic residues are packed in the core of the protein. As a result of this relocation, the non-polar side chains interact with each other. This type of interaction acts as a stabilising force for helices and consequently for protein folding (Kim and Baldwin, 1990; Pace *et al*., 1996; Dill, 1990; Makhatadze and Privalov, 1994).

Hydrogen bonds are the weak non-covalent interactions between two electronegative atoms formed by the sharing of a hydrogen atom. The electronegativity and the arrangement of the atoms which form a hydrogen bond determine the strength of the hydrogen bond. The bond formation occurs between a weakly acidic donor atom with a high electronegativity and an electron bearing highly electronegative acceptor atom. These donor and acceptor atoms are usually N, S and O which form hydrogen bonds in the peptide main chain and polar side chains. The secondary structure, due to the formation of backbone hydrogen bonds is in competition with water molecules and, therefore, will be formed mainly buried within the protein. Studies have shown that both main chain and side chain hydrogen bond formation have a fundamental impact on the stability of proteins, not individually but rather as the overall contribution of hydrogen bonds throughout the protein (Baldwin, 2003; Kim and Baldwin, 1990; Ragone, 2001; Schellman, 1980; Scholtz *et al*., 1991). Side-chain-side-chain interactions by means of hydrogen bonding are also suggested to contribute to the stability of α-helices (Armstrong *et al*., 1994; Scholtz *et al*., 1993; Padmanaban and Baldwin, 1994a; Padmanaban and Baldwin, 1994b; Viguera and Serrano, 1995).

pH also has an impact on the stability of α-helices especially where side-chain interactions are involved. The overall charge of a protein is determined by the pH of the solution. Any modification applied to pH will change the ionic phase of the side chain residues and the arrangement of charges in the entire protein which may cause hydrogen bonds to alter. This, therefore, affects the stability of α-helices. The proton binding affinity differs in the native and denatured states of proteins revealing how the dependence of the stability relies on the pH (Gowri Shankar *et al*., 2007).

The conformational entropy is the major force that opposes folding and reduces the conformational stability of proteins (Dill, 1990). When a protein folds, it forms a more ordered conformation (Brady and Sharp, 1997) which is unfavoured by the conformational entropy. In the native state, a protein possesses its lowest free energy as compared to the denatured state (Chan and Dill, 1990). Thus, the difference between the free energy and the conformational entropy determines the net stability of a protein. The Gibbs free energy of a protein in native state is determined using the Equation:

$$\Delta G = \Delta H - T\Delta S \qquad \textbf{Equation 1.1}$$

where ΔH is the net enthalpy contributed by the bond formation within the helices and β-sheets, T is the temperature in Kelvin and ΔS is the entropy which is divided into unfavourable conformational entropy of folding and the favourable entropy of solvation effect. As the interactions and bonds are formed between atoms and molecules within α-helices and β-sheets, the enthalpy of the formation of a helix increases. Therefore, strong packing in the core of the protein contributes to its stability to the secondary structure of the protein thus to the protein (Harpaz *et al*., 1994).

Electrostatic interactions have a major impact on the stability of α-helices and proteins (Huyghues-Despointes *et al*., 1993; Stellwagen *et al*., 1992; Sali *et al*., 1991; Zhou *et al*., 1994) because they are ampholyte structures. The two types of electrostatic interactions are: charge-charge interactions between charged species and dipole-dipole type interactions (Voet and Voet, 2004). Coulomb's law describes the energy separating the electrostatic interactions as follows:

$$U = \frac{kq1q2}{Dr} \qquad \textbf{Equation 1.2}$$

where *D*, q1, q2 and r indicate the dielectric constant of the *milieu*, the two charges and the distance between them, respectively. The equation expresses that the dielectric constant and energy are inversely proportional such that as the dielectric constant increases the energy

required for the charged molecules to interact drops. In an environment with high dielectric constant, as the distance between the charges increases the interaction between them becomes weakened. Salt bridges are formed between a charged and a neutral atom by means of hydrogen bonding. The distance between two groups in a salt bridge is found to be ≤ 3.5 A˚. The distance between charges of ion-pairs is ≤ 4 A˚. A salt bridge can also be a destabilising force to a protein when it is available to solvent that results in an unfavourable loss of solvation (Bosshard *et al*., 2004). The stability provided by salt bridges to a protein is approximately 2.1 kcal/mol when there is no connection between salt bridges and solvent (Takano *et al.,* 2000). Ion pairs also contribute significantly to the stability of α-helices and β-turns where two interactions take place between the same two residues. However, they have a more important function in anchoring the tertiary structure rather than the secondary structure of proteins (Gowri Shankar *et al.*, 2007).

1.2.2. The N-capping box as a stabilising motif in α-helices

The N-capping box is proposed to stabilise and initiate the α-helical conformation in a number of α-helices, peptides (Chakrabarty *et al*., 1993; Doig *et al*., 1994; Lyu *et al*., 1992; Lyu *et al*., 1993) and proteins (Bell *et al*., 1992; El-Masry and Fersht, 1994; Serrano *et al*., 1992a; Serrano *et al*., 1992b; Serrano and Fersht, 1989) by forming hydrogen bonds between side chains and backbones. An interaction between the backbone amide of a residue located three residues downstream from the N-cap (N3) and the side chain of the N-cap residue take place by means of hydrogen bonding (Figure 1) (Richardson and Richardson, 1988; Harper and Rose, 1993; Dasgupta and Bell, 1993). Reciprocally, the other hydrogen bond is formed between the side chain of the N3 and the amide backbone of the N-cap (Figure 1). Although the side-chain of an N-cap residue is commonly involved in stabilising the helix, this is not necessarily the case as was shown in a study of N-cap residues in 393 N-termini of α-helices from the PDB (Bernstein *et al*., 1977; Doig *et al*., 1997). The N-cap may also stabilise the helix by forming a bond between the N-cap carbonyl and the N3 amino group or by forming a stabilising interaction with water

molecule (Doig *et al*., 1997) which is called the hydration effect.

The helix propensities of amino acids play a significant role during helix formation. The intrinsic helical propensity of a given amino acid sequence is well described by using a tool called AGADIR (Lacroix *et al*., 1998) which predicts the behavior of helices in monomeric helix-forming peptides (Munoz and Serrano, 1994; Munoz and Serrano, 1997). Each of the 20 amino acids localised in a central helical position has been described in terms of their helical propensities (Karpen *et al*., 1992; Luque *et al*., 1996). Each amino acid varies in terms of their helical propensity levels according to their position in the helix. As mentioned earlier, serine, threonine, asparagine and aspartate have been found to be the most common N-capping residues (Harper and Rose, 1993; Richardson and Richardson, 1988). This is due to the fact that the side chain of these amino acid residues interacts with the amide groups of residues located at positions N1, N2, N3 and/or N4 by means of hydrogen bonding which stabilise the α-helix. This is confirmed by a study where serine at the N-cap position of α-helices of barnase contributes about 2 $kcal.mol^{-1}$ to the stability of the protein by forming a hydrogen bond with the residue, n+3 (Serrano and Fersht, 1989). This contribution varies as 1.3 $kcal.mol^{-1}$ when Asn or Asp is the N-cap and 0.5-1 $kcal.mol^{-1}$ when Gly or Ala is at the N-cap position.

So why does each amino acid residue have a different helical propensity and, therefore, contribute differently to the helix specificity? Conformational entropy (Lyu et al., 1990; Merutka *et al*., 1990; O`Neil and DeGrado, 1990; Padmanabhan *et al*., 1990; Zimm and Bragg, 1959) and electrostatic interactions (Fersht, 1984; Fersht, 1987) have been proposed to answer the question. Firstly, due to the fact that the formation of α-helices is an entropic process, the compensation of the loss in free energy is accomplished by strong interactions stabilising the helix (Blanco *et al*., 1998; Munoz *et al*., 1998). Secondly, the electrostatic environment caused by the helix dipole also has an impact on the stability of α-helices (Åqvist *et al*., 1991; Shoemaker *et al*., 1985; Shoemaker *et al*., 1987) in which the single amino acid backbone dipoles located at the beginning and end point of the helix contribute

a positive charge to the N-terminus and a negative charge to the C-terminus of the helix. Thus, the N-terminus will interact mostly with acidic residues while the C-terminus interacts with basic residues (Blagdon and Goodman, 1975; Chou and Fasman, 1978). Through these interactions, helix dipole and helix capping may cooperate via hydrogen bonding between side chains and backbone residues during the helix formation that result in a more stable α-helix (Zuhovsky *et al*., 1994).

A great deal of research has been done in terms of the contribution of the N-capping box to the helix formation and stability of proteins. The mutation at Ser71 and Glu74 at the N-capping box of the α2 helix of the human growth hormone (hGH) (Zuhovsky *et al*., 1994) show that the removal of a hydrogen bond at the N-capping box causes the protein to lose stability. A further research has been done on the capping box motif (Ser/Thr-Xaa-Xaa-Asp) which plays a significant role in the helix formation of glutathione S- transferase P1-1 (Dragani *et al.*, 1997). This motif, located in the α6 helix, is found in all GST members and GST-related proteins. The results showed that the mutation on the N-capping box residues located in the α6 helix, S150A and D153A, contributed destability not only to the α6 helix but also to the entire protein. Further study has been done on Alpha glutathione S-transferase with regards to the contributions of the N-capping motif to the stability and dynamics of the α9 helix of the protein (Dirr *et al.*, 2005). A conserved N-capping motif located at the C-terminal helix of hGSTA1-1 as well as a peptide that corresponds to the C-terminal helix of hGSTA1-1 was replaced with a glycine. As a result, the conformational dynamics and, therefore, the characteristics of the H-site, a hydrophobic site found on both domains of the protein and to which hydrophobic and non-substrate ligands bind, were modified (Dirr *et al*., 2005).

1.3. The role of stabilised α-helices in transmembrane domains

Most transmembrane and amphitropic proteins are comprised of α-helical transmembrane domains some of which function as membrane channels. Transmembrane helices play

significant roles in the folding, assembly and dynamics of these proteins. Therefore, the role of the α-helical transmembrane domains of membrane and amphitropic proteins will be further discussed.

1.3.1. Membrane proteins

The membrane spanning helices are mainly characterised by hydrophobic residues that are buried in the core of the membrane proteins with few or no polar side-chains (Rees *et al*., 1989; Engelman *et al*., 1986). The dynamic nature of the folding and stability of transmembrane helices is poorly understood. A 'two-stage' model of helical association was suggested in an early study in which the stability and folding pathway of membrane proteins occur in two thermodynamically independent events: the first step involves helix formation during which the helical regions of the membrane protein insert into the membrane, whereas the second step is accomplished by specific intermolecular or intramolecular interactions taking place between these helices within the membrane (Popot *et al*., 1987). Therefore, a tightly-packed helix bundle of membrane proteins is formed within the membrane. The helix-helix associations of the second stage are driven by several specific interhelical interactions which play crucial roles. These interactions are classified as: Van der Waals forces between closely packed small residues (Bowie, 2005; Fleishman and Ben-Tal, 2002; Lemmon and Engelman, 1994; Russ and Engelman, 2000; Senes *et al*., 2000; Schneide and Engelman, 2004; Finger *et al*., 2006), hydrogen bonds (Bowie, 2005; Fleishman and Ben-Tal, 2002; Zhou *et al*., 2000; Gratkowski *et al*., 2001; Dawson *et al*., 2003), salt bridges (Honig and Hubbel, 1984), aromatic interactions (Dougherty, 1996; Sal-Man *et al*., 2007; Johnson *et al*., 2007) and closely packed valines, isoleucines and leucines (Fleishman and Ben-Tal, 2002; Lemmon and Engelman, 1994; Senes *et al*., 2000; Gurezka et al., 1999). A more recent study on 15 transmembrane proteins suggested that these five types of interactions are observed in most of the helix bundles (Harrington and Ben-Tal, 2009). In addition, these interactions themselves facilitate the iterative assembly of the helix bundles.

1.3.2. Amphitropic proteins and CLICs

Amphitropic proteins are dual-form proteins that can exist in a soluble and membrane-inserted form and were first defined by Burn (1988). They are involved in various functions such as enzyme regulation, cellular communication, antimicrobial and cytotoxic activity of proteins (reviewed by Halskau *et al*., 2009). They are bacterial pore-forming toxins (PFTs), apoptotic proteins, annexins and chloride intracellular channel proteins (CLICs).

These proteins are distinct from regular membrane proteins in that they have more polar amino acid residues on their surface than the membrane proteins. These proteins are mainly α-helical in structure (Bell *et al*., 1997; Choe *et al*., 1992; Garcia-Saez *et al*., 2004; Harrop *et al*., 2001; Jiang and London, 1990; Lindeberg *et al*., 2000; Van der Goot *et al*., 1991; Manceva *et al*., 2004; Promdonkoy and Ellar, 2003; Schendel *et al*., 1997; Tejuca *et al*., 1996; Thuduppathy and Hill, 2005; Thuduppathy *et al*., 2006; Torry and Merrill, 1999; Ulrih *et al*., 2004; Zakharov and Cramer, 2002; Zakharov *et al*., 2004) and are present in either a water-soluble form in the cytosol or a membrane-bound form. This dual mechanism suggests that the hydrophobic 'dagger' is covered by an amphipathic 'sheath' allowing the protein to exist in a soluble state or to insert into the membrane under certain conditions (Donovan *et al*., 1982; Oh *et al*., 1996; Shin *et al*., 1993). Any biological functions such as toxic activity (Parker and Pattus, 1993; Geny and Popoff, 2006) and changes in environmental conditions (reviewed by Johnson and Cornell, 1999) may drive these proteins to transform from a soluble conformation to a membrane-bound conformation.

The low pH (pH5-5.5) on the membrane surface is found to play a fundamental role in the conformational changes of pore-forming toxins that take place during their conversion from soluble to membrane bound form. A high proportion of acidic residues at the surface of many α pore-forming toxins act as ''pH-sensors'' which are neutralised by the low pH. Several α pore-forming toxins, for instance, colicin A (van der Goot *et al*., 1991), exotoxin A (Jiang and London, 1990), diphtheria toxins (Jiang *et al*., 1991; Choe *et al*., 1992;

London, 1992), ANX12 (Langen *et al*., 1998), α-toxin (Bortoleto and Wart, 1999), Cyt1A δ-endotoxin (Manceva *et al.,* 2004) and equinatoxin (Ulrih *et al*., 2004) have been shown to exhibit pH sensitivity and partially unfold forming a molten globule state at low pH. A molten globule comprises a conserved secondary structure along with a loss of tertiary structural properties (Haynie and Freire, 1993) in which hydrophobic surfaces are more exposed than in the native conformation (Parker and Feil, 2005).

The Bcl-2 family of proteins are a family of amphitropic proteins that regulate cell death or apoptosis according to various apoptotic stimuli. This family of proteins can be divided into two subclasses: Bcl-x_L and Bax. The former promotes and the latter prevents apoptosis. Members of this family are found to incorporate into the membrane (*in vitro* and *in vivo)* particularly in the presence of acidic lipid bilayers with low dielectric constant and at low pH (Schendal *et al*., 1998; Shimizu *et al*., 1999; Shimizu *et al*., 2000, Thuduppathy and Hill, 2005). They act somehow as selective ion and/or protein channels that release apoptotic factors from the mitochondria to the cytoplasm (Garcia-Saez *et al*., 2004; Gross *et al*., 1999). Despite differences in sequence and function, there is a striking structural similarity between these proteins, and many pore-forming toxins in that two hydrophobic helices form a helical hairpin in the centre of a bundle surrounded by six to seven amphipathic α-helices which shield the helical hairpin (Muchmore *et al*., 1996; Chou *et al*., 1999; Suzuki *et al*., 2000; Garcia-Saez *et al*., 2004). Therefore, in the presence of lipid membranes, these proteins undergo a structural reorganisation in order to expose the hydrophobic helices for penetration into the membrane interior (Minn *et al*., 1997; Shimizu *et al*., 1999; Saito *et al*., 2000; Vander Heiden *et al*., 2001).

Annexins are another family of dual-form proteins. They are involved in ion channel formation, cell adhesion and other membrane related mechanisms (Cartailler *et al*., 2000; Gerke and Moss, 2002). Studies have shown that the membrane-related functions of these proteins are either Ca^{2+}-dependent or Ca^{2+}-independent membrane interactions. Ca^{2+}-independent membrane interaction is regulated by phospholipid composition

(Isas *et al.*, 2003) and/or by transient changes in pH (Isas *et al.*, 2000; Kohler *et al.*, 1997; Langen *et al.*, 1998; Sokolov *et al.*, 2000). Major protein refolding is also necessary for these interactions to take place (Isas *et al.*, 2003).

The chloride intracellular channel proteins (CLICs) are also amphitropic proteins and are one of the major classes of chloride channels. The other chloride channels are ligand-gated ion channels (GABA and glycine receptors), cystic fibrosis transmembrane conductance regulators (CFTR), and chloride channels (ClCs) (al-Awqati, 1995; Jentsch and Gunther, 1997). CLICs form a subclass of the glutathione transferases (GSTs, EC 2.5.1.18); a superfamily of intracellular multi-functional enzymes that exist in a wide range of organisms. CLIC proteins are found in most tissues and cells (Chuang *et al.*, 1999; Duncan *et al.*, 1999, Valenzuela *et al.*, 2000). To date, the human members identified in the CLIC family are as follows: CLIC1 (also known as nuclear chloride channel 27-NCC27), CLIC2, CLIC3, CLIC4, CLIC5A, CLIC5B and CLIC6. CLIC1 to CLIC5A are almost identical in size, approximately 240 amino acid residues. In contrast, CLIC5B and CLIC6 are two larger variants, comprising extended N-terminal domains (Dulhunty *et al.*, 2001).

In relation to their wide distribution throughout plasma and organellar membranes (Chuang *et al.*, 1999; Duncan *et al.*, 1999; Edwards, 1999; Valenzuela *et al.*, 2000), CLICs carry out significant functions including cell division (Valenzuela *et al.*, 2000), cell motility (Ronnov-Jessen *et al*., 2002), tubulogenesis (Berry *et al*., 2003), angiogenesis (Tung *et al*., 2009), kidney function (Landry *et al.*, 1989), formation of skeletal muscle and brain (Chalothorn *et al*., 2009) bone resorption (Schlesinger *et al.*, 1997), p53-regulated apoptosis (Fernandez-Salas *et al.*, 1999; Fernandez-Salas *et al*., 2002; Suh *et al*., 2004; Suh *et al*., 2005) as well as functioning in membrane potential, neurotransmission, transepithelial transport (Jentsch, 1994; Jentsch *et al.*, 1997), salt absorption and secretion control (Strange *et al.*, 1996) and PKA signaling (Shanks *et al*., 2002).

One of the striking characteristics of the CLIC family is their amphitropic nature whereby they either exist in a soluble state in the cytoplasm or bound to the membrane. CLICs can

insert themselves into the target membrane in the absence of a leading sequence where they form anion channels (Singh and Ashley, 2006).

The GST family of proteins contain a thioredoxin fold in their N-domains. This fold is utilised to regulate diverse redox reactions and thus is crucial in cellular growth, cell cycle, oxidative stress, mammalian cell apoptosis and carcinogenesis (Armer and Holdgren, 2006; Kakolyris *et al*., 2001; Povis and Montfort, 2001; Pekkari and Holmgren, 2004). A remarkable use of this fold is seen in the channel modulating activity of ryanodine receptors (RyR) by omega class GST (Dulhanty *et al*., 2001), membrane binding activity by kappa class GST (Ladner *et al*., 2004) and RyR regulation by calsequestrin, a member of the thioredoxin family and a Ca^{2+} storage protein in muscles (Wang *et al*., 1998; Wei *et al*., 2006). Therefore, the utility of the thioredoxin fold in some GST proteins such as CLIC2, GSTO1-1 and calsequestrin extends beyond the regular redox activity of the GST superfamily. Moreover, in light of recent studies (Codreaunu *et. al*., 2005; Cromer *et al*., 2007; Harrop *et al*., 2001; Li *et al*., 2006; Littler *et al*., 2005; Thompson *et al*., 2006) the contention is that the intrinsic flexibility of the thioredoxin fold of the N-terminal domain may promote the formation of a membrane-bound conformation of CLIC proteins.

1.4. CLIC1 overview

1.4.1. Structure of CLIC1

CLIC1 is a monomeric protein with a molecular weight of 26.9 kDa (Valenzuela *et al*., 1997). p*I* was calculated as 4.85 by the DNAStar software (Lasergene) (Ashley, 2003). The structure accommodates six cysteines, eight tyrosine residues spreading primarily in the C-domain and a unique tryptophan (Trp35 in the α1 helix). The sequence of the protein is unequal in distribution of charge, with 35 acidic residues and 27 basic residues.

The crystal structure of CLIC1, which was solved at 1.4 Å at pH5 (Harrop *et al*., 2001) reveals that the α-helical and β-sheet structures comprise 47.7% and 8.3% of the protein, respectively (Figure 2).

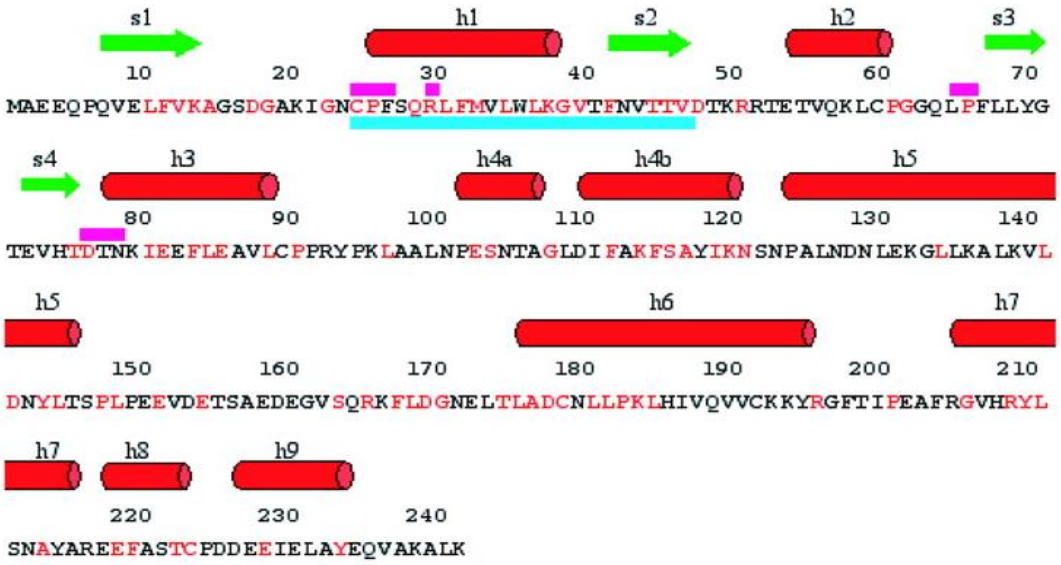

Figure 2: The topology of CLIC1. The Figure indicates the primary and secondary structural elements of CLIC1. The β-strands are shown by arrows and α-helices are shown by cylinders. The image is from PDBsum database (Laskowski *et al.*, 1997) using the PDB code 1k0m (Harrop *et al.*, 2001).

In common with GSTs, CLIC1 contains two domains: a thioredoxin-like N-domain with a mixture of α-helical/β-sheet components and an all α-helical C-domain (Figure 3). The N-domain of CLIC1 (residues 1- 90) contains a putative transmembrane region (residues forming α1 helix and β2 strand) (Figure 3) (Littler *et al*., 2010).

A highly hydrophobic region exists between the residues 25 to 40 in the N-terminal domain of CLICs (Figure 4) (Stoychev *et al*, 2009). This region is unique to CLICs amongst the GST family members and plays a crucial role in the membrane insertion of CLICs. The flexible nature of the N-domain may enable the transmembrane region of the protein to insert into the membrane by breaking contacts with the C-domain (Stoychev *et al*, 2009). This hydrophobic region also serves to form a network of contacts between the α1, α3 and α5 helices by the residues Glu81-Arg29 and Glu85-Lys37 joining the α1 helix and the α3 helix at the N-domain with the α5 helix at the C-domain by spanning the domain interfaces. Therefore, the amphipathic α1 helix, which contains the unique Trp35, is the major contact element forming the putative transmembrane region and making the most contacts between domain 1 and domain 2 (Fanucchi *et al.*, 2008).

1.4.2. Stability of CLIC1

The stability of a protein refers to the difference in free energies (ΔG) between native and denatured protein (Section 1.2.2). Thus, it is the potential energy that a protein will maintain its native folded state (Matthew, 1985; reviewed by Dill, 1990; Pace *et al*., 1996). Consequently, the structure and stability of a globular protein is accomplished via the equilibrium provided by the forces driving and opposing folding (reviewed by Dill, 1990). pH has a significant effect on the stability and the channel activity of CLIC1. CLIC1 displays its lowest channel activity at pH7.0 and highest activity at acidic pH (Warton *et al.*, 2002). Furthermore, CLIC1 is most stable at pH7 and soluble CLIC1 has a lower conformational stability and can form a partially unfolded intermediate state in the presence of mild denaturing conditions at low pH (Fanucchi *et al.*, 2008).

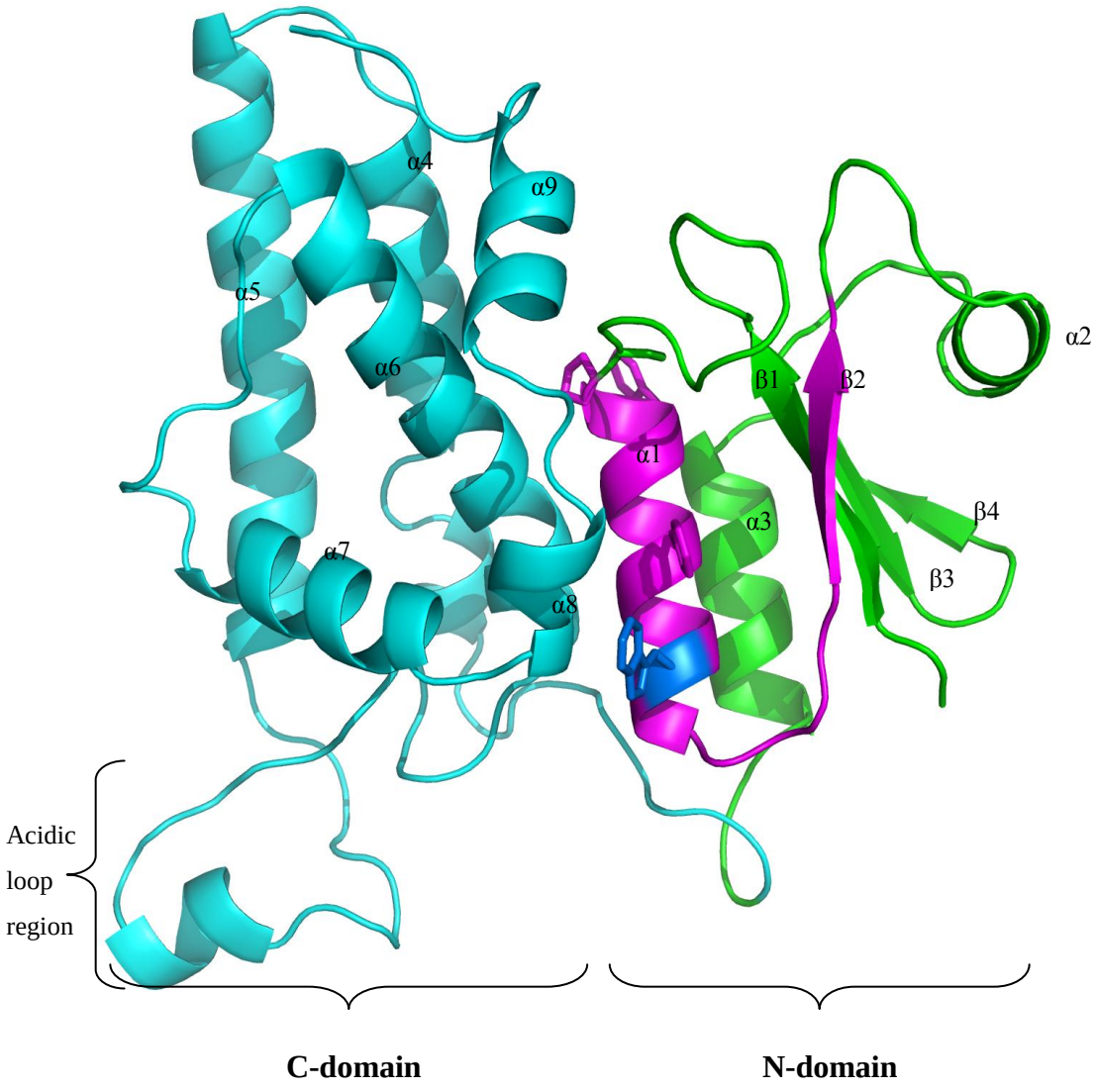

Figure 3: Schematic diagram of reduced CLIC1 in ribbon showing the putative transmembrane region of CLIC1. The N-and C-domains are shown in green and cyan, respectively. The putative transmembrane region (TMR) comprising the α1 helix and the β2 strand, located in the N-terminal domain is shown in purple. The single tryptophan (Trp35) is shown in blue. The acidic loop region exists in the C-domain of the protein. Image was generated using PyMOL™ v. 0.99 (DeLano Scientific, 2006). The PDB code was 1k0m (Harrop *et al*., 2001).

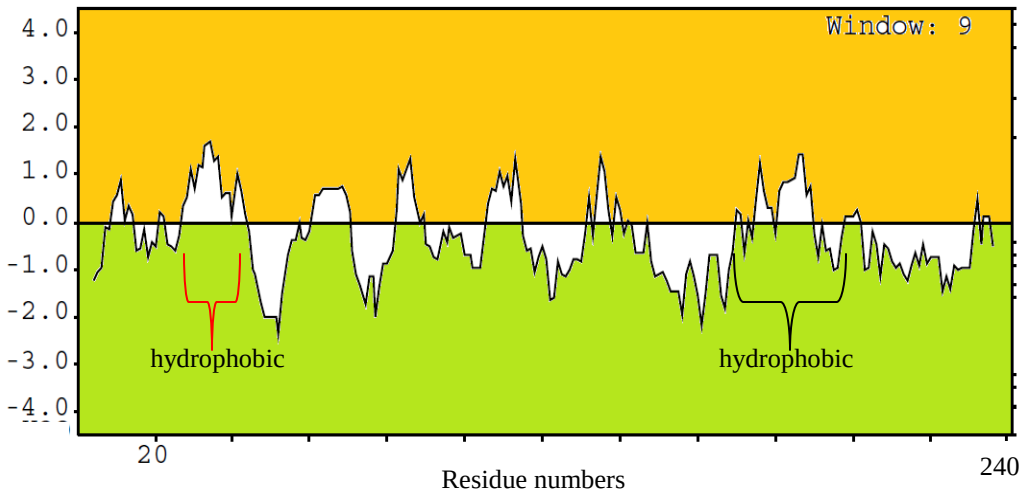

Figure 4: Hydrophobicity pattern of CLIC1. The hydrophobic regions of CLIC1 are indicated by the regions above 0.0 coloured in orange. According to the Figure, the regions between the residues Pro25-Leu36 (red bracket) indicating the putative transmembrane region in the α1 helix and Ala177-Lys193 (black bracket) in the α6 helix are highly hydrophobic. The Figure was generated using protscale from Expasy (http://www.expasy.org/tmp) (Kyte and Doolittle, 1982; Fauchere and Pliska, 1983).

Since the highest channel activity is observed when the structural stability of CLIC1 is reduced (Fanucchi *et al.*, 2008; Warton *et al.*, 2002), the free energy barrier to insert into the membrane may be lowered by formation of a stable intermediate at low pH.

An intermediate at equilibrium is a state of a protein that exists between its folded and denatured states and contains both partially folded and unfolded structures. Studies show that the intermediates of some proteins play an important role in protein folding and the formation of the native state (Roder *et al.*, 2000; Jemth *et al.*, 2004), although most small globular proteins display only the native and folded states (Grantcharova *et al.*, 2001). CLIC1 shows an equilibrium intermediate state which is highly dependent on both pH and temperature (Fanucchi *et al.*, 2008). The stable intermediate state of CLIC1 is native-like in secondary structure and is detectable at pH5.5/20˚C or pH7.0/37˚C. Moreover, in comparison with native and denatured states, the intermediate of CLIC1 exposes more hydrophobic surface (Fanucchi *et al.*, 2008).

An inter-domain lock-and-key motif is present as a stabilising component of CLIC1. The key residue, Met32, is located in the transmembrane region of CLIC1 (Legg, E`Silva, unpublished work). This key residue connects the N- and C-terminal domains of CLIC1 by extending its hydrophobic side chain from the N-domain into a hydrophobic region of the C-domain. This motif is suggested to play a role in interface packing of CLIC1 (Alves *et al.*, 2006; Luo *et al.*, 2002; Wallace *et al.*, 2000). The hydrophobic transmembrane region α1-β2, which is responsible for membrane insertion, must disengage from the C-domain, extend, and refold into the new membrane-bound form in order to achieve channel formation (Fanucchi *et al.*, 2008). It is proposed that the dissociation of the inter-domain lock-and-key motif in CLIC1 may lead the N- and C-domains to disconnect during the conversion of the soluble form into the membrane-bound form of CLIC1 (Stoychev, PhD Thesis, 2008) and may form a less stable intermediate species.

1.4.3. The α1 helix and β2 strands in the putative transmembrane region (PTM) in CLIC1

The putative transmembrane region is defined by the α1 helix and the β2 strands and between the residues Pro25 to Val46 (Goodchild *et al.,* 2010; Littler *et al.,* 2004; Singh and Ashley, 2006) (Figure 3). The α1 helix in CLIC1 comprises an N- (Ser27) and C- (Lys37) capping box (Stoychev *et al*., 2009). It is this N-cap residue (Ser27) that is the focus of this project.

The mechanism by which the putative transmembrane region of CLIC1 inserts into and spans the membrane was first proposed by Tulk and Edwards (1998) following their research on the resistance of CLIC1 to alkaline extraction. A study performed by Tonini *et al.* (2000) subsequently revealed that CLIC1 behaves as an integral membrane protein which, interacts with the membrane by inserting into- and spanning the membrane. Later, a study (Berry *et al.,* 2003) using CLIC-like proteins showed that the first 55 residues at the N-terminal domain are necessary for membrane insertion. Moreover, functional studies have shown that the putative transmembrane region in the N-domain is a key component in terms of localisation to a membrane and functioning *in vivo* in invertebrate CLIC proteins (Berry and Hobert, 2006). Electrophysiological studies performed on transfected CHO-K1 cells by using a FLAG epitope tag have shown that CLIC1 inserts and spans the membrane an odd number of times and is associated with ion channel activity (Tonini *et al*., 2000). Hydrogen exchange studies have found the N-domain to be more flexible and less stable than the C-domain (Stoychev *et al*., 2009) probably in order to partially unfold prior to membrane insertion at low pH (Fanucchi *et al*., 2008). A recent study performed using fluorescence resonance energy transfer (FRET) spectroscopy and electron paramagnetic resonance (EPR) also supports the concept by which when CLIC1 interacts with membranes, the N- and C-domains are located on the opposite sides of the membrane (Goodchild *et al*., 2010). Moreover, in order to form a channel by inserting into the membrane, the hydrophobic transmembrane region (β1-α1-β2) of CLIC1 must undergo a

structural reorganisation involving a rapid unfolding and refolding of the N-terminal domain. These studies suggest that the putative transmembrane region exists and functions as a channel in the presence of membranes.

Since CLIC and GST families are known to utilise the thioredoxin fold to give rise to a channel (section 1.3.2), some members of these families were chosen for helix and N-cap-forming propensity (Stoychev *et al*., 2008) and analysed using the AGADIR algorithm (Munoz and Serrano, 1994; 1997) (Table 1). The results confirmed the proposed transmembrane region of CLIC1 (α1 and β2) and that the other CLIC members possess high helical propensity and that this propensity is conserved throughout the CLIC family.

However, except for kappa class GST, none of the GST members display high helical propensity in a similar region and they do not contain an N-cap residue, (Stoychev *et al*., 2008). In addition to the α1 helix of CLIC1 having high helical propensity, it also shows a high N-cap propensity by means of the N-capping box residue (Ser27) (Table 1). It is interesting to note that, according to the alignment of the α1 helix sequences of CLIC and GST members (Nathaniel, PhD, 2007), the α1 helix in kappa class GST comprises a weak N-cap residue (Gly22).

1.5. Objective and aims

Studies performed on many proteins suggest that N-cap residues play a crucial role in the stability of proteins. However, the highly conserved N-capping box in CLICs has not been studied yet. Thus, the objective of this project is to study the significance of the N-capping box in the α1 helix on the structure and the stability of CLIC1. The results would determine the significance of the N-capping box to the structure and the stability of the α1 helix in CLIC1 which may give insight into the role of the putative transmembrane helix. It possibly has functional roles in the mechanism by which the protein transforms from a soluble to a membrane-bound conformation.

Table 1: Prediction of helical and N-capping propensities of residues in the α1 helix of CLICs and GST kappa using AGADIR (Munoz and Serrano, 1994; 1997). The Table is adapted from Nathaniel (PhD, 2008).

	CLIC1		CLIC2			CLIC3			CLIC4			CLIC5			CLIC6			GST Kappa		
Res	H	**N**	**Res**	**H**	**N**	**Res**	**H**	**N**	**Res**	**H**	**N**	**Res**	**H**	**N**	**Res**	**H**	**N**	**Res**	**H**	**N**
S27	5.4	16.1	C19	0.9	21.3	P23	5.8	2.1	P23	5.6	1.51	P23	5.6	1.5	C21	0.2	5.47	W20	3.4	1.88
E28	21.5	1.15	P20	22.3	6.08	S24	7.9	25.9	F24	7.2	2.08	F24	7.1	2.06	P22	5.7	1.53	L21	5.2	0.6
R29	22.7	1.32	F21	28.3	7.97	C25	33.9	4.84	S25	9.2	27.6	S25	9.2	27.5	F23	7.2	2.1	G22	5.8	11.7
L30	24	0.39	C22	36.2	13.1	Q26	38.7	1.35	Q26	36.9	1.99	Q26	36.6	1.98	S24	9.3	27.8	F23	17.4	1.23
F31	24.2	0.38	Q23	49.4	2.53	R27	40	1.16	R27	38.8	2.4	R27	38.6	2.39	Q25	37.2	2.01	E24	18.6	1.01
M32	24.3	0.14	R24	51.9	2.25	L28	41.2	0.35	L28	41.2	0.44	L28	40.9	0.43	R26	39.2	2.43	V25	19.6	1.65
V33	24.4	0.04	L25	54.1	0.42	F29	41.3	1.17	F29	41.6	0.4	F29	41.3	0.4	L27	41.6	0.44	L26	21.2	1.18
L34	24.4	0	F26	54.4	0.37	M33	42.1	0.28	M30	41.7	0.15	M30	41.4	0.14	F28	41.9	0.4	C27	22.3	2.94
W35	24	0.01	M27	54.5	0.14	V31	42.3	0.1	I31	41.9		I31	41.6	0.03	M29	42.1	0.15	R28	24.3	0.58
L36	19.4	0.01	I28	54.7	0.05	L32	42.3	0.02	L32	41.8		L32	41.5	0.01	I30	42.3	0.04	Y29	22.3	0.14
K37	9.8	0	L29	54.6	0.01	L33	41.7	0	W33	41.1		W33	40.9	0.03	L31	42.2	0.01	Q30	21.5	0.03
			W30	53.9	0.04	L34	36.9	0	L34	35.2		L34	34.9	0.01	W32	41.5	0.05	H31	21.3	0.38
			L31	47.4	0.01	K35	18.8	0	K35	16.9		K35	16.6	0	L33	35.6	0.01	L32	21.6	0.11
			K32	27.5	0	G36	4.8	0	G36	1.9		G36	2	0	K34	17.3	0	W33	21.5	0.37
			G33	7.9	0										G35	2.8	0	N34	18.4	1.85
			V34	7	0										V36	2.3	0	I35	20.2	0.05
			K35	1.4	0										I37	2.2		K36	16.5	0
																		L37	14.9	0
																		K38	9.4	0.02
																		L39	6.9	0.02

The helical (H) and N-cap (N) propensities of the residues in the α1 helices of the members of CLIC family and the Kappa class GST are shown in percentages. The N-cap residues with their helical and capping propensities are shown in yellow shaded blocks.

Therefore, the aims of this project are as follows:

1) to generate the mutant by changing serine, Ser27, to proline,

2) to characterise the secondary and tertiary structures of wild-type (CLIC1-WT) and cap mutants of CLIC1 (CLIC1-S27P) in terms of, and

3) to investigate the thermodynamic stability of the wild-type and the mutant using equilibrium unfolding.

CHAPTER 2. EXPERIMENTAL PROCEDURES

2.1. Materials

The cDNA encoding wild-type GST-CLIC1 fusion protein, cloned into the pGEX-4T-1 plasmid, was a gift from S. N. Breit (Centre for Immunology, St. Vincent`s Hospital and University of New South Wales, Sydney Australia) (Valenzuela *et al.*, 1997). *Escherichia coli* BL21 (DE3) pLysS cells as well as the QuikChange® Site-Directed Mutagenesis kit were obtained from Strategene (La Jolla, California, USA). E. Cloni® cells were acquired from Lucigen (Middleton, WI, USA). Dithiothreitol (DTT), reduced glutathione (GSH), thrombin from human plasma, glutathione-agarose and 8-anilino-1-naphthalene sulphonate (ANS) were obtained from Sigma-Aldrich (St. Louis, MO, USA). The SDS-PAGE protein markers (#SM0431) and isopropyl-1-thio-β-D-galactopyranoside (IPTG) were purchased from Fermentas (Ontario, Canada). Ultrapure urea was obtained from Merck laboratory supplies (Darmstadt, Germany). All other chemicals used were of analytical grade.

2.2. Experimental procedures

2.2.1. Plasmid verification and transformation of *E. coli* cells

Prior to working on any protein, the plasmid containing CLIC1 DNA was sent to Inqaba Biotec (Pretoria, South Africa) for sequencing and was confirmed to contain the CLIC1 sequence.

In order to make glycerol stocks for subsequent purifications, the transformation of the *Escherichia coli* BL21 (DE3) pLysS cells was carried out using the pGEX-4T-1 plasmid containing cDNA encoding wild-type GST-CLIC1 fusion protein as described by Chung *et al*., (1989). A glycerol stock of cells (50 µl) was thawed on ice and plasmid DNA (1 µL) added on ice and incubated (30 min). Heat-shock on a heating block (42 °C, 45 sec) was applied to allow the DNA access to the cells. The samples were placed on ice (2 min) and

SOC media (2% tryptone (w/v), 0.5% yeast (w/v), 1 M NaCl (1%) (w/v) and 1 M KCl (0.2%) (w/v)) was added to the mixture and placed in a shaking incubator (250 × g, 1 h, 37ºC).

Samples were subsequently spread onto sterile plates containing Lysogeny-Bertani (LB) - ampicillin agar (1% tryptone (w/v), 0.5% yeast extract (w/v), 0.5% NaCl (w/v), 1.5% agar (w/v) and ampicillin (10 mg/ml) and incubated (16-17 h, 37°C). A single colony was collected from the transformants and incubated in 100 ml of sterile LB medium containing ampicillin (10 mg/ml) in a rotating incubator (250 × g, 16-17 h, 37°C).

2.2.2. Construction of CLIC1 mutant (CLIC1-S27P)

As the N-capping box residue of the α1 helix, Ser27 was chosen for experimental studies (Section 1.4.3). Proline has a closed structure which prevents this amino acid from interacting with other residues and thus is called a helix breaker (Richardson and Richardson, 1988). Therefore, a CLIC1-S27P mutant was designed in order to investigate the effects of the modification of the N-capping box on the thermodynamic stability and structure of CLIC1.

The wild-type nucleotide sequence of CLIC1 (NCBI reference sequence: NM_001288.4) was used to design the primers with a single point mutation through the Primer-X software (**http://bioinformatics.orf/primerx**). The QuikChange® Site-Directed Mutagenesis kit along with the protocol (Strategene) (Papworth *et al.*, 1996) was used to generate the single point mutation via PCR amplification where the TCC, at position 79 in the pGEX-4T-1 vector, was substituted with CCC. The sample reaction was made up of 5 µl (10×) reaction buffer (100 mM KCl, 100 mM $(NH_4)_2SO_4$, 200 mM Tris-HCl (pH 8.8), 20 mM $MgSO_4$, 1% (v/v) Triton® X-100), 1% (w/v) nuclease-free bovine serum albumin (BSA), 2 µL (50 ng) double stranded DNA template (dsDNA), 2 µl (125 ng) forward primer, 2 µl (125 ng) reverse primer, 1 µl dNTP mix, 37 µl milli-Q water and 1 µl (2.5 U/µl) *Pfu*Turbo DNA

polymerase, to reach a final volume of 50 µl. The reaction products corresponding to the mutant coding sequence were amplified with 16 cycles of 30 seconds at 95 °C to denature the wild-type dsDNA, 60 seconds at 55 °C to anneal the mutant primers and 60 seconds at 68 °C for the extension of the DNA. *Escherichia coli* XL1-Blue super-competent cells provided with the kit were plated onto the LB agar containing 100 µg/µl ampicillin after transforming the reaction products into the cells and incubated for 16 hours at 37°C. A single colony was picked and sent for sequencing. It was confirmed that the engineered mutation was accomplished and no other mutations were produced during the PCR amplification reaction.

The sequence of CLIC1-WT as well as CLIC1-S27P open reading frame (ORF) that were obtained from DNA sequencing at Inqaba Biotec are shown in Table 2. The codon where the mutation was incorporated is shown in blue where the codon for serine is exchanged with that for proline.

2.2.3. Over-expression and purification of CLIC1-WT and CLIC1-S27P

Over-expression and purification of CLIC1-WT and CLIC1-S27P were performed as described by Tulk *et al.* (2002). A glycerol stock of cells containing the cDNA of the wild-type and the mutant (50 µl) was separately added to 200 ml LB media containing 100 µg/ml ampicillin and the cells were grown rotating at 250 × g for 6 hours at 37°C for the wild-type and 16 hours at 20°C for the mutant since the cells that express the mutant protein was insoluble when they were grown at 37°C. A 50-fold dilution of this overnight culture was added into fresh LB media containing 100 µg/µl ampicillin and incubated for approximately 3 hours to reach an OD_{600} of ~0.9. Isopropylthiogalactoside (IPTG) (1 mM) was subsequently added to induce the over-expression of the fusion protein and cells were left for further growth for 6 hours at 37°C for the CLIC1-WT and overnight at 20°C for the CLIC1-S27P to achieve optimum over-expression.

Table 2: Open reading frame of CLIC1-WT and CLIC1-S27P used to generate the mutant, CLIC1-S27P.

CLIC1-WT	5` GGGAACTGCCCATTCTCCCAGAGACTG 3`
CLIC1-S27P	5` GGGAACTGCCCATTCCCCCAGAGACTG 3`

The cells were subsequently centrifuged for 15 minutes in a Sorvall RC5C centrifuge using an SLA3000 rotor at 5000 × g and 4°C.

The resulting pellet was resuspended in about 15 ml of resuspension buffer (10 mM Tris, 200 mM NaCl, 1 mM EDTA, 0.02% (w/v) NaN_3, 1 mM DTT added fresh pH7.5) and left at -20°C overnight for the initiation of cell lysis. The frozen cells were defrosted on a rotator at 4°C and $MgCl_2$ (1µl, 1 M), DNase (1 µl/ml) and lysozyme (10 µl, 10% (w/v) dissolved in resuspension buffer, pH7) were added before the cells were mechanically lysed on ice by sonication for 3×30 seconds, pulsed (intensity 3, pulse 0.5 sec) by using a Sonicator™ Ultrasonic Processor XL (Misonix Inc.).

The crude lysate was further centrifuged using an SS34 rotor (15 000 × g, 30 min, 4°C). The resulting supernatant was filtered to eliminate any remaining cell debris after diluting twice times with an equal volume of resuspension buffer at pH7.5. The supernatant was loaded onto a glutathione-Sepharose column pre-equilibrated with equilibration buffer (10 mM Tris-HCl, 150 mM NaCl, 1 mM EDTA, 1 mM DTT added fresh and 0.02% (w/v) NaN_3) at pH 8.0. This column has glutathione which is the immobilised ligand bound to the Sepharose matrix. The soluble GST-CLIC1 fusion protein in the supernatant of the *Escherichia coli* BL21 (DE3) pLysS lysate binds via the GST to glutathione while the rest of the protein solution passes through the column. Hence, CLIC1-GST fusion protein is isolated from other proteins produced by the *Escherichia coli* cells. The column was subsequently washed with 10-column volumes of the equilibration buffer containing 1 M NaCl to eliminate any other bacterial proteins that bound non-specifically to the column. Thereafter, the column was equilibrated with 5-column volumes of thrombin cleavage buffer at pH 8.4 (200 mM Tris-HCl, 150 mM NaCl, 1 mM EDTA).

Human thrombin (80 units per 1 litre of culture) was added to 15 ml of thrombin cleavage buffer and loaded onto the glutathione-Sepharose column containing the bound fusion protein. The column was sealed and digestion was allowed to occur on a rotator for 16 hours at 20°C resulting in the cleavage of CLIC1 from GST and, therefore, CLIC1 released

from the matrix. The CLIC1 cleaved from GST and the thrombin used for cleavage was collected from the column. A GSH-elution buffer, pH 8.0 (50 mM Tris-HCl and freshly added 10 mM reduced glutathione) was loaded onto the column to elute off the GST and any uncleaved fusion protein that was bound to the column.

DEAE anion-exchange chromatography was used to separate the CLIC1-thrombin mixture. The DEAE anion exchange column was attached to an ÄKTAprime purification system (Amersham® Biosciences) and pre-equilibrated with DEAE-equilibration buffer at pH 6.5 (20 mM Tris-HCl, 0.02% (w/v) NaN_3). This step was included so as to purify CLIC1 from thrombin. At the pH of the ion exchange buffer which is 6.5, CLIC1 has a negative charge (p*I*~5.0) and bound to the positively charged matrix of the DEAE column. Thrombin, however, has a positive charge at pH 6.5 (p*I*~8) and passed through the column without binding. The high concentration of salt in the thrombin cleavage buffer prevents the mutant from binding to the column under the specific conditions while the wild-type binds. Mutant proteins tend to aggregate in high salt and, therefore, lose their binding ability to columns (Chiti *et al*., 2002; Stoychev, PhD, 2008) while the wild-type of these proteins do not. Therefore, after recovery from the GSH column, CLIC1-S27P was dialysed against DEAE equilibration buffer (pH 6.5, at 4 °C, for less than 3 h) to decrease the salt concentration since it causes it to aggregate rapidly. Both the wild-type and mutant CLIC1–S27P were eluted from the DEAE column by the addition of 300 mM NaCl to the buffer. The high affinity of the high concentration of salt for the charged matrix leads to a reduction in the interaction between the ion exchanger and CLIC1. Therefore, CLIC1 is eluted while the salt is remained bound to the column. Protein purity was analysed using SDS-PAGE and various samples of the prime elution peak (Section 3.1). Once the proteins were purified, they were snap-frozen or dialysed every 6-7 days Snakeskin™ Pleated dialysis tubing MWCO 10 000 (Pierce), against 3 changes of CLIC1 storage buffer at pH7 (50 mM sodium phosfate buffer, 0.02 w/v NaN_3, 1 mM DTT added) in order to keep the proteins in reduced form. The wild-type and mutant were also dialysed against acetate buffer (5 mM sodium acetate buffer, 0.02% (w/v) NaN_3, pH5.5) 1 mM DTT (for the wild-type) and 5 mM DTT

(for the mutant since it aggregates at pH5.5) freshly added for the studies at pH5.5.

2.2.4. Sodium dodecyl sulfate polyacrylamide gel electrophoresis (SDS-PAGE)

Reducing sodium dodecyl sulfate polyacrylamide gel electrophoresis (SDS-PAGE), a technique used to separate and characterise proteins according to their molecular weight, was used to determine the purity and homogeneity of the expressed CLIC1-WT and CLIC1-S27P, proteins anticipated to give a band of 26.6 kDa. A 15% separating gel (30% (w/v) acrylamide, 1% (w/v) bisacrylamide, 10% (w/v) sodium dodecyl-sulfate (SDS), 10% (w/v) ammonium persulfate, 0.1% (w/v) TEMED and 1.5 M Tris-HCl, pH 8.8) and a 4% stacking gel (30% (w/v) acrylamide, 1% (w/v) bisacrylamide, 10% (w/v) SDS, 10% (w/v) ammonium persulfate, 0.1% (w/v) TEMED and 0.5 M Tris-HCl, pH 6.8) were used to construct the discontinuous SDS-PAGE gel and run as described by Laemmli (1970). The differences in stacking and separating gel acrylamide concentrations along with the differences in ionic strength and pH values of the stacking and separating gel buffers are employed to concentrate protein-SDS complexes in the stacking gel. Sample buffer (100 mM β-mercaptoethanol, 20% (w/v) glycerol, 10% (w/v) SDS, 0.05% (w/v) bromophenol blue and 0.5 M Tris-HCl, pH 6.8) was used to dilute samples 2-fold and added before loading samples to the gel in a 1:4 sample to sample buffer ratio after denaturing by boiling (5 min). Molecular markers (Fermentas SM0431) containing proteins of various molecular weights [β-galactosidase (116.0 kDa), bovine serum albumin (66.2 kDa), ovalbumin (45.0 kDa), lactate dehydrogenase (35.0 kDa), REase Bsp98l (25.0 kDa), β-lactoglobulin (18.4 kDa) and lysozyme (14.4 kDa)] were simultaneously run with the samples at 40 V in electrophoretic buffer [25 mM Tris-HCl, 200 mM glycine, and 0.1% (w/v) SDS, 3 h]. Coomassie Blue R250 staining solution [2% (w/v) (13.5% (v/v) glacial acetic acid and 18.8% (v/v) ethanol] was used to stain the gels (90 min). The gels were subsequently destained with a 40% destainining solution [25% (v/v) ethanol and 10% (v/v) glacial acetic acid].

2.2.5. Protein concentration determination

Ultraviolet (UV) absorbance spectroscopy was used to determine the concentration of purified CLIC1. The protein concentration was calculated by using the Beer-Lambert law:

$$A = \varepsilon_{\lambda} cl \qquad \textbf{Equation 2.1}$$

where A represents the absorbance measured at 280 nm and ε_{λ} represents the molar extinction coefficient (M^{-1} cm^{-1}) of the protein at wavelength λ (Equation 2.2). c and l show the concentration of the protein (M) and the cuvette path length (cm), respectively. The method generated by Perkins (1986) was used to determine the molar extinction coefficient of the wild-type and mutant species using the absorbance of tryptophan, tyrosine and cysteine residues (Equation 2.2).

$$\boldsymbol{\varepsilon_{280}\ (M^{-1}cm^{-1}) = 5550\Sigma Trp + 1340\Sigma Tyr + 150\Sigma Cys} \qquad \textbf{Equation 2.2}$$

$$\boldsymbol{= 5550(1) + 1340(8) + 150(6)}$$

$$\boldsymbol{= 17\ 170\ M^{-1}cm^{-1}}$$

Five serial dilutions (4×, 5×, 6×, 8× and 10×) were prepared from the stock CLIC1 and a dilution curve was constructed using A_{280} and A_{340}. Protein concentration was determined by fitting a linear regression to the five points from the serial dilution. All readings were buffer corrected. Possible aggregates absorb at 340 nm that may interfere with the absorbance readings at 280 nm, therefore, the determination of protein concentration was corrected for the absorbance by aggregates using the Equation (Reed *et al.*, 2003):

$$\boldsymbol{A_{280(corrected)} = A_{280(protein)} - A_{280(buffer)} - (A_{340(protein)} - A_{340(buffer)})(A_{280(buffer)}/A_{340(buffer)})}$$

Equation 2.3

Protein concentration was checked before each experiment. Possible contamination by DNA was checked using the ratio $A_{280}/A_{260.}$ All absorbance measurements were done at 20°C using a Jasco V-550 UV/VIS spectrophotometer.

2.2.6. Circular dichroism measurements

Far-UV circular dichroism (CD) spectroscopy was used to study the secondary structure of CLIC1. The technique is based on the asymmetry of the proteins in solution when they are exposed to polarised light (Woody, 1995). It measures the differential absorption of the right- and left- handed circularly polarised light by optically active chromophores such as the peptide backbone, disulphide groups and aromatic residues at a specific wavelength. Far-UV CD detects the changes in secondary structure of a protein at a wavelength range of 170-250 nm (Woody, 1995). This measures the different absorbance levels of specifically peptide bonds of the protein backbone. In this study, far-UV CD was employed for the characterisation of the secondary structure of native, intermediate (for the wild-type only) and unfolded states of CLIC1-WT and CLIC1-S27P. Proteins at a concentration of 10 µM in storage buffer (5 mM sodium phosphate buffer, 1 mM DTT, 0.02% (w/v) NaN_3, pH7), and acetate buffer (5 mM sodium acetate buffer, 1 mM DTT, 0.02% (w/v) $NaN_{3,}$ pH5.5) were used for the measurements using a 2 mm path length quartz cuvette at 20°C. A Jasco J810 spectropolarimeter and the software Spectra Manager for windows v1.5.00 was used for all circular dichroism measurements. All readings were obtained as an average of 10 readings with sensitivity at high (10 mdeg), a data pitch at 0.5 nm, a response of 1 second and a band width of 0.5 nm. All spectra were corrected for buffers and the raw data were converted to mean residue ellipticity (MRE) (ϕ) ($deg.cm^2.dmol^{-1}.residue^{-1}$) using the following Equation (Woody, 1995):

$$[\phi] = (100 \times \theta) / cnl \qquad \textbf{Equation 2.4}$$

where [θ] is the ellipticity (mdeg), the difference in absorbance of left and right handed circularly polarised light, c is the concentration of proteins (mM), n is the number of

residues in the protein and l is the path length of the cuvette (mm) (Woody, 1995). The data were plotted using SigmaPlot v11.0. The negative exponential smoothing technique in Sigmaplot v. 11.0 with a 0.1 sampling proportion was used to smooth the spectra.

2.2.7. Intrinsic fluorescence measurements

Fluorescence occurs when the excitation of electrons of a molecule takes place upon the absorption of light. The electrons subsequently emit light at a lower energy and, therefore, higher wavelength (Lakowicz, 1999). The intrinsic protein chromophores for this technique are tryptophan and tyrosine residues (Pain, 2004) where the electrons are excited at a wavelength of 280 nm for both tyrosine and tryptophan, and at 295 nm for only tryptophan. Fluorescence spectroscopy is used to characterise the tertiary structure, especially the packing and local environment of the chromophores in a protein (Lakowicz, 1999). Fluorescence therefore was used as a probe to study the tertiary structure of CLIC1-WT and CLIC1-S27P. CLIC1 has a unique tryptophan (Trp35) and eight tyrosine residues. The emission spectra are dominated by the single tryptophan residue, however (Lakowicz, 1999). Because of its indole group, Trp35 is highly sensitive to the polarity of its environment. The fluorescence emission spectra give characteristic signals which are varied according to the polarity of the environment in which tryptophans are packed (Lakowicz, 1983). A red shifted maximum emission wavelength is seen when the exposure of a tryptophan to the polar environment becomes greater which causes the energy of the excited states to drop (Royer, 1995).

All the fluorescence measurements were conducted at 20°C on Perkin-Elmer Luminescence Spectrometer LS50B using FLWinLab v4.00.0 software. Excitation and emission slit widths were 4 or 5 nm using a quartz cuvette of 1 cm path length for 5 µM protein. Spectra were recorded at a wavelength range of 280-450 nm with excitation at 280 nm for tyrosine and tryptophan, and 295 nm for tryptophan with a scan speed of 200 nm/min. All spectra were obtained as an average of 3 accumulations and all data were corrected for buffer. The

data were plotted using SigmaPlot v11.0 and smoothed using the negative exponential method.

The quenching of the fluorescence of Trp35 by acrylamide was used as a probe to provide more information on the environment of tryptophan in the native and intermediate states of the wild-type and the mutant. The method investigates not only conformational changes of a polypeptide but also the dynamic structure of the protein. It gives information on the frequency and amplitude of structural fluctuations permitting solutes to diffuse into the internal regions of a globular fold (Lacowicz and Weber, 1973; Eftink and Ghiron, 1977). A modified form of the Stern-Volmer Equation which was used to analyse the dynamic acrylamide quenching of the single tryptophan residue is:

$$\mathbf{F_0/\ F = (1 + \mathit{K}_{SV}\ [Q])} \qquad \textbf{Equation 2.5}$$

where K_{SV} is the Stern-Volmer constant, F_0 and F are fluorescence intensities at 0 M acrylamide and under increasing acrylamide concentrations, respectively and [Q] is the concentration of acrylamide. Acrylamide quenching of tryptophan in the native and intermediate conformations of the wild-type and the mutant was performed in the following way: acrylamide stocks were prepared at a final concentration of 1 M in 50 mM sodium phosphate (pH7) or 50 mM acetate buffer (pH5.5). The various concentrations of acrylamide between 0 M-0.3 M were added to 2 µM protein and mixed. All measurements were recorded between 295-550 nm at an excitation of 295 nm as an average of 3 readings at a scan speed of 250 nm/min and using slit widths of 4 nm for the mutant and 5 nm for the wild-type.

2.2.8. Extrinsic fluorescence measurements

8-Anilino-1-naphthalene sulphonate (ANS) was used as an extrinsic fluorescent probe for unfolding studies of CLIC1-WT and CLIC1-S27P. ANS is an amphipathic dye with an affinity to bind hydrophobic patches of a protein (Rosen and Weber, 1969; Brand and

Gohlke, 1972) allowing partially folded species such as intermediate species, to be detected during the unfolding of proteins (Struyer, 1965) as the hydrophobic surfaces of the unfolded protein are exposed to the solvent. Binding of ANS emits light more intensely at a shorter wavelength.

The changes in tertiary structure and detection of intermediate species that are formed during the unfolding of CLIC1 were assessed by using ANS binding at a specific excitation wavelength of 390 nm and emission at 460 nm throughout the unfolding pathway. ANS stock was prepared at a concentration of 2 mM in the 50 mM sodium phosphate buffer, pH7 with 1 mM DTT or 50 mM acetate buffer, pH5.5 with 1 mM (for the wild-type) or 5 mM (for the mutant) fresh DTT in which CLIC1 was dialysed. Stock urea solutions were prepared at a concentration of 10 M using filtered dialysis buffers into which CLIC1 had been dialysed against every week. pH was adjusted by titration using orthophosphoric acid for pH7 or acetic acid for pH5.5. The concentration of stock urea was calculated using the following equation (Pace, 1986b):

$$\mathbf{[Urea] = 117.66\ (\Delta N) + 29.753\ (\Delta N)^2 + 185.56\ (\Delta N)^3} \qquad \textbf{Equation 2.6}$$

where (ΔN) is the difference between the refractive index of urea and buffer. Dilutions of the wild-type and mutant with urea (0-8 M) were prepared and incubated at 20°C for 2 hours to reach equilibrium. Subsequently, ANS was added at a concentration of 200 µM and left for a further hour to ensure ANS binding to any hydrophobic patches that are exposed to the solvent before performing measurements. Slit widths were kept at 4 nm and a cuvette of 1 cm pathlength was used throughout. Scan speed was 250 nm/min. All spectra were recorded as an average of 3 accumulations and corrected for free ANS.

The K_d value was calculated to determine the affinity of the protein for any ligand. This study was performed at pH7 and 5.5 for the wild-type intermediate (in the presence of 3.8 M urea) and the native mutant in the absence of urea since the mutant binds to ANS in the native state. K_d values were obtained by plotting and fitting the graphs using nonlinear

regression. Various concentrations of ANS (0-200 µM) were added to 2 µM wild-type and mutant and left for an hour to ensure that any hydrophobic patches exposed to the solvent bind to ANS. Subsequently, measurements were performed as explained above. All fluorescence measurements were plotted using SigmaPlot v11.0 and the data smoothed using negative exponential method. The K_d value was calculated using the Equation:

$$f=a^* (1-\exp^{(-b.x)}) \qquad \textbf{Equation 2.7}$$

where f is the $f_{max}/2$, a is f_{max}, b is the concentration of ANS at which the protein binds at maximum and x is the K_d which indicates the affinity of the protein to bind ANS.

2.2.9. Recovery studies

The reversibility of protein unfolding has to be established so as to ensure that the reaction can achieve equilibrium in order to perform equilibrium unfolding studies. The equilibrium constant, K_{eq} is necessary to calculate the thermodynamic parameters, such as ΔG and *m*-values which describe the stability of proteins (Shirley, 1995).

Fluorescence was used as a probe to investigate the recovery of the wild-type and the mutant at pH7 and pH5.5. For the refolding, the wild-type and mutant were unfolded in 8 M urea at a concentration of 10 µM. They were left for two hours at pH7 and an hour at pH5.5 to denature. Proteins were diluted 10-fold with CLIC1 phosphate buffer, pH7 or acetate buffer, pH5.5, into decreasing concentrations of urea (range 0.8 M to 8 M). They were allowed to refold for two hours at pH7 or an hour at pH5.5. A series of control samples for refolding were prepared for comparison purposes and consisted of 1 µM protein and concentrations of urea range (8 M to 0.8 M). For the recovery studies, the refolded samples that contain 0.8 M urea and the control samples with 0.8 M urea were used for comparison purposes at both pH values. Fluorescence readings of the sample were recorded at a wavelength range of 280-450 nm with excitation at 280 nm. All spectra were measured as triplicates at 20°C, buffer-corrected and plotted using SigmaPlot v. 11.0.

2.2.10. Urea-induced equilibrium unfolding

The stability of a protein can be estimated by constructing protein equilibrium unfolding curves under specific conditions. This study also gives information about the folding mechanism of a protein and may allow for the detection of possible intermediate conformations (Pace, 1986). The equilibrium is shifted from the native to the unfolded states (N↔U) with or without the accumulation of intermediates by the addition of a denaturant (Pace, 1986a) which is urea in this case.

Thermodynamic parameters can be calculated from unfolding data; the reaction should be both reversible and at equilibrium before starting any measurements (Pace, 1986a). Monophasic (native↔unfolded) and biphasic (native↔intermediate↔unfolded) equilibrium unfolding curves indicate whether two-state or three-state models exist during the unfolding process.

The wild-type and mutant species of CLIC1 (2 µM) were added to various concentrations of urea ranging from 0 M to 8 M along with phosphate buffer, pH7 or acetate buffer, pH5.5 and incubated at 20°C for 120 minutes to reach equilibrium at pH7 and for 90 minutes to reach equilibrium at pH5.5, respectively. The unfolding of CLIC1 at equilibrium was followed using fluorescence at an excitation of 280 nm and CD as probes and the results were recorded for samples at each urea concentration. The CD data were collected at ellipticity of 222 nm because the α-helical content gives a distinct trough at 222 nm. The unfolding fluorescence data were collected by plotting fluorescence intensities at 310 nm, 320 nm, 345 nm and the intensity averaged emission wavelength (IAEW) (Royer *et. al.*, 1993) against urea concentration. The IAEW was calculated as:

$$\lambda = \sum_{i=1}^{N} \frac{\mathbf{I}i\lambda i}{\sum_{i=1}^{N} (\mathbf{I}i)}$$

Equation 2.8

where I is the intensity, i is the each point in the spectrum, and λ is the wavelength. All spectra for fluorescence and circular dichroism were average of triplicates which were analysed by using SigmaPlot® v11.0.

Stock urea solutions were prepared as described in Section 2.2.8. After preparing the stocks, urea was kept at -20°C for no longer than a week since cyanate which forms during the urea decomposition can modify the chemical composition of the amino groups of proteins (Stark, 1965).

The parameters of conformational stability in the absence of denaturant (ΔG_{H20}) and the dependence of the free energy of unfolding on denaturant concentration (*m*-value) were determined using linear extrapolation (Greene and Pace, 1973).

2.2.11. Data fitting

Savuka is a computer-based program used for the global fitting of equilibrium unfolding data to obtain the thermodynamic parameters, *m*-value and ΔG (Zitzewitz *et al.*, 1995; Bilsel *et al.*, 1999). The program analyses multiple sets of data and thus simultaneous fits can be generated with minimal errors (Beecham, 1992).

A two-state unfolding curve represents two species that are present during the transition: the native (N) and the unfolded (U) species (N↔U). This type of fit consists of three regions (Pace and Stoltz, 1997):

i. The pre-transition region in which the protein is predominantly in the native conformation
ii. The transition state in which cooperative unfolding of the protein takes place and varying concentrations of native and unfolded species exist
iii. The post-transition region in which the protein is predominantly in its unfolded conformation

According to this mechanism, the equation for the fraction of protein in native state (F_N) and unfolded state (F_U) is as follows:

$$F_N + F_U = 1 \qquad \textbf{Equation 2.9}$$

The raw value recorded using circular dichroism or fluorescence is represented by y at which any point along with the unfolding curve and can be calculated as:

$$y = Y_N F_N + Y_U F_U \qquad \textbf{Equation 2.10}$$

where Y_N and Y_U represent the y values of the native and unfolded proteins, respectively.

The Gibbs free energy of this transition, ΔG *is* calculated as:

$$\Delta G = -RT\ln K_{eq} \qquad \textbf{Equation 2.11}$$

where R is the universal gas constant (1.987 cal mol^{-1} K^{-1}) and T is the temperature in Kelvin. The equilibrium constant, K_{eq}, is calculated as:

$$K_{eq} = F_U / F_N$$

$$= F_U / 1 - F_U$$

$$= (Y_N - y) / (y - Y_U) \qquad \textbf{Equation 2.12}$$

Inserting Equation 2.12 into Equation 2.11;

$$\Delta G = -RT\ln (Y_N - y) / (y - Y_U) \qquad \textbf{Equation 2.13}$$

The thermodynamic parameters of unfolding, $\Delta G_{(H_2O)}$ and m-value were calculated using the linear extrapolation method generated by Greene and Pace (1973). The ΔG values and the concentration of the denaturant have a linear relationship where the urea concentration is extrapolated back to 0 M to get the ΔG value in the absence of urea according to this

method (Greene and Pace, 1973) as shown below:

$$\Delta G = \Delta G_{(H_20)} - m\,[\text{urea}] \qquad \textbf{Equation 2.14}$$

The *m*-value represents the slope of the curve and expresses the dependence of the free energy of ΔG on the urea concentration (Shirley, 1995).

C_m values representing the midpoint of the transition curves were obtained using the equation:

$$C_m = \Delta G_{(H_2O)} / m \qquad \textbf{Equation 2.15}$$

The two-state model is only applicable if the unfolding curve is a single step transition with no shoulders or plateaus seen in the curve. Moreover, different probes that are used to study unfolding of the protein should reflect results that are consistent and overlaying with each other. However, intermediate states are seen for many proteins showing at least two unfolding transitions. This requires three-state or multi-state models in order to fit the data. Hence, the intermediate species of the mutant and the wild-type fitted to a three-state model using the equation as follows:

$$Z_i = y_i - Y_N / Y_U - Y_N \qquad \textbf{Equation 2.16}$$

where Z_i is the point of the urea concentration at which an intermediate is formed. As mentioned earlier, a three-state model includes native, intermediate, and denatured species at equilibrium (Pace, 1986a) where the transition seems to be N↔I↔U. In this model, the intermediate species at equilibrium exists when the observed extent of unfolding (F_{obs}) along the unfolding transition is different from the fraction of the protein in the unfolded conformation in the two-state transition (F_U) (Pace, 1986a). Therefore:

$$F_{obs} = F_U + \sum_i F_i Z_i \qquad \textbf{Equation 2.17}$$

where F_i is the the concentration of the stable intermediate species.

Thus, using Equation 2.12, the $\Delta G1$ (H_2O) and $\Delta G2$ (H_2O) can be calculated as:

$$\Delta G1\ (H_2O) = -RTln\ (y - Y_N / y_i - Y_N) \text{ and}$$

$$\Delta G2\ (H_2O) = -RTln\ (y - Y_i / Y_U - y)$$

and m_{NI} and m_{IU} can be obtained using Equation 2.13:

$$m_{NI}\ [denaturant] = \Delta G / \Delta G1\ (H_2O)$$

and $$m_{IU}\ [denaturant] = \Delta G / \Delta G2\ (H_2O)$$

where NI denotes the N↔I transition and IU denotes the transition of I↔U.

CHAPTER 3: RESULTS

3.1. CLIC1-WT and CLIC1-S27P purification

The SDS-PAGE gels of samples from the various purification steps for the wild-type and mutant is shown in Figure 5.

CLIC1-WT and CLIC1-S27P were expressed as a GST fusion protein which has a theoretical size of 52.4 kDa. Cells grown at 37°C for 5-6 hours gave a high yield of GST-CLIC1-WT fusion protein that was found to be soluble in the supernatant. GST-CLIC1-S27P fusion protein was insoluble when expressed at 37°C however (results not shown), and subsequently cells containing the cDNA encoding mutant GST-CLIC1 were incubated for 16 hours at 20°C. Even so, a small amount of insoluble GST-CLIC1-S27P was found to be in the pellet (Figure 5, lane 2). However, a thick band corresponding to a molecular weight of 54 kDa (Figure 5 A, lane 3) indicates that the majority of the fusion protein is soluble in the supernatant under these conditions. Figure 5 A lane 4 shows the flow through off the GSH-Sepharose column indicating that a large amount of fusion protein bound to the affinity matrix. Figure 5 A lane 5 shows the CLIC1-S27P and thrombin mixture that was recovered from the GSH-Sepharose column after 16 hours agitation with thrombin. *Sj*26GST was subsequently removed from the GSH-Sepharose column by the addition of glutathione (Figure 5, A, lane 8).

The mixture of CLIC1-S27P and thrombin was separated using the DEAE column. Since thrombin has a positive charge at pH 6.5, it does not bind to the DEAE-column and was washed off the column in the flow though (Figure 5 A, lane 6 and Figure 6). CLIC1 is negatively charged at pH 6.5 and bound to the DEAE column. CLIC1-S27P was successfully recovered from the DEAE column with 300 mM NaCl at pH 6.5 (Figure 6). The single large band in Figure 5 A lane 7 indicates that the CLIC1-S27P was successfully purified.

A.

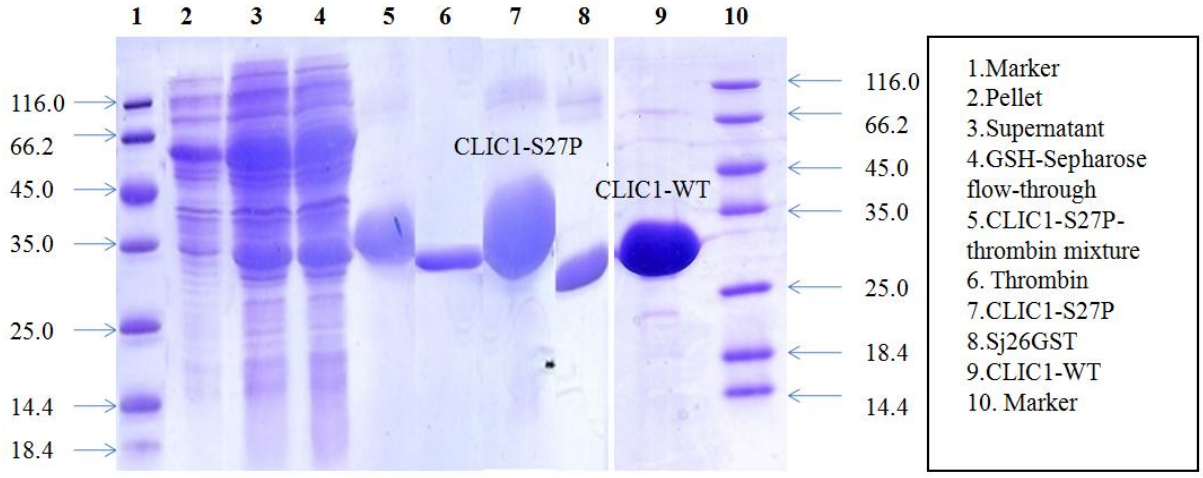

B.

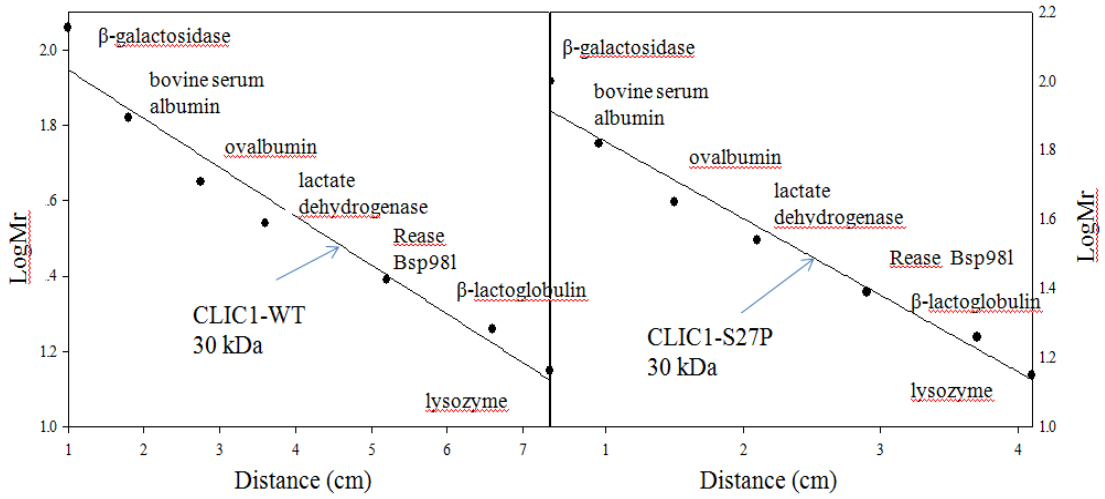

Figure 5: SDS-PAGE gel showing a representative CLIC1 purification

A. A 15% polyacrylamide SDS-PAGE gel illustrating a representative CLIC1-WT and CLIC1-S27P purification. Lane 1 is the marker. The pellet and the supernatant of the lysate of the mutant are shown in lane 2 and 3, respectively. Lane 4 contains the flow-through off the GSH-Sepharose column indicating that an amount of GST-CLIC1-S27P fusion protein bound to the matrix while a fraction of it did not bind. CLIC1-S27P and thrombin mixture

is shown in lane 5. The thrombin separated from CLIC1 is shown in lane 6. Lane 7 indicates a band of successfully purified CLIC1-S27P with a molecular mass of 30 kDa along with a negligible amount of contaminants. The cleaved *Sj*26GST is shown in lane 8. Lane 9 and 10 show a second gel indicating successfully purified CLIC1-WT and molecular weight markers, respectively.

B. The calibration curves constructed by using the electrophoretic mobilities of standard proteins of different molecular masses (in kDa) on the SDS-PAGE gel (r^2=0.95). The proteins used are β-galactosidase (116.0 kDa), bovine serum albumin (66.2 kDa), ovalbumin (45.0 kDa), lactate dehydrogenase (35.0 kDa), REase Bsp98l (25 kDa), β-lactoglobulin (18.4 kDa), lysozyme (14.4 kDa). As the arrows indicate, CLIC1-WT and CLIC1-S27P were found to be 30 kDa.

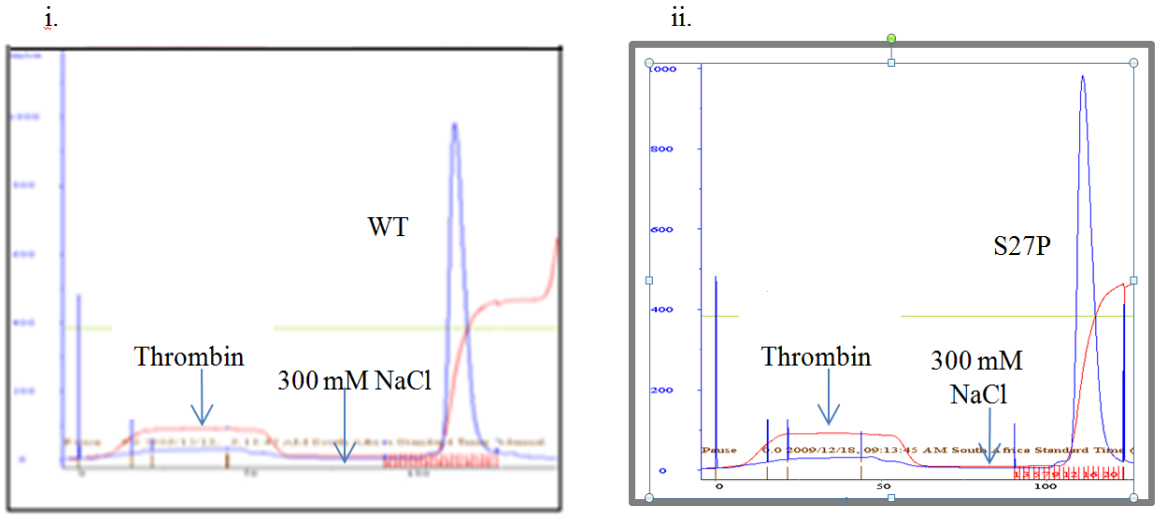

Figure 6: A representative CLIC1-WT and CLIC1-S27P purification from the DEAE column. The elution profile of CLIC1-WT (i) and CLIC1-S27P (ii) along with thrombin off the DEAE-Sepharose anion exchange column is shown above. Absorbance was recorded at 280 nm. Thrombin (red line shown with the arrow) was first eluted from the column since it does not bind to the DEAE column. Both the wild-type and the mutant were recovered as single peaks from the column using 20 mM Tris-HCl, 300 mM NaCl, pH 6.5.

The faint bands indicating the presence of proteins other than CLIC1 are negligible due to the fact that the gels were overloaded and the concentration of CLIC1 present far supersedes that of the contaminants.

The theoretical mass of CLIC1 is 26.9 kDa. However, according to the mobility of standard proteins of different molecular masses (in kDa) on the SDS-PAGE gel, the molecular weight of both the wild-type and the mutant was found to be 30 kDa (Figure 5, B). The explanation for this may be that since CLIC1 has a net charge of -7 at pH7, the acidic nature of the protein may cause a lower mobility than expected and thus diminish the mass:charge ratio and SDS binding (Dunker and Rueckert, 1969; Lehotvaara, 1978; Pitt-Rivers and Impiombato, 1968; Reynolds and Tanford, 1970).

The absorbance spectra of both the wild-type and the mutant are shown in Figure 7. The ratio of absorbance at 280 nm to absorbance at 260 nm is about 1.8 and 1.7 for the wild-type and the mutant, respectively. This indicates that there is no significant DNA contamination in both the proteins.

3.2. Structural characterisation

3.2.1. Secondary structural properties

Secondary structural characterisation of CLIC1-WT and CLIC1-S27P was performed using far-UV circular dichroism. The far-UV CD spectra of the wild-type and the mutant were recorded over the wavelength range of 190-250 nm at pH7 and pH5.5. The spectra show characteristics of a predominantly α-helical protein displaying two troughs; one at 208 nm and one at 222 nm (Figure 8).

The wild-type is known to form an intermediate at pH5.5 in the presence of urea (3.8 M) (Fanucchi *et al*., 2008).

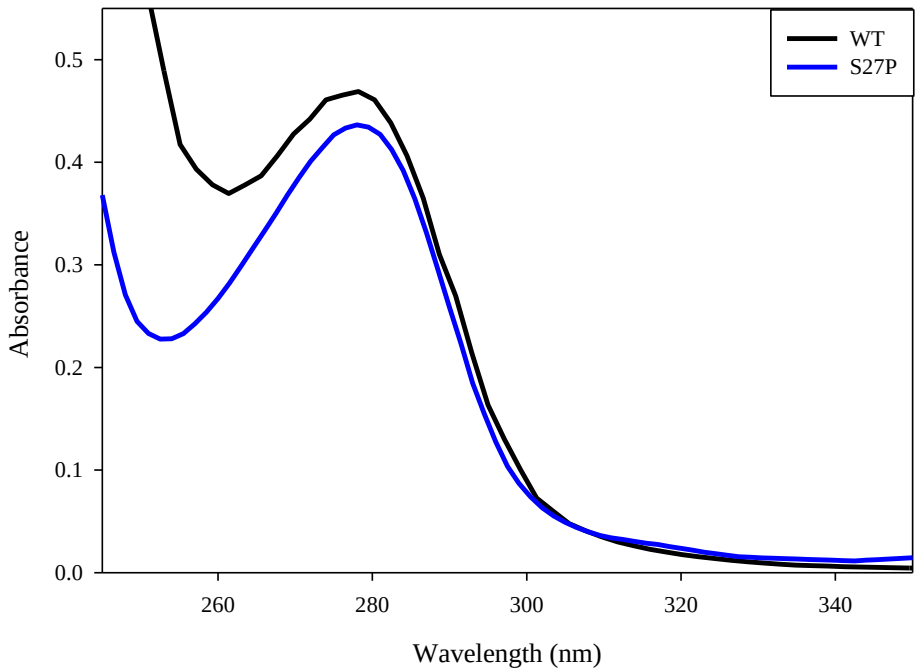

Figure 7. Absorbance spectra of purified CLIC1-WT and CLIC1-S27P. The concentration of the wild-type (black line) and the mutant (blue line) were found using the Beer-Lambert law and absorbance at 280 nm to be 66.6 mg/ml and 42 mg/ml, respectively. The A_{280}/A_{260} ratio is about 1.8 and 1.7 for the wild-type and the mutant, respectively which corresponds to no significant DNA contamination. There is also no aggregation indicated by the negligible absorbance at 340 nm for both the proteins.

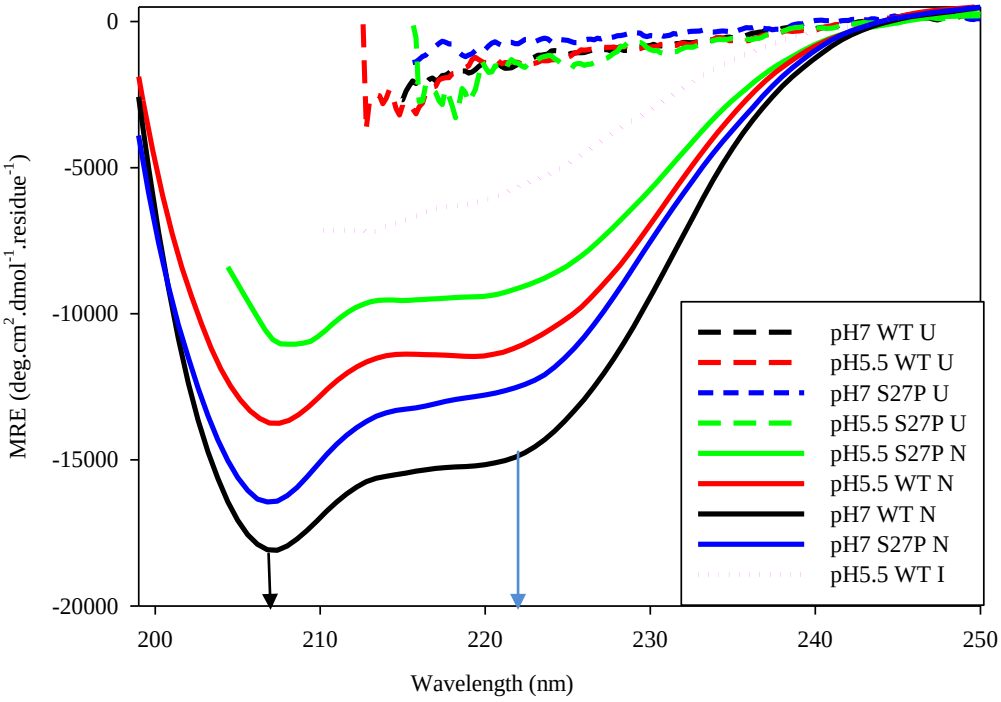

Figure 8: Far-UV circular dichroism spectra of CLIC1-WT and CLIC1-S27P. The native (N) and the unfolded (U) proteins are represented as solid lines and dashed lines, respectively. The wild-type intermediate (I) is indicated by a dotted line. The spectra exhibit two troughs that represent α-helical proteins, one at 208 nm (black arrow) and the other at 222 nm (blue arrow). The buffer used was 50 mM phosphate buffer, pH7 with 1 mM DTT and 50 mM acetate buffer, pH5.5 with 1 mM DTT (for the wild-type) and 5 mM DTT (for the mutant). The intermediate species of the wild-type (I) was recorded in the presence of 3.8 M urea in 50 mM acetate buffer, 1 mM DTT, pH5.5. Spectra were corrected for the buffer blank and show an average of ten accumulations at 100 nm/min at 20°C. The data were smoothed using a negative exponential methodology.

However, the mutant does not form a clearly defined equilibrium intermediate (Section 1.4.2) and thus the native, intermediate and unfolded states of CLIC1- WT were compared only with the native and the unfolded states of CLIC1-S27P in this study.

Secondary structural features of the native, intermediate and denatured states of CLIC1-WT and the native and the denatured states of CLIC1-S27P have been studied at pH7 and 5.5 since these pH values are the approximate pH of the cytoplasm and at the membrane surface, respectively (Bortoleto and Ward, 1999; Chenal *et al.,* 2002; Menestrina *et al.,* 1989; van der Goot *et al.,* 1991).

CLIC1-WT and CLIC1–S27P both exhibit helical secondary conformation with two troughs in the far-UV CD spectra at pH7 though the mutant shows 17% decrease in secondary structure compared to the wild-type at pH7 (Figure 8). Similarly, the spectra of the wild-type and mutant at pH5.5 indicate a helical structure with the mutant displaying an 18% loss of helical structure as compared to the wild-type. Both the wild-type and the mutant appear less α-helical at pH5.5 than at pH7 (Figure 8). The intermediate species of the wild-type possesses less secondary structure than the native states of both the wild-type and the mutant. The spectra of the denatured states of both the proteins in the presence of 8 M urea no longer indicate α-helical secondary structure at either pH7 or pH5.5 and are indicative of mainly random-coil structure (Figure 8).

3.2.2. Tertiary structural properties

Fluorescence spectroscopy was used as a probe to explore the local environment of the lone tryptophan and to detect any hydrophobic patches that are exposed to the solvent and will bind ANS for CLIC1-WT and CLIC1-S27P. In terms of the environment of the tryptophan, the chromophores (8 tyrosines and a single tryptophan) were excited at 280 nm. The unique tryptophan, Trp35, gives information about the environment where it is located and makes an excellent probe for the putative transmembrane region since this is where it is located (Figure 3).

Furthermore, it is located in the α1 helix that is affected by the N-cap, Ser27, and is an excellent probe for changes caused by the mutation. The emission spectra for the wild-type and the mutant when excited at 280 nm are given in Figure 9.

The spectra for the native state of both the wild-type and the mutant at pH7 indicate no significant difference with a single peak in the fluorescence intensity ($\lambda_{em\ max}$) at 341 nm for both proteins (Figure 9, A). The denatured species of both the proteins are also similar with a red-shifted peak indicating a more exposed tryptophan to the solvent as the protein unfolds (Figure 9, A). At pH5.5, the spectrum of the wild-type peaks at 343 nm while for the mutant it is blue-shifted to 338 nm with a lower intensity (Figure 9, B). The intermediate species of the wild-type (in the presence of 3.8 M urea) displays a blue-shifted peak to 336 nm and an enhanced intensity. Both the native mutant and the wild-type intermediate at pH5.5, therefore, appear to contain a more buried tryptophan compared to the native wild-type at pH7.

8-Anilino-1-naphthalene sulfonic acid (ANS) was used as a probe to detect hydrophobic patches that are exposed to the solvent. The fluorescence emission spectra of CLIC1-WT and CLIC1-S27P in the presence of 200 μM ANS along with the spectra of unbound ANS are shown in Figure 10. The spectrum for unbound ANS peaks at 512 nm in the absence of protein and is identical at pH7 and pH5.5. Hence, ANS emission signal is not pH-dependent. Any enhancement in fluorescence intensity in the presence of protein is indicative of ANS binding to hydrophobic patches on the surfaces of these proteins. It is interesting to note that at pH7 ANS bound to the native CLIC1-S27P shows an enhanced fluorescence intensity with $\lambda_{em\ max}$ of 467 nm as compared to CLIC1-WT that does not show binding of ANS at pH7 (Figure 10, A). The enhancement in fluorescence intensity of ANS bound to the mutant suggests an increase in the number of hydrophobic patches while the blue shift is indicative of the hydrophobicity of the binding patch. At pH5.5, ANS does not bind to the native wild-type although it binds to the native mutant at this pH value.

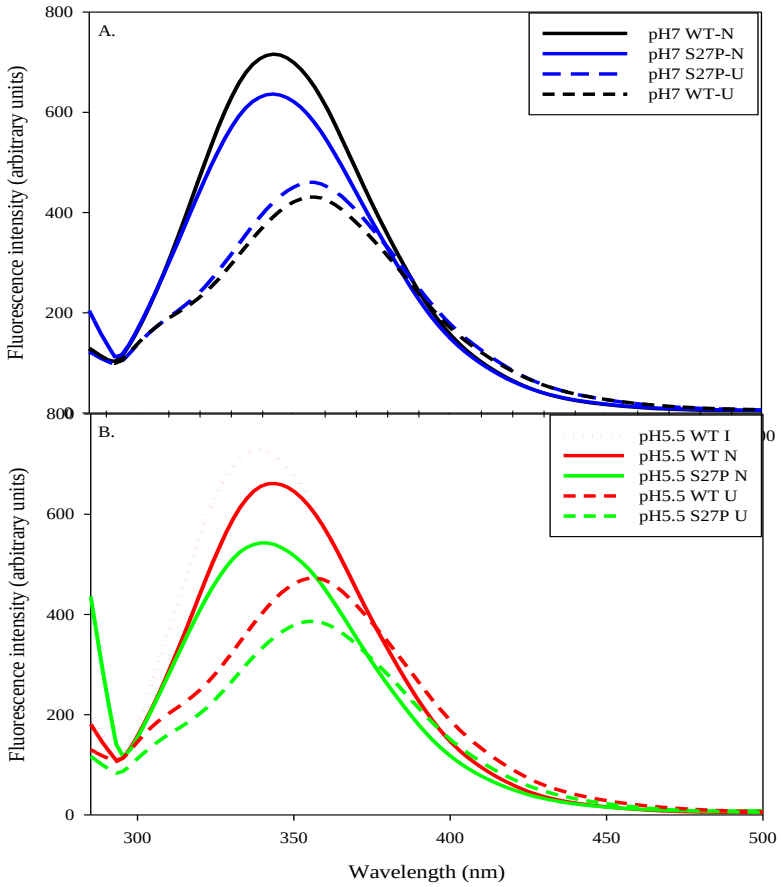

Figure 9: Fluorescence emission spectra of CLIC1-WT and CLIC1-S27P. The spectra of 5 µM native (N) and unfolded (U) CLIC1-WT and CLIC1-S27P were recorded by exciting the proteins at 280 nm at pH7 (A) and pH5.5 (B) at 20°C. The wild-type intermediate (I) (dotted line) in the presence of 3.8 M urea was also recorded at pH5.5. The denatured species are indicated as dashed lines with the same colours as the native ones. The spectra of both the proteins are similar except that a blue-shift in the peak to the lower wavelength is observed in the native mutant and the wild-type intermediate spectra at pH5.5. The buffer that was used is 50 mM sodium phosphate buffer, pH7 with 1 mM DTT and 50 mM acetate buffer, pH5.5 with 1 mM DTT (wild-type) and 5 mM DTT (mutant).

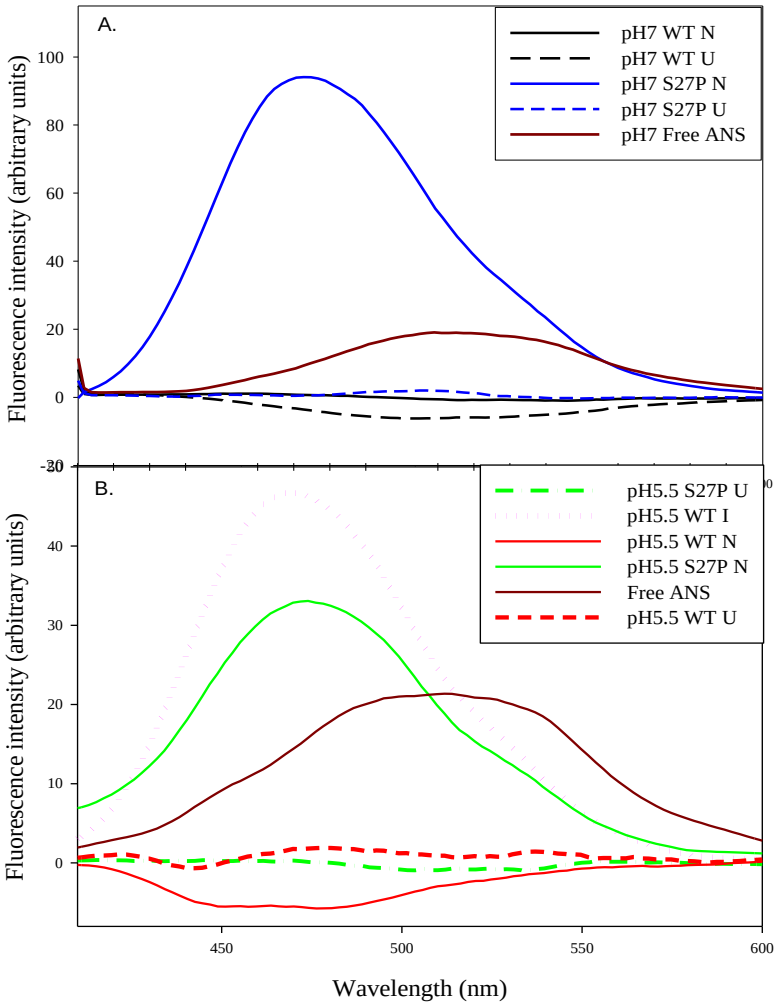

Figure 10: Binding of ANS to CLIC1-WT and CLIC1-S27P. The fluorescence emission spectra of ANS bound to CLIC1-WT and CLIC1-S27P (2 μM) were measured by using fluorescence at pH7 (A) and pH5.5 (B) at 20°C. The buffer that was used is 50 mM phosphate buffer, pH7 and 50 mM acetate buffer, pH5.5 with the addition of 200 μM ANS. ANS was excited at 390 nm. Native (0 M urea) (N) and unfolded (8 M urea) (U) proteins in the presence of ANS are shown as solid and dashed lines, respectively. The wild-type intermediate (I) (3.8 M urea) is indicated by the dotted line. ANS that bound to the native CLIC1-S27P shows enhanced fluorescence intensity and a blue-shift as compared to CLIC1-WT that does not bind ANS at either pH7 (A) or pH5.5 (B). The wild-type intermediate (I) (3.8 M urea, pH5.5) binds ANS unlike the wild-type native and denatured states but similar to the mutant native state.

The wild-type intermediate exhibits a similar spectrum to the native mutant at pH5.5 and shows binding of ANS at a $\lambda_{em\ max}$ of 469 nm (Figure 10, B). ANS does not bind to the denatured state of either the wild-type or the mutant at pH7 or pH5.5.

The fluorescence intensity of ANS (0 µM -100 µM) in the CLIC1-WT and CLIC1-S27P protein solutions was also recorded at 460 nm in order to calculate the K_d values which determine the affinity of the proteins for ANS (Figure 11). K_d values as an average of three replicates for native CLIC1-S27P were found to be 17.5 µM and 23.3 µM at pH7 and 5.5, respectively. The K_d for the wild-type was calculated for only the intermediate state of the protein since the native wild-type does not bind ANS. The K_d for the wild-type intermediate was found to be 14 µM. A lower K_d value is indicative of higher binding affinity to ANS. Thus, the intermediate state of the wild-type at pH5.5 has slightly higher affinity for ANS compared to the mutant. In the case of CLIC1-S27P, the native protein binds ANS with a higher affinity at pH7 than at pH5.5.

3.2.3. Acrylamide quenching

The accessibility of the single tryptophan (Trp35) localised in the putative transmembrane region of CLIC1 to the solvent was probed by using acrylamide quenching of tryptophan fluorescence (Figure 12). The study was to investigate the effect that the mutation has on the vicinity of the single tryptophan (Trp35) by determining whether it becomes more buried or exposed. Modified Stern-Volmer plots for the fluorescence quenching of tryptophan by acrylamide were used to calculate the *K*sv values for both CLIC1-WT and CLIC1-S27P at pH7 and pH5.5. The *K*sv value shows the efficiency of quenching of the tryptophan by acrylamide.

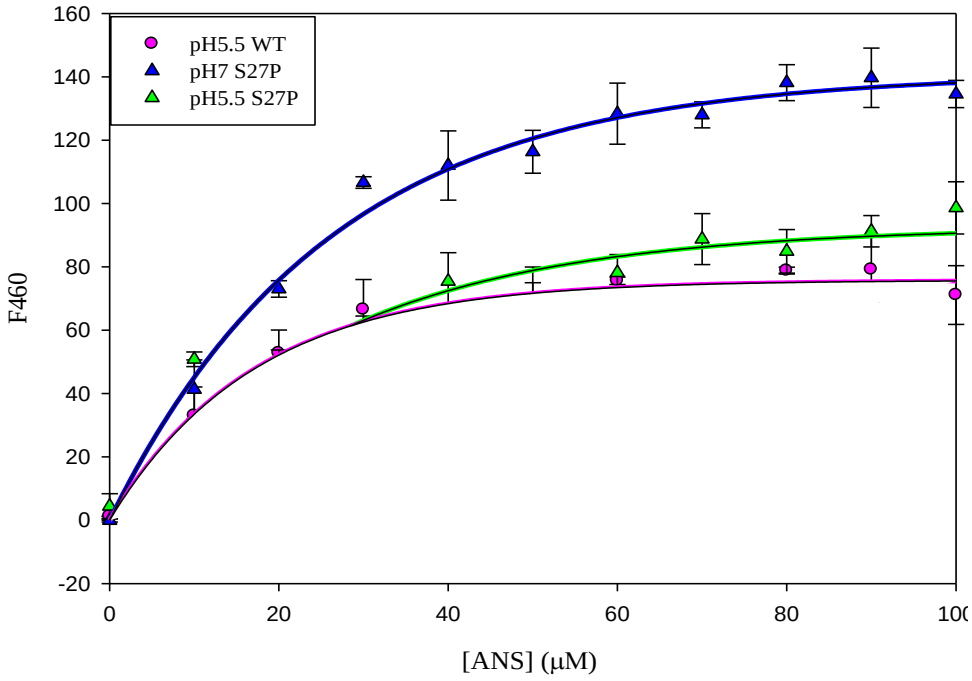

Figure 11: K_d of ANS binding.

The fluorescence intensities of various concentrations of ANS (0-100 μM) bound to CLIC1-WT intermediate (●) (in the presence of 3.8 M urea, at pH5.5) and native CLIC1–S27P at pH7 (▲) and pH5.5 (▲) at 460 nm were recorded at 20°C. The data were fitted to non-linear regression. K_d values were calculated using Equation 2.6. The K_d values for the mutant at pH7 and 5.5 were found to be 17.5 μM (R^2=0.88) and 23.3 μM (R^2=0.90), respectively, and the K_d of wild-type was 14 μM (R^2=0.97).

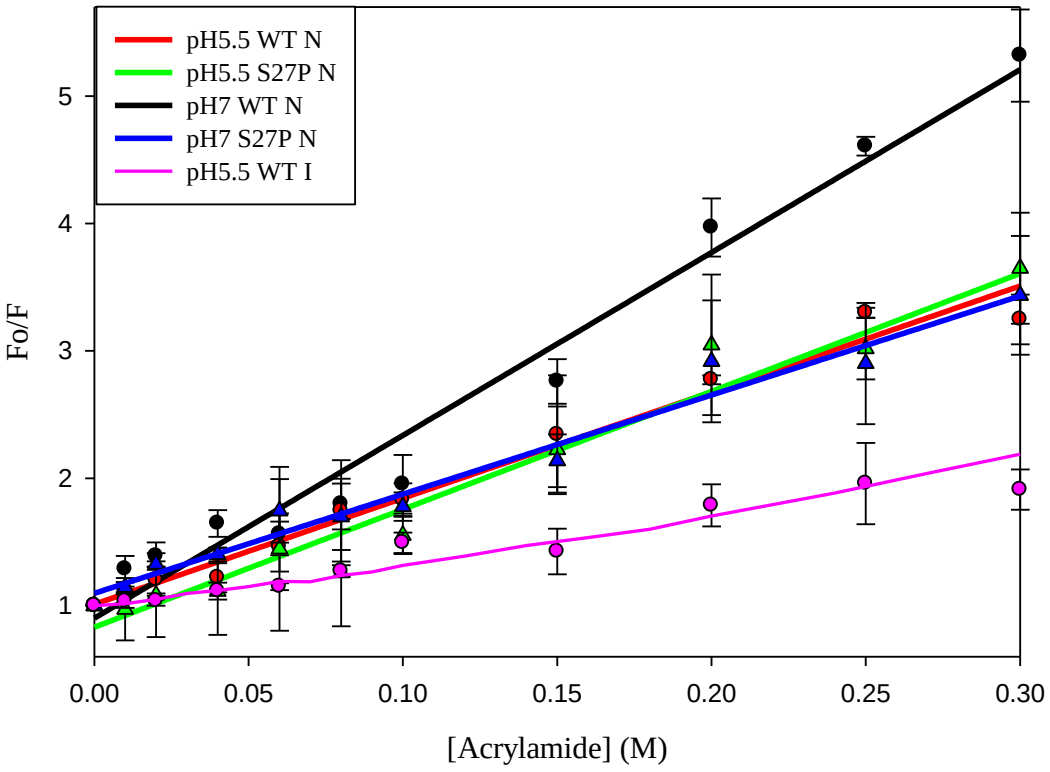

Figure 12: Modified Stern-Volmer plots for fluorescence quenching of Trp35 by acrylamide in CLIC1-WT and CLIC1-S27P.

F_0/F as a function of acrylamide quenching is illustrated for the native CLIC1-WT at pH7 (●) (R^2=0.86), at pH5.5 (●) (R^2=0.96) and the intermediate state of CLIC1-WT (●) (I) (Fanucchi *et al*., 2008) (in the presence of 3.8 M at pH5.5) (R^2=0.87). The F_0/F for the native CLIC1-S27P is shown for pH7 (▲) (R^2=1) and pH5.5 (▲) (R^2=0.93). The proteins were incubated in 50 mM phosphate buffer, pH7 with 0.02% NaN_3, 1 mM DTT and 50 mM acetate buffer, pH5.5 with 0.02% NaN_3, 1 mM DTT (for the wild-type) and 5 mM DTT (for the mutant) and increasing concentration of acrylamide (0 M-0.3 M).

The higher *K*sv value indicates that tryptophan is more quenched by acrylamide and hence is more exposed to the solvent, whereas the lower *K*sv value shows a more buried tryptophan conformation. The Stern-Volmer plots clearly indicate that tryptophan is the most accessible in the native wild-type at pH7 showing the highest *K*sv value (Table 3) suggesting the tryptophan is more exposed to the aqueous phase under these conditions. The lowest *K*sv value was observed in the native mutant at pH5.5 which therefore has the tryptophan most buried (Table 3).

3.2.4. Urea-induced equilibrium unfolding of CLIC1-WT and CLIC1-S27P

The reversibility of the unfolding reactions and recovery of the native fold are necessary to be able to calculate the thermodynamic parameters, ΔG (H_2O) and *m*-value (Pace, 1986) from an equilibrium unfolding curve. A reversibility study performed for CLIC1-WT has shown that the unfolding of the protein is reversible (McIntyre, PhD, 2008). Fluorescence was used as a probe to monitor the recovery of the tertiary structure of the mutant. Figure 13 shows the fluorescence spectra of native and refolded species along with the refolding curves of CLIC1-S27P at pH7 and pH5.5. At pH7, the mutant recovered approximately 95% of native structure (Figure 13, A). At pH5.5, the recovery of the native structure was observed to be 99% (Figure 13, B). The refolding was found to be consistent along the entire unfolding curve and no hysteresis was observed (Figure 13, C and D).

Table 3: The comparison of Stern-Volmer constants (*K*sv) of CLIC1-WT and CLIC1-S27P determined by fluorescence quenching of Trp35 by acrylamide.

***K*sv (M^{-1} urea)**			
	pH7 Native	**pH5.5 Native**	**Intermediate (3.8 M urea,pH5.5)**
CLIC1-WT	14.3 (± 0.49)	8.3 (± 0.41)	2.2 (± 0.7)
CLIC1-S27P	7.7 (± 0.47)	3.4 (± 0.28)	ND

The *K*sv values (M^{-1} urea) at pH7 and 5.5 of the native mutant and wild-type and intermediate species of the wild-type in the presence of 3.8 M are shown with the standard deviations in brackets.

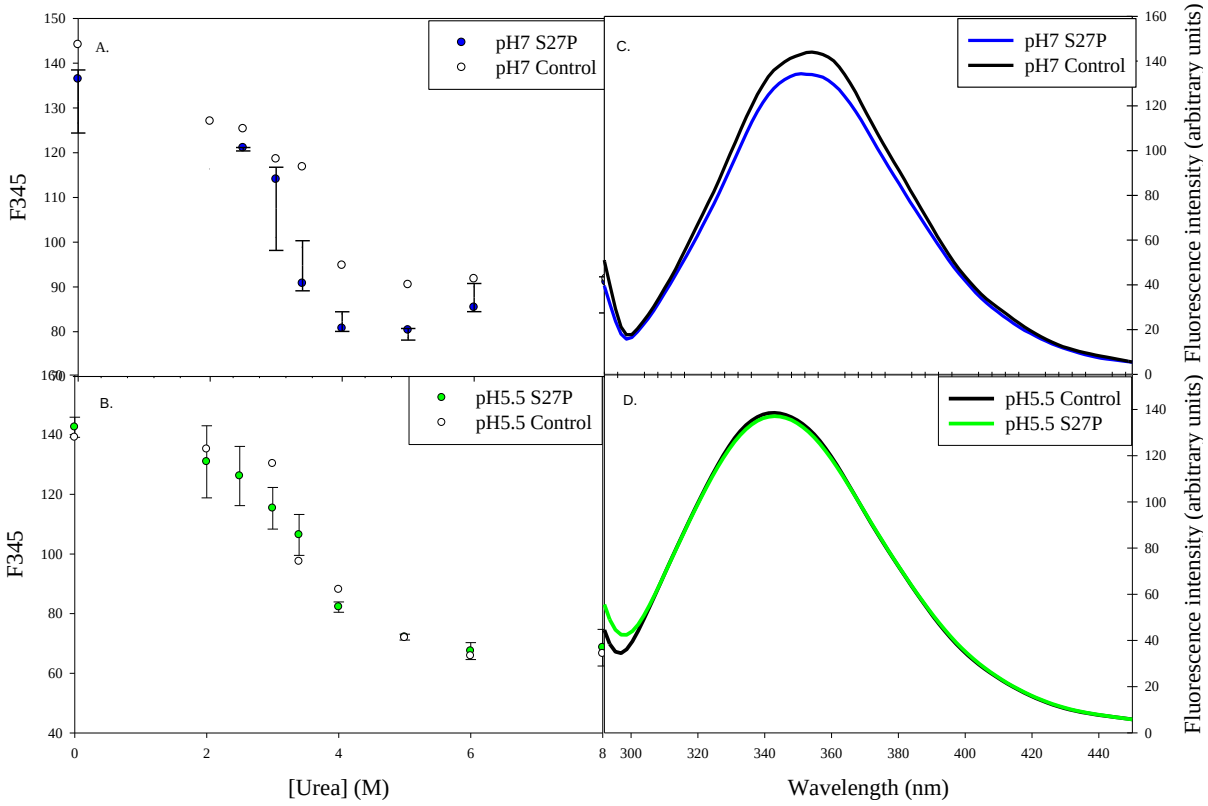

Figure 13: Reversibility of CLIC1-S27P unfolding.

CLIC1-S27P was in 50 mM phosphate buffer, pH7 with 0.02% NaN_3, 1 mM DTT or in 50 mM acetate buffer, pH5.5 with 0.02% NaN_3, 5 mM DTT. Fluorescence excitation was at 280 nm and emission was monitored at 345 nm.

A. Refolding curve of CLIC1-S27P at pH7. The refolding and the unfolding are indicated by (●) and (○), respectively.

B. Refolding curve of CLIC1-S27P at pH5.5. The refolding and the unfolding are indicated by (●) and (○), respectively.

C. Recovery of CLIC1-S27P fluorescence at pH7. The protein and the control are indicated by a blue line and a black line, respectively. The native structure is recovered 95% at 0.8 M urea concentration.

D. Recovery of CLIC1-S27P fluorescence at pH5.5. The protein and the control are indicated by a green line and a black line, respectively. The native structure is recovered 99% at 0.8 M urea concentration.

Far-UV circular dichroism and fluorescence were used as probes to monitor the urea-induced equilibrium unfolding of CLIC1-WT and CLIC1-S27P (Figure 14). The study was to monitor secondary (far-UV CD) and tertiary (fluorescence) structural alterations upon unfolding and as a result, the conformational stability of both the proteins.

The F310, F320, F345, IAEW and E222 plotted as a function of urea concentration were globally fitted by using Savuka 6.2.26 to obtain the stability parameters (Zitzewitz *et al*., 1995; Bilsel *et al*., 1999) (Figure 14). The reason why various wavelengths of the fluorescence data were chosen is that there is a difference in the unfolding transition between these specific wavelengths.

Both the fluorescence and CD-monitored transitions of CLIC1-WT are monophasic and superimposable at pH7 indicating the unfolding transitions to be highly cooperative (Figure 14, A). CLIC1-S27P also exhibits a two-state transition although the slope is far less steep compared to CLIC1-WT at pH7 (Figure 14, C and E). Furthermore, lower concentrations of urea are sufficient to initiate the denaturation of the mutant which may indicate the mutant being less stable than the wild-type at pH7. The curves measured using fluorescence and circular dichroism as probes are no longer superimposable at pH5.5 for both proteins. Both CLIC1-WT and CLIC1-S27P exhibit a biphasic transition at pH5.5 (Figure 14, D and F). This may be a result of a decrease in cooperative folding of both the wild-type and the mutant at pH5.5 compared to at pH7. Furthermore, the unfolding transitions of CLIC1-S27P are less cooperative as compared to CLIC1-WT at both pH7 and pH5.5.

Fluorescence intensities of binding of ANS to CLIC1-WT and CLIC1-S27P at 460 nm are shown (in the presence of 0 M to 8 M urea and 200 µM ANS) (Figure 14, G and H). At pH7, ANS does not bind to both the native and denatured wild-type (Figure 14, G). However, ANS binds to the native mutant with enhanced fluorescence intensity (by approximately 100 units) at pH7 (Figure 14, G).

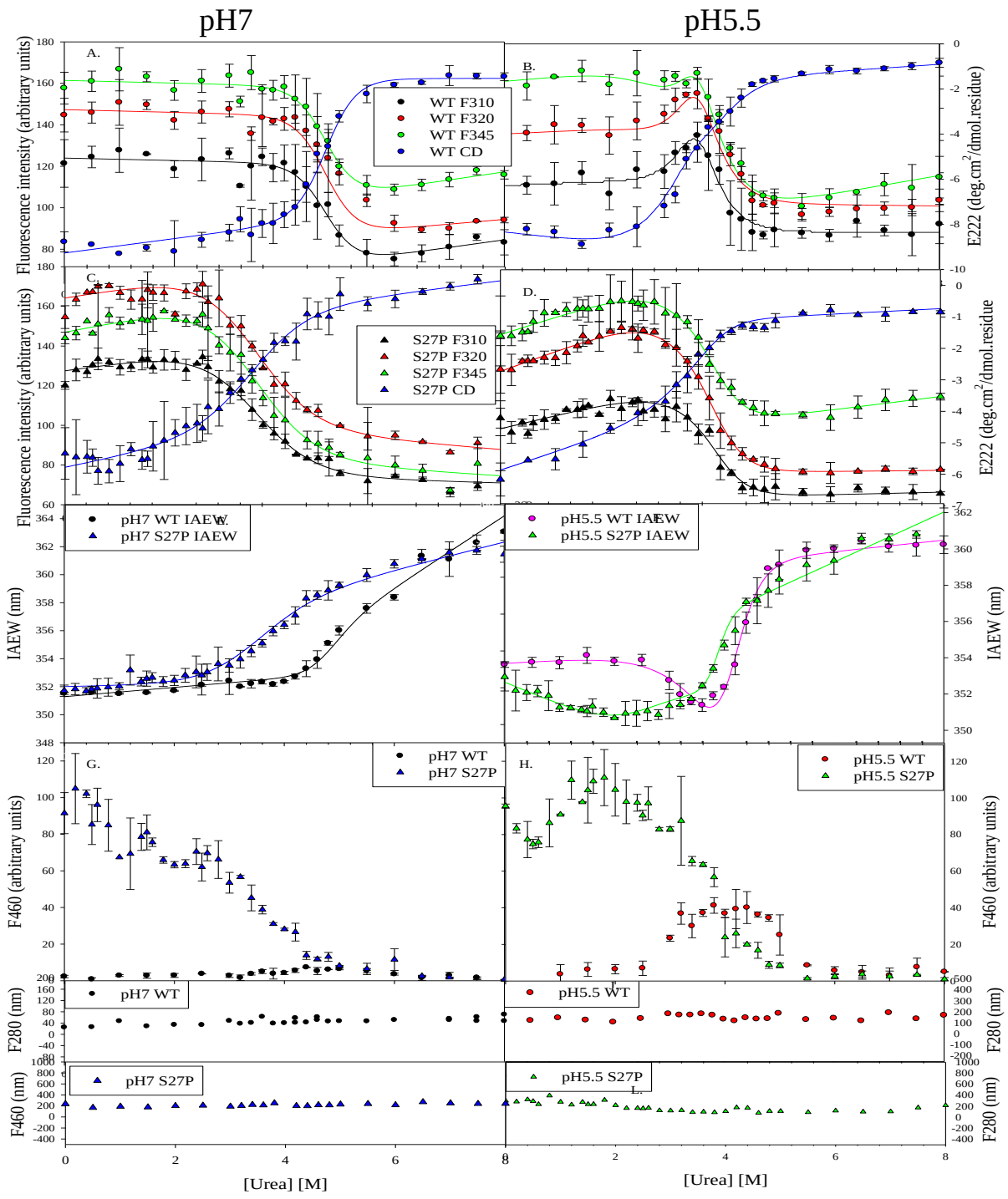

Figure 14: Comparison of equilibrium unfolding curves of CLIC1-WT and CLIC1-S27P at pH7 and 5.5.

A. B. Equilibrium unfolding curves of CLIC1-WT using the fluorescence intensities at F310 (●), F320 (●), F345 (●) and CD (●) ellipticity at E222 nm as probes at pH7 (A) and pH5.5 (B). The transition of the wild-type is monophasic at pH7 when monitored with both fluorescence and CD indicating a highly cooperative unfolding transition. However, it displays a biphasic transition between 3.2 and 3.8 M urea at pH5.5 that is indicative of an intermediate state at this region. The CD curve does not detect the intermediate state at pH5.5 showing a smooth transition.

C. D. Equilibrium unfolding curves of CLIC1-S27P using the fluorescence intensities at F310 (▲), F320 (▲), F345 (▲) and CD (▲) ellipticity at E222 nm as probes at pH7 (C) and pH5.5 (D). The transition is monophasic at both pH7 and pH5.5 although the slope is less steep as compared to CLIC1-WT under both conditions. The protein initiates unfolding at lower concentrations of urea (2 M urea) as compared to CLIC1-WT (3.2-4 M urea). There is no noticeable inflection which would be indicative of an intermediate state as is the case in CLIC1-WT.

E. F. Intensity averaged emission wavelength of CLIC1-WT and CLIC1-S27P fluorescence at pH7 (E) and pH5.5 (F). The transition is monophasic and sigmoidal for both the wild-type (●) and the mutant (▲) at pH7. The mutant, however, shows a less steep slope upon unfolding as compared to the wild-type. At pH5.5, the shift to shorter wavelength in CLIC1-WT (●) upon increasing urea concentrations (0 M-8 M) is indicative of an intermediate state. A similar shift is also observed in CLIC1-S27P (▲) at lower concentrations of urea and over a broader range of denaturant concentration than the wild-type (1.6 M-2.5 M).

G. H. Fluorescence intensities of binding of ANS (200 µM) to CLIC1-WT and CLIC1-S27P at 460 nm at pH7 (G) and pH5.5 (H). At pH7, CLIC1-S27P (▲) binds ANS in the native state and the presence of urea at a concentration range of 0 M to 4 M while CLIC1-WT (●) shows no binding. At pH5.5, CLIC1-WT (●) binds ANS in the presence of urea at

a range of 3 M to 4.5 M where the protein forms the intermediate species. CLIC1-S27P (▲) binds ANS in both the native state and the presence of urea concentrations of 0 M to 4.5 M.

I. J. The Raleigh scatter at 280 nm of CLIC1-WT is shown at pH7 (●) (I) and pH5.5 (●) (J). There is no aggregation observed along the entire transition at the both pH values.

K. L. The Raleigh scatter at 280 nm of CLIC1-S27P is shown at pH7 (▲) (K) and pH5.5 (▲) (L). There is no significant aggregation observed along the entire unfolding transition in the protein at both pH values.

The data were fitted to a two-state (N→U) model at pH7 and a three-state (N→I→U) monomer model at pH5.5 using Savuka (Zitzewitz *et al*., 1995; Bilsel *et al*., 1999) (Table 4) (also see Section 2.2.13). The goodness of fit for the models of both the proteins at pH7 and pH5.5 was 1. The thermodynamic parameters obtained from the curves clearly indicate that CLIC1 is destabilised by the mutation on the N-cap position with a ΔG (H_2O) value of approximately 4 kcal/mol at pH7 while CLIC1-WT is found to be 10 kcal/mol at pH7 (Table 4). At pH5.5, calculated $\Delta G1_{(H2O)}$ and $\Delta G2$ (H_2O) values of CLIC1-WT are found to be 4 and 13 kcal/mol, respectively. The calculated *m*-values which refer to the dependence of the free energy of unfolding on denaturant concentration, of both proteins are also shown (Table 4). The *m*-value of CLIC1-S27P is significantly decreased compared to CLIC1-WT at both pH7 and pH5.5. The transition mid-points (C_m values), point at which half of the population of the protein is unfolded, of CLIC1-WT and CLIC1-S27P were calculated using the global parameters. The C_m value at pH7 is reduced for the mutant compared to the wild-type. Similarly, the C_m of the first transition at pH5.5 is reduced for the mutant compared to the wild-type indicating a potential loss of stability of the native state of CLIC1-S27P at both pH values.

Table 4: Comparison of stability parameters obtained from the 2-state and 3-state fits of the equilibrium unfolding data of CLIC1-WT and CLIC1-S27P at pH7 and 5.5.

pH7 (two state monomer)		
Parameters	**CLIC1-WT**	**CLIC1-S27P**
Δ*G* (H_2O)(kcal/mol)	10 (±0.9)	3.7 (±0.3)
m (kcal/mol/M urea)	2 (±0.2)	1 (±0.1)
C_m (M urea)	5	3.7
Reduced χ^2	0.2	0.15
pH5.5 (three state monomer)		
Δ*G* 1 (H_2O) (kcal/mol)	3.7 (±0.3)	4.2 (±0.9)
*m*1 (kcal/mol/M urea)	0.7 (±0.4)	1.2 (±0.4)
C_m 1 (M urea)	3.4 (±0.1)	3.5
Δ*G2* (H_2O) (kcal/mol)	8.1 (±4.9)	7.3 (±1.8)
*m*2 (kcal/mol/M urea)	2.1 (±2.1)	1.8 (±0.4)
C_m 2 (M urea)	4.2 (±0.1)	4.0
Reduced χ^2	0.2	0.18

The $\Delta G_{(H_2O)}$ and *m*-values obtained by plotting F310, F320, F345, IAEW and E222 as a function of urea concentration and globally fitting the data to either two-state (pH7) or three-state (pH5.5) monomer models. The values in brackets represent the standard deviations obtained from the fits.

CHAPTER 4: DISCUSSION

Recently it was found that CLIC1 is comprised of an N- and C-capping box in the α1 helix that forms part of the transmembrane region (Nathaniel, PhD, 2007). The impact of N-capping boxes on the α-helices of specific proteins has been studied by several groups (Kim and Baldwin, 1990; Cochran *et al*., 2001; Zuhovsky, 1994; Dragani *et al*., 1997; Dirr *et al*., 2005). These studies suggest that the N-capping boxes contribute significantly to the stability of proteins. Although the N-capping box of the α1 helix is conserved throughout the CLIC family, the significance of the N-capping box of the α1 helix on the stability and the function of CLIC1 was unknown. The aim of this study was to examine the importance and contributions of the N-capping box, Ser27, to the structure and stability of the α1 helix, the putative transmembrane helix in CLIC1, using the engineered mutant CLIC1-S27P. In creating the mutant to explore the contribution of the N-capping box in the structure and stability of CLIC1, the introduction of a proline was favoured as its as it is a helix-breaker and its closed side chain would disrupt the α1 helix.

4.1. Structural components of native CLIC1-S27P

4.1.1. The global native structure of CLIC1-S27P is affected by the mutation

There are significant alterations in secondary and tertiary structure of CLIC1-S27P compared to CLIC1-WT (Section 3.4). According to the far-UV circular dichroism studies, CLIC1 is mainly alpha helical in structure (Figure 8). This is confirmed by the crystal structure of CLIC1 that reveals 10 α-helices and 4 β-strands (Figure 3) (Harrop *et al*., 2001). However, according to the far-UV circular dichroism spectra (Figure 8), changing serine to proline at the N-cap position of the α1 helix, contributes a loss of α-helical content to the protein as compared to that of the wild-type. There is also a difference in α-helical

structure at both pH7 and pH5.5 that is observed in both the wild-type and the mutant. The loss in ellipticity observed at pH5.5 compared to that at pH7 suggests the proteins have a less α-helical content at pH5.5 than at pH7 (Figure 8). The loss of α-helical content at pH5.5 has been explained in a recent study using hydrogen exchange mass spectrometry (Stoychev *et al*., 2009). The study suggested that at low pH the α1, α3 and α8 helices of CLIC1 take on a more flexible conformation. The reason for this is probably the neutralisation of acidic residues at the surface of the protein at the lower pH. This may break two interactions that are formed at pH7: the salt-bridge that is formed between Arg29 and Glu81 and the interaction between the α1 and α8 helices and could explain the reduction in helicity with lowered pH in the wild-type and a similar event is likely in the mutant as discussed in Section 4.1.2. In addition to this, the change in the secondary structure of the mutant compared to the wild-type could be affected by the breakage of the connection between the α1 helix and β1 strand of CLIC1 induced by the mutation as discussed in section 4.1.2.

In terms of tertiary structural alterations, the reduction in fluorescence intensity and the blue-shifted $\lambda_{em\ max}$ of the native mutant at pH5.5 as compared to the wild-type imply that the tryptophan (Trp35) of the mutant becomes more buried at pH5.5 compared to pH7 (Figure 9). The CLIC1-WT intermediate state also exhibits a more buried tryptophan compared to the native wild-type structure (Fanucchi *et al*., 2008). This can be explained as: First, it suggests that the mutant may take on an intermediate conformation at pH5.5 as is seen in the wild-type at that pH under mild denaturing conditions (Fanucchi *et al*., 2008). The second is that the mutant may exhibit an altered native state at pH5.5. This is because although the fluorescence studies do not show significant alterations in the structure, the native mutant shows structural alterations as its hydrophobic surface becomes exposed to the solvent and, thus, binds ANS at pH5.5.

The fluorescence intensity measurements in the presence of ANS of the wild-type and mutant used to detect the hydrophobic patches that are exposed to the solvent suggest

significant structural alterations induced by the mutation at the N-cap of the α1 helix (Figure 10). The native CLIC1-S27P, in the absence of urea, binds ANS at both pH7 and 5.5 indicating hydrophobic patches being exposed in the native conformation which are not detected in the native wild-type conformation (Figure 10). ANS binds to the native CLIC1-S27P relatively tightly with K_d values of 17.5 μM and 23.3 μM at pH7 and pH5.5, respectively, in the presence of 0 M urea, while the wild-type binds to ANS only at pH5.5 and under mild denaturing conditions (Figure 11). Therefore, the mutation significantly affects the position of the hydrophobic residues of the α1 helix and hence the tertiary structural properties of the protein, with greater exposure of the hydrophobic regions occurring. This may be a result of the loose packing of the helices and thus lack of packing interactions such as short-range Van der Waals interactions in the protein.

The environment of the single tryptophan, Trp35, was further investigated using acrylamide quenching as a probe (Section 3.4.3). As the *K*sv values calculated from the Stern-Volmer plots indicate, Trp35 in the native wild-type is found to be most solvent accessible at pH7 (14.3 M^{-1}) and at pH5.5 (8.3 M^{-1}) while the mutant displays a more buried tryptophan conformation at pH7 (7.7 M^{-1}) and at pH5.5 (3.4 M^{-1}) compared to the wild-type (Figure 12 and Table 3). This result is consistent with the fluorescence studies where the lone tryptophan of the mutant adopts a more buried conformation and is accompanied by a blue-shifted $\lambda_{em\ max}$ and a decrease in fluorescence intensity (Figure 9). The burial of the lone tryptophan is suggested to attribute to local structural alterations under mild denaturing conditions (McIntyre, 2007). Since the mutation was engineered in the vicinity of the single tryptophan (Trp35), any alterations at this point may affect the tryptophan causing to be buried or exposed to the solvent. Changing a polar amino acid, serine, with a hydrophobic amino acid, proline, may have caused breakage of interactions between this residue and other residues. Therefore, although the tryptophan is more buried, the overall helical structure shows a more exposed conformation. The latter is supported by ANS studies (Figure 10). Moreover, the effect of pH on the behaviour of CLIC1 has previously been mentioned. The protein shows a lower degree of secondary structure at pH5.5 and is

proposed to form an intermediate state under these conditions where the major structural alterations in the tertiary structure take place in the α1 helix (Fanucchi *et al*, 2008; Littler *et al*., 2010). The mutant displays similar characteristics to the wild-type with exhibiting intermediate species under mild denaturing conditions at pH5.5 and thus this may affect the location of tryptophan as taking on a more buried conformation at pH5.5.

4.1.2. The helical interactions are affected by the mutation

The α1 helix is composed of two polar, two basic and nine hydrophobic amino acid residues. The impact of the mutation at the N-capping box in terms of interactions between the residues forming the α1 helix has been examined (Figure 15). The analysis shows that each of the amino acid residues interacts with the others by means of hydrogen bonding according to the n-(n+4) formula that describes a classical α-helix and is observed with all the amino acids in the α1 helix of CLIC1 (Figure 15). Moreover, these amino acid residues also form backbone hydrogen bonds with the residues located three residues downstream formulated as n-(n+3) in the α1 helix. The backbone amide and carbonyl group of the N-cap residue, Ser27, interacts with Cys24 by means of hydrogen bonding (Figure 16). This type of interaction between the n-(n+3) corresponds to the N-cap motif (Richardson, Richardson, 1988) although the hydroxyl group of serine is not directly active in interactions with residues in the helix as is the case with most of the serine N-capped proteins (Doig *et al*., 1997).

The residue does, however, form hydrogen bonds with two water molecules nearby. This stabilising interaction has been shown to occur with some N-cap residues (Doig *et al*., 1997). In the case of the mutant, S27P, the hydrogen bond formation of Ser27 with the two water molecules (H_2O355 and H_2O356) is disrupted when the serine is mutated to a proline (Figure 15). These interactions with water molecules also function as a bridge between the α1 helix and β1 strand where Lys13 forms hydrogen bonds with these water molecules when serine is at the N-cap position. This bridge is, therefore, broken by the mutation.

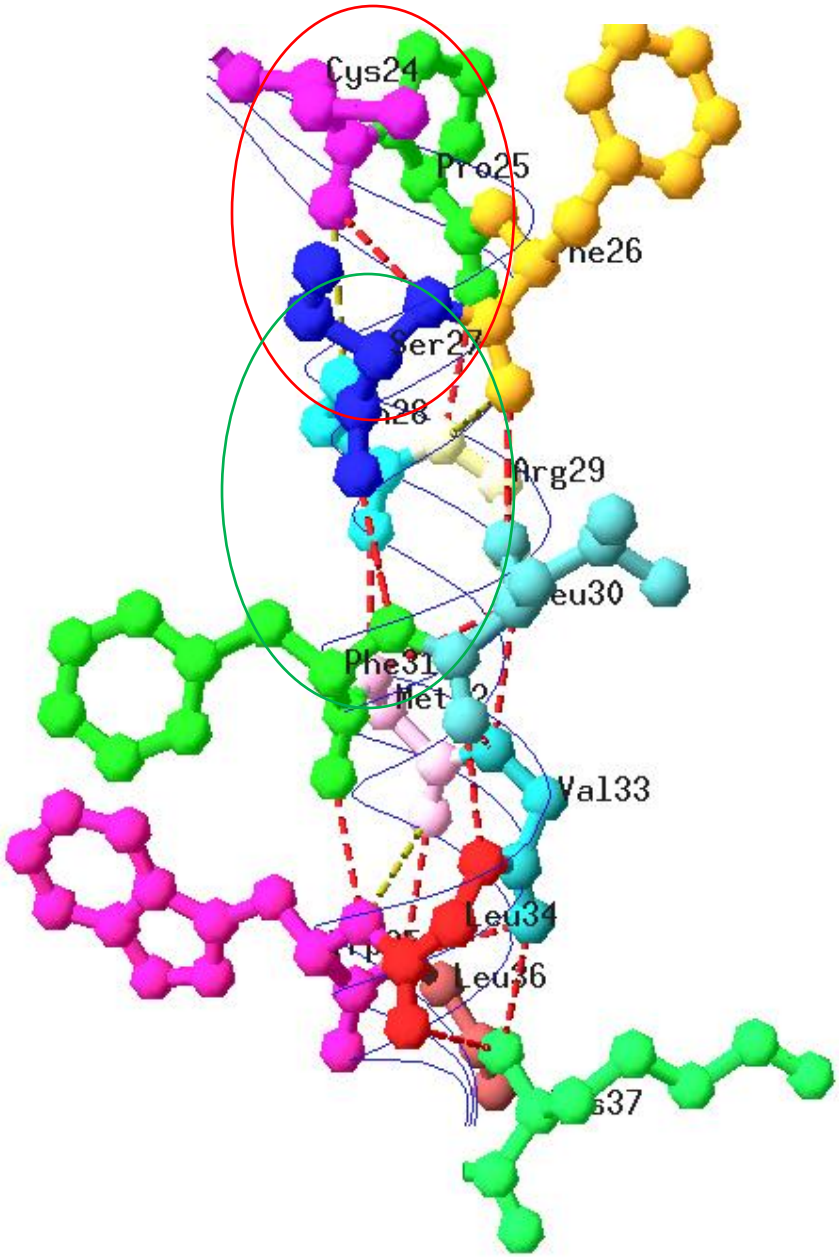

Figure 15: The hydrogen bond formation of the α1 helix of CLIC1. Red and yellow dashed lines indicate the strong and weak hydrogen bond formations between the backbone residues, respectively. The backbone hydrogen bonds formed between Ser27-Cys24 and Ser27-Phe31 are indicated in red and green circles, respectively. The Figure was generated using Swiss PDB Viewer (Guex and Peitsch, 1997). The PDB code is 1k0m (Harrop *et al.*, 2001) for CLIC1.

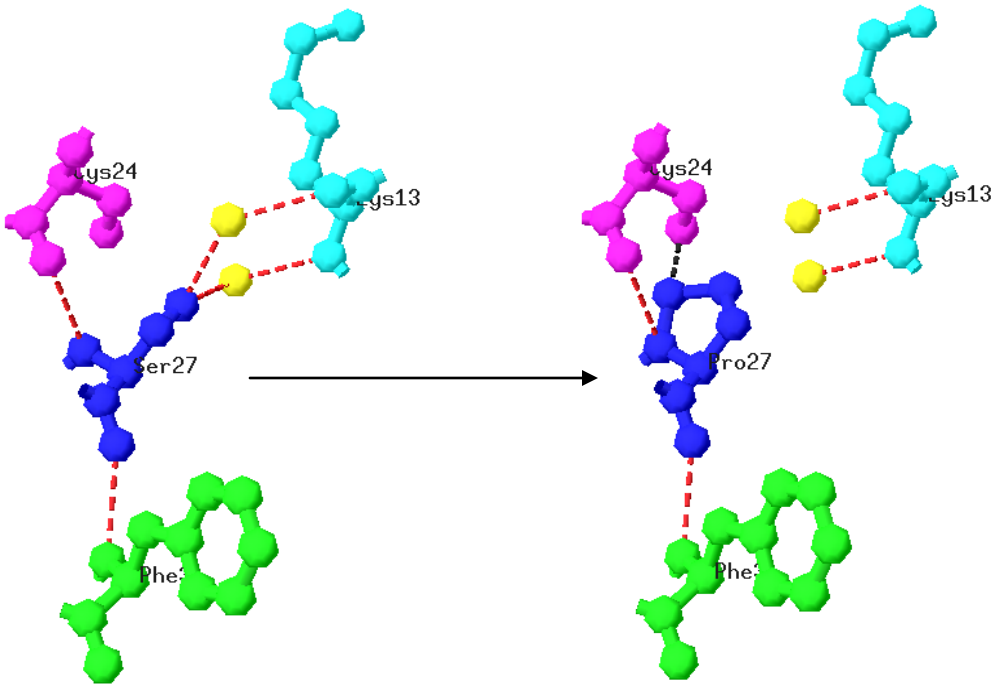

Figure 16: The hydrogen bond formation of the N-capping box (Ser27) of the α1 helix in CLIC1-WT and CLIC1-S27P. Ser27 and Pro27 are indicated in blue. Cys24 and Phe31 are shown in pink and green, respectively. Lys13 is shown in cyan. Both Ser27 and Pro27 form backbone hydrogen bonds with Cys24 and Phe31 as shown in the illustration. The hydrogen bond formations between the Ser27 side chain and water molecules (yellow spheres) are also shown. These are not present when proline is at the N-cap position. There is also a clash (black dashed lines) observed between the proline and the cysteine residues which implies structural alterations in the mutant. The Figure was generated using Swiss PDB Viewer (Guex and Peitsch, 1997). The PDB code is 1k0m (Harrop *et al.,* 2001) for CLIC1.

Moreover, both rotamers of Pro27 form a clash with Cys24, caused by the steric hindrance of the proline side chain and possibly causing the proline in this position to break the helix (Figure 16). This may attribute more flexibility to the α1 helix and thus to the protein, contributing to a less compact and less stable structure.

It is clear that even though hydrophobic interactions have a fundamental role in stabilising proteins, hydrogen bonding should also be satisfied in order to provide stability to the protein and may overcome the hydrophobic effect (discussed in Gilis and Rosman, 1996) as may be the case with the mutant. Furthermore, Ser27 was found to be one of the hot spots found in the domain interface of CLICs (Stoychev, PhD, 2008). This residue is proposed to have fundamental roles in the structure and have interactions with other conserved residues in the interior part of the CLICs as seen in CLIC1.

Serine itself is a prominent amino acid residue in many transmembrane proteins. Serine motifs are found to be common in twelve transmembrane segments searched in the SWISS-PROT database (Dawson *et al*., 2002) and this residue has been found to exist predominantly on the lipid-exposed surface of membrane proteins (Gratkowski *et al*., 2001). Serines are also proposed to give membrane proteins their self interacting property (Senes *et al*., 2000). Therefore, even though further studies are required to discover the contributions of this single residue to the membrane function of the CLIC proteins, there is no doubt that a number of serines have had a fundamental role in stabilising the interactions in transmembrane helices (Kolbe *et al*., 2000).

The helical propensities of CLIC1-WT and CLIC1-S27P were obtained using AGADIR (Munoz and Serrano, 1994; 1997) showing that serine at the N-cap position of the α1 helix contributes 5.55% to the α1 helix propensity while this value is 3.27% when proline is at the N-cap position. This finding is confirmed by the circular dichroism data where the α-helical content decreases in the mutant at both pH7 and pH5.5 (Figure 9).

Similar results have been suggested in previous studies done elsewhere (Lattman and Rose, 1993; Zuhovsky *et al*., 1994). Thus, helix capping interactions of the α1 helix of CLIC1 are significant properties providing the α1 helix with its helical propensity. Overall, there were significant alterations induced by the mutation in terms of secondary structure with loss of helical components and tertiary structure with a buried tryptophan along with more exposed hydrophobic surfaces. Moreover, the breakage of interactions in the α1 helix and a decrease in helix propensity also arose from the mutation, although these speculations need to be proved in future by solving the crystal structure of this mutant.

4.2. Changes in the stability and unfolding of CLIC1 induced by S27P mutation

The concept by which the N-capping boxes stabilise proteins is supported by this study where CLIC1 is destabilised by the N-cap mutation. A similar result was observed in a mutant generated by changing the N-cap of the α9 helix, D209G, of GST alpha (Dirr *et al*., 2005). Here the results suggested that the N-cap motif of the α9 helix is important in the folding and the stabilisation of GST alpha although the mutation did not alter the secondary and tertiary structure of the protein. CLIC1-S27P shows 37% decrease in the free energy of unfolding and 50% decrease in the *m*-value compared to CLIC1-WT at pH7 (Table 4). Trp35 may be quenched by other residues that result in burial of this residue, and hence it is not accessible to the solvent. The increase in *m*-value with a decrease in pH is generally correlated with an increase in the solvent accessible surface area (SASA) of the denatured state (Whitten *et al*., 2001). The decrease in the *m*-value of the mutant at pH7 refers to a significant decrease in SASA upon unfolding and the stabilisation of less compact states of the protein. This is consistent with the fluorescence and CD-monitored results. The increase in the *m*-value of the mutant in the transition of N→I at pH5.5 as compared to the wild-type may refer to a more compact intermediate state of the mutant. In addition, the drop in the C_m value in the mutant implies that lower concentrations of urea are sufficient to initiate the denaturation of the mutant suggesting a loss of the tertiary compactness of the protein

(Table 4). Therefore, the mutation causes a reduction in the compactness of the native state or an increase in the compactness of the denatured state compared to the wild-type. Thus, the composition of the ensemble of proteins in solution available at equilibrium has altered. A three-state transition is observed in both the proteins at pH5.5 with a highly populated intermediate species for each (Figure 14) (Zitzewitz *et al*., 1995; Bilsel *et al*., 1999). The ΔG value of the N↔I transition is lower (4.2 kcal/mol) than the I↔U transition (7.3 kcal/mol) suggesting that the intermediate is stabilised by the mutation. A stabilised intermediate species is also observed in the wild-type at pH5.5 (Table 4).

4.3. Conclusion

The main focus of this project has been to study the significance of the N-capping box of the α1 helix on the structure and stability of CLIC1 through a mutation at the N-cap. Both the wild-type and the mutant proteins have been investigated in terms of their secondary and tertiary structure and thermodynamic stability at pH7 and pH5.5.

It has been found that a single mutation at the N-cap position of the α1 helix has significantly affected the secondary and tertiary structure of CLIC1. Firstly, the mutant was found to become less helical. Moreover, the helical propensity of the α1 helix is significantly dropped when mutated at the N-cap which contributes a less compact helical structure to the protein. Secondly, the tertiary structure of the protein was altered by the burial of the lone tryptophan and exposure of hydrophobic regions. Thirdly, the interactions between Ser27 and two water molecules and hence the bridge between the α1 helix and β1 strand was broken as a result of the mutation. Finally, the equilibrium unfolding study has shown that the protein is significantly destabilised by the N-cap mutation although the mutant exhibits a stabilised intermediate species similar to the wild-type at pH5.5.

Serine is a significant amino acid in transmembrane proteins as it is often found in the transmembrane region (Ballesteros *et al*., 2000; Dawson *et al*., 2002; Gratkowski *et al*, 2001; Senes *et al.,* 2001) where it is implicated in oligomerisation prior to membrane

insertion (Dawson *et al*., 2002). The work presented in this dissertation gives significant information about the contributions of Ser27 at the N-cap position of the α1 helix to the structure and the stability of CLIC1. Its contributions to the function of CLIC1 in the presence of membranes can be elucidated further by functional studies.

References

Adler, V., Yin, Z., Fuchs, S., Benezra, M., Rosario, L., Tew, K. D., Pincus, M. R., Sardana, M., Henderson, C. J., Wolf, C. R., Davis, R. J., and Ronai, Z. (1999) Regulation of JNK signaling by GSTp. *EMBO J.* **18,** 1321-1334.

Al-Awqati, Q. (1995) Chloride channels of intracellular organelles. *Curr. Opin. Cell Biol*. **7,** 504-508.

Allured, V.S., Collier, R.J., Carroll, S.F., and McKay, D.B. (1986) Structure of exotoxin A of *Pseudomonas aeruginosa* at 3.0 Å resolution. *Proc. Natl. Acad. Sci.USA* **83,** 1310**–**1324.

Alves, C. S., Kuhnert, D. C., Sayed, Y., and Dirr, H. W. (2006) The intersubunit lock-and-key motif in human glutathione transferase A1-1: role of the key residues Met51 and Phe52 in function and dimer stability. *Biochem.* **393,** 523-528.

Åqvist, J., Luecke, H., Quiocho, F. A., and Warshel, A. (1991) Dipoles localized at helix termini of proteins stabilize charges. *Proc. Natl. Acad. Sci.* **88,** 2026-2030.

Arkin, I. T., and Brunger, A. T. (1998) Statistical analysis of predicted transmembrane alpha-helices. *Biochim. Biophys. Acta*. **1429,** 113-128.

Armstrong, K. M., Fairman, R., and Baldwin, R. L. (1994) The (i, i+4) Phe-His interaction studied in an alanine-based α-helix. *J. Mol. Biol.* **230,** 284-291.

Armstrong, R. N. (1997) Structure, catalytic mechanism and evolution of the glutathione transferases. *Chem. Res. Toxicol*. **10,** 2-18.

Ashley, R. H. (2003) Challenging accepted ion channel biology: p64 and the CLIC family of putative intracellular anion channel protein. *Mol. Membr. Biol*. **20,** 1-11.

Atkins, W. M., Wang, R. W., Bird, A. W., Newton, D. J., and Lu, A. Y. H. (1993) The catalytic mechanism of glutathione S-transferase (GST). Spectroscopic determination of the pKa of tyrosine-9 in rat α1-1 GST. *J. Biol. Chem*. **268,** 19118-19191.

Aurora, R., Srinivasan, R., and Rose, G. D. (1994) Rules for α-helix termination by glycine. *Science* **264,** 1126-1129.

Awasthi, Y. C., and Singh, S. V. (1985) Subunit structure of human and rat glutathione S-transferases. *Comp. Biochem. Physiol*. **82B,** 17-23.

Baldwin, R. L. (2003) In search of the energetic role of peptide hydrogen bonds. *J. Biol. Chem*. **278,** 17581-17588.

Ballard, J., Crabtree, J., Roe, B. A., and Tweten, R. K. (1995) The primary structure of *Clostridium septicum* alpha-toxin exhibits similarity with that of *Aeromonas hydrophila* aerolysin. *Infect. Immun*. **63,** 340–344.

Ballesteros, J. A., Deupi, X., Olivella, M., Haaksma, E. E., and Pardo, L. (2000) Serine and threonine residues bend alpha-helices in the chi (1)=g(-) conformation. *Biophys. J*. **79,** 2754-2760.

Barelli, S., Canellini, G., Thadikkaran, L., Crettaz, D., Quadroni, M., Rossier, J. S., Tissot, J. D., and Lion, N. (2008) Oxidation of proteins:Basic principles and perspectives for blood proteomics. *Proteomics Clin. Appl*. **2,** 142-157.

Barlow, D. J., and Thornton, J. M. (1983) Ion-pairs in proteins. *J. Mol. Biol*. **169,** 867-885.

Barrick, D., and Baldwin, R. L. (1993a) The molten globule intermediate of apomyoglobin and the process of protein folding. *Protein Sci.* **2,** 869-876.

Barrick, D., and Baldwin, R. L. (1993b) Three-state analysis of sperm whale apomyoglobin folding. *Biochem.* **32,** 3790-3796.

Baskakov, I. V., and Bolen, D. W. (1998) Monitoring the sizes of denatured ensembles of staphylococcal nuclease proteins: implications involving *m*-values, intermediates and thermodynamics. *Biochem.* **37,** 18010-18017.

Bechinger, B. (1996) Towards membrane protein design: pH-sensitive topology of histidine-containing polypeptides. *J. Mol. Biol*. **263,** 768-775.

Bell, J. A., Becktel, W. J., Sauer, U., Baase, W. A., and Matthews, B. W. (1992) Dissection of helix capping in T4 Lysozyme by structural and thermodynamical analysis of six amino acids substitutions at Thr59. *Biochem.* **31,** 3590-3596.

Bell, C. E., Poon, P. H., Schumaker, V. N., and Eisenberg, D. (1997) Oligomerisation of a 45 kilodalton fragment of diphtheria toxin at pH5 to a molecule of 20-24 subunits. *Biochem.* **36,** 15201-15207.

Bernstein, F. C., Koetzle, T. F., Williams, G. J., Meyer, E. F. Jr., Brice, M. D., Rodgers, J. R., Kennard, O., Shimanouchi, T., and Tasumi, M. (1977) The Protein Data Bank: a computer-based archival file for macromolecular structures. *J. Mol. Biol*. **112 (3),** 535-542.

Berry, K. L., and Hobert, O. A. (2006) Mapping functional domains of chloride intracellular channel (CLIC) proteins in vivo. *J. Mol. Biol.* **359,** 1316–1333.

Berry, K. L., Bulow, H. E., Hall, D. H., and Hobert, O. A. (2003) A *C. elegans* CLIC-like protein required for intracellular tube formation and maintenance. *Science.* **302,** 2134–2137.

Berry, K. L., and Hobert, O. (2006) Mapping functional domains of chloride intracellular channel (CLIC) proteins in vivo. *J. Mol. Biol.* **359,** 1316-1333.

Berryman, M., and Bretscher, A. (2000). Identification of a novel member of the chloride intracellular channel gene family (CLIC5) that associates with the actin cytoskeleton of placental microvilli. *Mol. Biol. Cell.* **11,** 1509-1521.

Bhuyan, A. K., and Udgaonkar, J. B. (1998) Multiple kinetic intermediates accumulate during the unfolding of horse cytochrome c in the oxidised state. *Biochem.* **37,** 9147-9155.

Bilsel, O., Zitzewitz, J. A., Bowers, K. E., and Matthews, C. R. (1999) Folding mechanism of the R-subunit of tryptophan synthase, an α/β barrel protein: Global analysis highlights the interconversion of multiple native, intermediate and unfolded forms through parallel channels. *Biochem.* **38(3),** 1018–1029.

Birnboim, H. C., and Doly, J. (1979) A rapid alkaline extraction procedure for screening recombinant plasmid DNA. *Nucleic Acids Res*. **7,** 1513-1523.

Blagdon, D. E., and Goodman, M. (1975) Mechanism of proteins and polypeptide helix initiation. *Biopolymers*. **14,** 241-245.

Blanco, S., Figliola, A., Quiroga, R. Q., Rosso, O. A., and Serrano, E. (1998) Time-frequency analysis of electroencephalogram series. III. Wavelet packets and information cost function. *Phys. Rev. E*. **57,** 932-940.

Bortoleto, R. K., and Ward, R. J. (1999) A stability transition at mildly acidic pH in the alpha-hemolysin (alpha toxin) from *Staphylococcus aureus*. *FEBS Lett.* **459,** 438-442.

Bosshard, H. R., Marti, D. N., and Jelesarov, I. (2004) Protein stabilization by salt bridges: concepts, experimental approaches and clarification of some misunderstandings. *J. Mol. Recognit*. **17,** 1–16.

Brady, G. P., and Sharp, K. A. (1997) Entropy in protein folding and in protein-protein interactions, *Curr. Opin. Struct. Biol.* **7,** 215–221.

Bowie, J. U. (2005) Solving the membrane protein folding problem. *Nature* **438,** 581-589.

Burn, P. (1988) Talking point Amphitropic proteins: a new class of membrane proteins. *Tr. Biochem.Sci.* **13,** 79-83.

Campbell, T. J., Breit, S. N., and Curmi, P. M. G. (2001) Crystal structure of a soluble form of the intracellular chloride ion channel CLIC1 (NCC27) at 1.4 Å resolution. *J. Biol. Chem.* **276,** 44993–45000.

Carra, J. H., Anderson, E. A., and Privalov, P. L. (1994) Three-state thermodynamic analysis of the denaturation of staphylococcal nuclease mutants. *Biochem.* **33,** 10842-10850.

Cartailler, J.P., Haigler, H.T., and Luecke, H. (2000) Annexin XII E105K crystal structure: identification of a pH-dependent switch for mutant hexamerization. *Biochem.* **39,** 2475-83.

Chakrabartty, A., Kortemme, T., Padmanabhan, S., and Baldwin, R. L. (1993) Aromatic side-chain contribution to far-ultraviolet circular dichroism of helical peptides and its effect on measurement of helix propensities. *Biochem.* **32,** 5560-5562.

Chakrabarty, S., Bhinge, A., and Varadarajan, R. (2002) A procedure for detection and quantitation of cavity volumes in proteins. *J. Biol. Chem*. **277,** 31345-31353.

Chalothorn, D., Zhang, H., Smith, J. E., Edwards, J. C., and Faber, J. E. (2009) Chloride intracellular channel-4 is a determinant of native collateral formation in skeletal muscle and brain. *Circ Res*. **105(1),** 89-98.

Chan, H. S., and Dill, K. A. (1990) Origins of structure in globular proteins. *Proc. Natl. Acad. Sci*. **87(16),** 6388–6392

Chasseaud, L. F. (1979) The role of glutathione and glutathione S- transferases. *Adv. Cancer Res*. **29,** 175-274.

Chen, J., and Stites, W. E. (2001) Packing Is a Key Selection Factor in the Evolution of Protein Hydrophobic Cores. *Biochem.* **40,** 15280-15289.

Chenal, A., Savarin, P., Nizard, P., Guillain, F., Gillet, D., and Forge, V. (2002) Membrane protein insertion regulated by bringing electrostatic and hydrophobic interactions into play: A case study with the translocation domain of the diphtheria toxin. *J. Mol.Biol*. **277,** 43425-43432.

Chiti, F., Calamai, M., Taddei, N., Stefani, M., Ramponi, G., and Dobson, C. M. (2002) Studies of the aggregation of mutant proteins in vitro provide insights into the genetics of amyloid diseases. *PNAS* **99,** 16419-16426.

Choe, S., Bennett, M. J., Fujii, G., Curmi, P. M., Kantardjieff, K. A., Collier, R. J., and Eisenberg, D. (1992) The crystal structure of diphtheria toxin. *Nature* **357,** 216-222.

Chou, P. Y., and Fasman, G. D. (1978) Empirical predictions of protein conformation. *Annu. Rev. Biochem.* **47,** 251-276.

Chuang, J. Z., Milner, T. A., Zhu, M., and Sung, C. H. (1999). A 29 kDa intracellular chloride channel p64h1 is associated with large dense-core vesicles in rat hippocampal neurons. *J. Neurosci*. **19,** 2919-2928.

Cochran, D. A., Penel, S., and Doig, A. J. (2001) Effect of the N1 residue on the stability of the alpha-helix for all 20 amino acids. *Protein Sci*. **10,** 1305-1311.

Codreanu, S. G., Thompson, L. C., Hachey, D. L., Dirr, H. W., and Armstrong, R. N. (2005) Influence of the dimer interface on Glutathione Transferase structure and dynamics revealed by amide H/D exchange mass spectrometry. *Biochem.* **44,** 10605-10612.

Collier, H. B. (1973). Letter: A note on the molar absorptivity of reduced Ellman's reagent, 3-carboxylato-4-nitrothiophenolate. *Anal. Biochem.* **56,** 310-311.

Cromer, B.A., Morton, C. J., Board, P. G., and Parker, M. (2002) From glutathione transferase to pore in a CLIC. *Eur. Biophys. J.* **31,** 356-364.

Cromer, B.A., Gorman, M.A., Hansen, G., Adams, J.J., Coggan, M., Littler, D.R., Brown, L.J., Mazzanti, M., Breit, S.N., Curmi, P.M.G., Dulhunty, A.F., Board, P.G., and Parker, M.W. (2007) Structure of the Janus protein human CLIC2. *J.Mol. Biol.* **374,** 719–731.

Dasgupta, S., and Bell, J. A. (1993) Design of helix ends: Amino acid preferences, hydrogen bonding and electrostatic interactions. *Int. J. Pept. Protein Res*. **41,** 499-511.

Dawson, J. P., Weinger, J. S., and Engelman, D. M. (2002) Motifs of Serine and Threonine can Drive Association of Transmembrane Helices. *J. Mol. Biol*. **316,** 799-805.

Dawson, J. P., Melnyk, R. A., Deber, C. M., and Engelman, D. M. (2003) Sequence context strongly modulates association of polar residues in transmembrane helices. *J. Mol. Biol*. **331,** 255-262.

Dean, P. D. G., Johnson, W. S., and Middle, F. A. (1985) (Eds.), *Affinity Chromatography. A practical approach*, IRL Press.

Dill, K. A. (1990) Dominant forces in protein folding. *Biochem.* **29,** 7133-7155.

Dirr, H. W., Reinemer, P., and Huber, R. (1994) X-ray crystal structures of cytosolic glutathione S-transferases. Implications for protein architecture, substrate recognition and catalytic function. *Eur. J. Biochem*. **220,** 645-661.

Dirr, H. W., Tessa, L., Kuhnert, D. C., and Sayed, Y. (2005) A conserved N-capping motif contributes significantly to the stabilization and dynamics of the C-terminal region of class Alpha Glutathione S-Transferases. *J.Biol.Chem*. **280,** 19480-19487.

Doig, A. J., Chakrabartty, A., Klinger, T. M., and Baldwin, R. L. (1994) Determination of the free energies of N-capping in a-helices by modification of the Lifson-Roig helix-coil theory to include N- and C-capping. *Biochem.* **33,** 339-3403.

Donovan, J. J., Simon, M. I., and Montal, M. (1992) Insertion of diphtheria toxin into and across membranes: role of phosphoinositide asymmetry. *Nature* **298 (5875),** 669-672.

Dougherty, D. (1996) Cation-pi interactions in chemistry and biology: a new view of Benzene, Phe, Tyr and Trp. *Science* **271,** 163-168.

Dragani, B., Stenberg, G., Melino, S., Petruzzelli, R., Mannervik, B., and Aceto, A. (1997) Conserved N-capping box in the hydrophobic core of Glutathione *S*-Transferase P1–1 is essential for refolding. *J. Biol. Chem*. **272,** 25518–25523.

Dulhunty, A., Gage, P., Curtis, S., Chelvanayagam, G., and Board, P. (2000) The glutathione transferase structural family includes a nuclear chloride channel and a ryanodine receptor calcium release channel modulator. *J. Biol. Chem*. **276,** 3319-3323.

Dulhunty, A., Gage, P., Curtis, S., Chelvanayagam, G. and Board, P. (2001) The glutathione transferase structural family includes a nuclear chloride channel and a ryanodine receptor calcium release channel modulator. *J. Biol. Chem*. **276,** 3319-3323.

Duncan, R. R., Westwood, P. K., Boyd, A., and Ashley, R. H. (1997) Rat brain p64H1, expression of a new member of the p64 chloride channel protein family in endoplasmic reticulum. *J. Biol Chem*. **272(19),** 12575–12582.

Dunker, A. K., and Rueckert, R. R. (1969) Observations on molecular weight determinations on polyacrylamide gel. *J. Biol. Chem.* **244,** 5074-5080.

Edwards, J. C. (1999). A novel p64-related Cl^- channel: subcellular distribution and nephron segment-specific expression. *Am. J. Physiol*. **276,** F398-F408.

Edwards, J. C. (2000) A novel p64-related Cl- channel: subcellular distribution and nephron segment-specific expression. *Am. J. Physiol.* **276,** F398-F408.

Eftink, M. R., and Ghiron, C. A. (1975) Dynamics of a protein matrix revealed by fluorescence quenching. *Proc. Natl. Acad. Sci*. **72,** 3290-3294.

Elmasry, N. F., and Fersht, A. R. (1994) Mutational analysis of the N-capping box of the alpha-helix of chymotrypsin inhibitor-2. *Protein Eng.* **7,** 777-782.

Ellman, G. L. (1959) Tissue sulfhydryl groups. *Arch. Biochem. Biophys.* **82 (1),** 70–77.

Engelhard, M., and Evans, P. A. (1995) Kinetics of interaction of partially folded proteins with a hydrophobic dye: evidence that molten globule character is maximal in early folding intermediates. *Prot. Science*. **4(8),** 1553–1562.

Engelman, D. M., Steitz, T. A., and A. Goldman (1986) Identifying nonpolar transbilayer helices in amino acid sequences of membrane proteins. *Annu. Rev. Biophys. Biophys. Chem.* **15,** 321-353

Ericksson, A. E., Baase, W. A., Wozniak, J. A., and Matthews, B. W. (1992) A cavity-containing mutant of T4 lysozyme is stabilised by buried benzene. *Nature* **355,** 371-373.

Fanucchi, S., Adamson, R., and Dirr, H. W. (2008) Formation of an Unfolding Intermediate State of Soluble Chloride Intracellular Channel Protein CLIC1 at acidic pH. *Biochem.* **47 (44),** 11674–11681.

Fauchere, J. L., and Pliska, V. E. (1983) Amino acid hydrophobicity scale. *Eur. J. Med. Chem*. **18,** 369-375.

Fernandez-Salas, E., Sagar, M., Cheng, C., Yuspa, S.H., and Weinberg, W. C. (1999) P53 and tumor necrosis factor alpha regulate the expression of a mitochondrial chloride channel protein. *J. Biol. Chem*. **274,** 36488–36497.

Fernandez-Salas, E., Suh, K. S., Speransky, V. V., Bowers, W. L., Levy, J. M., Adams, T., Pathak, K. R. Edwards, L. E., Hayes, D. D. , Cheng, C., Steven, A. C., Weinberg, W. C., and Yuspa, S.H. (2002) mtCLIC/CLIC4, an Organellular Chloride Channel Protein, Is Increased by DNA Damage and Participates in the Apoptotic Response to p53. *Mol. Cell. Biol*. **22,** 3610-3620.

Fersht, A. R. (1984). Basis of biological specificity. *Trends Biochem. Science* **9,** 145-147.

Fersht, A. R. (1987) The hydrogen-bond in molecular recognition. *Trends Biochem. Science* **12,** 301-304.

Finger, C., Volkmer, T., Prodohl, A., Otzen, D. E., Engelman, D. M., and Schneider, D. (2006) The stability of transmembrane helix interactions measured in a biological membrane. *J. Mol. Biol*. **358,** 1221-1228.

Fleishman, S. J., and Ben-Tal, N. (2002) A novel scoring function for predicting the conformations of tightly packed pairs of transmembrane alpha-helices. *J. Mol. Biol*. **321,** 363-378.

Forood, B., Feliciano, E. J., and Nambiar, K. P. (1993): Stabilization of α-helical structures in short peptides via end capping. *Proc. Natl. Acad. Sci.* **90,** 838-842.

Fujiwara, Arai, M., Shimizu, A., Ikeguchi, M., Kuwajima, K., and Sugai, S. (1999) Folding-unfolding equilibrium and kinetics of equine b-lactoglobulin: equivalence between the equilibrium molten globule state and a burst-phase folding intermediate. *Biochem.* **38,** 4455-4463.

García-Sáez, A. J., Mingarro, I., Pérez-Payá, E., and Salgado, J. (2004) Membrane-insertion fragments of Bcl-xL, Bax and Bid. *Biochem.* **43,** 10930-10943.

Geny, B., and Popoff, M. R. (2006) Bacterial protein toxins and lipids: pore formation or toxin entry into cells. *Biol Cell*. **98(11),** 667-78.

Gerke, V. and Moss, S.E. (2002) Annexins: From Structure to Function. *Physiol.Rev.***82,** 331-371.

Gildenhuys, S., Wallace, L. A., and Dirr, H. W. (2009) Stability and Unfolding of Reduced Escherichia coli Glutaredoxin 2 : A Monomeric Structural Homologue of the Glutathione Transferase Family. *Biochem.* **47 (40),** 10801-10808.

Gilis, D., and Rosman, M. (1996) Stability changes upon mutation of solvent-accessible residues in proteins evaluated by database-derived potentials. *J. Mol. Biol*. **257,** 1112-1126.

Goodchild, S. C., Howell, M. W., Cordina, N. M., Dene, R. L., Breit, S. N., Curmi, P. M. G., and Brown, L. J. (2009) Oxidation promotes insertion of the CLIC1 chloride intracellular channel into the membrane. *Eur. Biophys. J.* **39,** 129-138.

Goodchild, S. C., Howell, M. W., Littler, D. R., Mandyam, R. A., Sale, K. L., Mazzanti, M., Breit, S. N., Curmi, P. M. G., and Brown L. J. (2010) Metamorphic response of the CLIC1 chloride intracellular ion channel protein upon membrane interaction. *Biochem.* **49,** 5278-5289.

Goto, Y., Calciano, L.J., and Fink, A.L. (1990) Acid-induced folding of proteins. *Proc. Natl. Acad. Sci.* **87,** 573-577.

Gouaux, E. (1997) Channel-forming toxins: tales of transformation. *Curr. Opin. Struct. Biol.* **7,** 566-573.

Gowri Shankar, B.A., Sarani, R., Michael, D., Mridula, P., Ranjani, C.V., Sowmiya, G., Vasundhar, B., Sudha, P., Jeyakanthan, J., Velmurugan, D., and Sekar, K. (2007) Ion pairs in non-redundant protein structures. *J. Biosci*. **32,** 693–704.

Grantcharova, V., Alm., E. J., Baker, P., and Horwich, A. L. (2001) Mechanisms of protein folding. *Curr. Opin. Strict. Biol*. **11,** 70-82.

Gratkowski, H., Lear, J. D., and DeGrado, W. F. (2001) Polar side-chins drive the association of model transmembrane peptides. *Proc.Natl. Acad. Sci.* **98,** 880-885.

Greene, R. F. Jr., and Pace, C. N. (1973) Urea and guanidine hydrochloride denaturation of ribonuclease, lysozyme, a-chymotrypsin and b-lactoglobulin. *J.Biol. Chem.* **249,** 5388-5393

Guex, N., and Peitsch, M. C. (1997) **SWISS-MODEL** and the Swiss-PdbViewer: An environment for comparative protein modeling. *Electrophoresis* **18,** 2714-2723. http://expasy.org/spdbv/

Guha, S., and Bhattacharyya, B. (1995) A partially folded intermediate during tubulin unfolding: its detection and spectroscopic characterisation. *Biochem.* **34,** 6925-6931.

Gurezka, R., Laage, R., Brosig, B., and Langosch, D. A. (1999) Heptad motif of leucine residues found in membrane proteins can drive self-assembly of artificial transmembrane segments. *J. Biol. Chem*. **274,** 9265-9270.

Hall, A. G., Autzen, P., Cattan, A. R., Malcolm, A. J., Cole, M., Kernahan, J., and Reid, M. M. (1994) Expression of mu class glutathione S-transferase correlates with event-free survival in childhood acute lymphoblastic leukemia. *Cancer Res*. **54,** 5251-5254.

Haltia, T., and Freire, E. (1995) Forces and factors that contribute to the structural stability of membrane proteins. *Biochim. Biophys. Acta* **1241,** 295-322.

Halskau, O., Muga, A., and Martinez, A. (2009) Linking new paradigms in protein chemistry to reversible membrane-protein interactions. *Curr. Prot.Pept.Sci*. **10,** 339-359.

Hammes, G. H. (2005) *Spectroscopy for the biological sciences*. 1st Ed. 1-17, 35-89, John Wiley and Sons Inc., Canada.

Harrington, S. E., and Ben-Tal, N. (2009) Structural determinants of transmembrane helical proteins. *Structure* **17,** 1092-1103.

Harpaz, Y., Gerstein, M., and Chothia, C. (1994) Volume changes on protein folding. *Structure* **2,** 641–649.

Harper, E. T., and Rose, G.D. (1993) Helix stop signals in Proteins and Peptides: The Capping Box. *Biochem.* **32,** 7604-7609.

Harrop, S. J., De Maere, M. Z., Fairlie, W. D., Rezstsova, T., Valenzuela, S. M., Mazzanti, M., Tonini, R., Qiu, M. R., Jankova, L., Warton, K., Bauskin, A. R., Wu, W. M., Pankhurst, S., Hayes, J. D. and Wolf, C. R. (1988) *in Glutathione Conjugation: Mechanisms and Biological Significance* (Sies, H. and Ketterer, B. eds.), pp.316-356, Academic Press, London.

Harrop, S. J., De Maere, M. Z., Fairlie, W. D., Rezstsova, T., Valenzuela, S. M., Mazzanti, M., Tonini, R., Qiu, M. R., Jankova, L., Warton, K., Bauskin, A. R., Wu, W. M., Pankhurst, S., Campbell, T. J., Breit, S. N., and Curmi, P. M. G (2001) Crystal structure of a soluble form of the intracellular chloride ion channel CLIC1 (NCC27) AT 1.4˚ resolution. *J. Biol. Chem*. **276,** 44993-45000.

Hayes, J. D., Flanagan, J. U., and Jowsey, I. R. (2005) Glutathione transferases. *Annu. Rev. Pharmacol. Toxicol.* **45,** 51-88.

Haynie, D. T., and Freire, E. (1993) Structural energetics of the molten globule state. *Proteins* **16(2),** 115-140.

Heiss, N. S., and Poustka, A. (1997) Genomic structure of a novel chloride channel gene, CLIC2, in xq28. *Genomics* **45,** 224-228.

Honig, B. H., Hubbell, W. L., and Flewelling, R. F. (1986) Electrostatic interactions in membranes and proteins. *Annu. Rev. Biophys. Biophys. Chem*. **15,** 163-193.

Huyghues-Despointes, B. M. P., Scholtz, J. M. , and Baldwin, R. L. (1993) Helical peptides with three pairs of Asp-Arg and Clu-Arg residues in different orientations and spacings. *Protein Sci* **2,** 80-85.

Ionescu, R. M., Smith, V. F., O'Neill, J. C. Jr., and Matthews, C. R. (2000) Multistate equilibrium unfolding of *Escherichia coli* dihydrofolate reductase: thermodynamic and spectroscopic description of the native, intermediate and unfolded ensembles. *Biochem.* **39,** 9540-9550.

Isas, M. J., Cartailler, J. P., Sokolov, Y., Patel, D. R., Langen, R., Luecke, H., Hall, J. E., and Haigler, H. T. (2000) *Biochem.* **39,** 3015-3022.

Isas, M. J., Darshana, R. P., Jao, C., Jayasinghe, S., Cartailler, J. P., Haigler, H. T., and Langen, R. (2003) Global structural changes in Annexin 12. *J.Biol.Chem*. **278,** 30227-20234.

Ish-Horowicz, D., and Burke, J. F. (1981) Rapid and efficient cosmid cloning. *Nucleic Acids Res.* **9(13)**, 2989.

Jacobs, R. E., and White, S. H. (1989) The nature of the hydrophobic binding of small peptides at the bilayer interface: implications for the insertion of transbilayer helices. *Biochem.* **28,** 3421-3437.

Jakobsson, P. J., Morgenstern, R., Mancini, J., Ford-Hutchinson, A., and Persson, B. (1999) Common structural features of MAPEG- a widespread superfamily of membrane associated proteins with highly divergent functions in eicosanoid and glutathione metabolism. *Protein Sci.* **8,** 689-692.

Jean, Y. C., and Ache, H. J. (1978) Determination of critical micelle concentrations in micellar and reversed micellar systems by positron annihilation techniques. *J. Am. Chem. Soc.,* **100,** 984-985.

Jemth, P., Gianni, S., Day, R., Li, B., Johnson, C. M., Daggett, V., and Fersht, A. R. (2004) Demonstration of a low energy on pathway intermediate in a fast-folding protein by kinetics, protein engineering, and simulation. *Proc. Natl. Acad. Sci*. **101,** 6450-6455.

Jentsch, T. J. (1994) Trinity of cation channel. *Curr. Opin. Cell. Biol*. **6,** 600-601.

Jentsch, T. J., and Gunther, W. (1997) Chloride channels: an emerging molecular picture. *Bioessays* **19,** 117-126.

Jiang, J.X., and London, E. (1990) Involvement of denaturation-like changes in *Pseudomonas* exotoxin A hydrophobicity and membrane penetration determined by characterisation of pH and thermal transitions. Roles of two distinct conformationally altered states. *J. Biol. Chem.* **265,** 8636-8641.

Jiang, J. X., Chung, L. A., and London, E. (1991) Self-translocation of diphtheria toxin across model membranes. *J. Biol. Chem*. **266(35),** 24003-10.

Johnson, C. E., and Cornell, R. B. (1999) Amphitropic proteins: regulation by reversible membrane interactions (review). *Mol. Membr. Biol.* **16(3),** 217-235.

Johnson, R. M., Hecht, K., and Deber, C. M. (2007) Aromatic and cation-pi interactions enhance helix-helix association in a membrane environment. *Biochem.* **46,** 9208-9214.

Kakolyris, S., Giatromanolaki, A., Koukourakis, M., Powis, G., Souglakos, J., Sivridis, E., Georgoulias, V., Gatter, K. C., and Harris, A. L. (2001) Thioredoxin expression is associated with lymph node status and prognosis in early operable non-small cell lung cancer. *Clin Cancer Res*. **7(10),** 3087-91.

Karpen, M. E., Haseth, P. L., and Neet, K. E. (1992) Differences in the amino acid distributions of 3_{10}-helices and α-helices. *Protein Sci.* **1,** 1333-1342.

Kim, M. K., and Kang, Y. K. (1999). Positional preference of proline in alpha-helices. *Protein Sci*. **8,** 1492-1499.

Kim, P. S., and Baldwin, R. L. (1990) Intermediates in the folding reactions of small proteins. *Annu. Rev. Biochem*. **59,** 631-660.

Kleinschmidt, J. H., and Tamm, L. K. (1996) Folding intermediates of a beta-barrel membrane protein. Kinetic evidence for a multi-step membrane insertion mechanism. *Annu. Rev. Biochem*. **59,** 631-660.

Kohler, G., Hering, U., Zschoring, O., and Arnold, K. (1997) Annexin V interaction with phosphatidylserine-containing vesicles at low and neutral pH. *Biochem.* **36,** 8189-8194.

Kuwajima, K. (1996) The molten globule state of α-lactalbumin. *FASEB J*. **10,** 102-109.

Kyte, J., and Doolitlle, R.F. (1982) A simple method for displaying the hydropathic character of a protein. *J. Mol. Biol.* **157,** 105-132.

Lacroix, E., Viguera A. R., and Serrano, L. (1998). Elucidating the folding problem of a-helices: Local motifs, long-range electrostatics, ionic strength dependence and prediction of NMR parameters. *J. Mol. Biol.* **284,** 173-191.

Lacy, D. B., and Stevens, R. C. (1998) Unravelling the structures and modes of action of bacterial toxins. *Curr. Opin. Struct. Biol.* **6,** 778–784.

Laemmli, U. K., (1970) Cleavage of structural proteins during the assembly of the head of bacterioophage T4. *Nature* **227,** 680-685.

Lakowicz, J. R. (1999) *Principles of fluorescence spectroscopy*. Plenum Press, New York.

Lambert, O., Gerke, V., Bader, M. F., and Brisson, A. (1998) Structural analysis of junctions formed between lipid membranes and several annexins by cryo-electron microscopy. *J. Struct. Biol.* **272,** 42-55.

Lamoreaux, G. L., and Rusness, L. (1989) *in Glutathione-Chemical, Biochemical and Medical Aspects* (Dolphin, D., Poulser, R. and Avramovic, O., eds.), part B, pp. 153-196, John Wiley, New York.

Landry, D. W., Akabas, M. H., Redhead, C. R., Edelman, A., Cragoe, E. J. Jr, and al-Awqati, Q. (1989). Purification and reconstitution of chloride channels from kidney and trachea. *Science* **244,** 1469-1472.

Landry, D., Sullivan, S., Nicolaides, M., Redhead, C.R., Edelman, A., Field, M., al-Awqati, Q., and Edwards, J. (1993). Molecular cloning and characterisation of p64, a chloride channel from kidney microsomes. *J. Biol. Chem*. **268,** 14948-14955.

Langen, R., Isas, J.M., Lueke, H., Haigler, T.H., and Hubbell, W.L. (1998) Membrane-mediated assembly of annexins studied by site-directed spin labeling. *J. Biol. Chem*. **273,** 22453-22457.

Langen, R., Isas, J. M., Hubbell, W. L., and Haigler, T.H. (1998) A transmembrane form of annexin XII detected by site-directed spin labelling. *Proc.Natl.Acad.Sci.* **95,** 14060-14065.

Larkin, M. A., Blackshields, G., Brown, N. P., Chenna R., McGettigan P. A., McWilliam, H., Valentin F., Wallace, I. M., Wilm, A., Lopez, R., Thompson, J. D., Gibson, T. J., and Higgins, D. G. (2007) ClustalW and ClustalX version 2. *Bioinformatics* **23(21),** 2947-2948.

Lehtovaara, P. (1978) Anomalous migration of leghaemoglobin on sodium dodecyl sulfate/polyacrylamide-gel electrophoresis. *Biochem. J.* **169,** 251-253.

Lemmon, M. A., and Engelman, D. M. (1994) Specificity and promiscuity in membrane protein interactions. *Q. Rev. Biophys*. **27,** 157-218.

Li, J., Carrol, J., and Ellar, D.J. (1991) Crystal structure of insecticidal deltaendotoxin from *Bacillus thuringiensis* at 2.5 Å resolution. *Nature* **353,** 815-821.

Li, Y. F., Li, D. F., Zang, Z. H., and Wang, D. C. (2006) Trimeric structure of the wild soluble chloride intracellular ion channel CLIC4 observed in crystals. *Biochem. Biophys. Res. Commun.* **1565,** 333–346.

Lindeberg, M., Zakharov, S. D., and Cramer, W. A. (2000) Unfolding pathway of the colicin E1 channel protein on a membrane surface. *J. Mol. Biol.* **295,** 679-692.

Littler, D. R., Harrop, S. J., Fairlie, W. D., Brown, L. J., Pankhurst, G. J., Pankhurst, S., DeMaere, Z., Campbell, J. T., Bauskin, A. R., Tonini, R., Mazzanti, M., Breit, S. N., and Curmi, P. M. G. (2004) The intracellular chloride ion channel protein CLIC1 undergoes a redox-controlled structural transition. *J. Biol. Chem.* **279,** 9298-9305.

Litwack, G., Ketterer, B., and Arias, I. M. (1971) Ligandin: a Hepatic Protein which Binds Steroids, Bilirubin, Carcinogens and a Number of Exogenous Organic Anions. *Nature* **234,** 466-467.

Liu, S., Zhang, P., Ji, X., Johnson, W. W., Gilliland, G. L., and Armstrong, R. N. (1992) Contribution of tyrosine 6 to the catalytic mechanism of isoenzyme 3-3 of glutathione S-transferase. *J. Biol. Chem*. **267,** 4296-4299.

Lockhart, D. J., and Kim, P. S. (1992) Internal stark effect measurement of the electric field at the amino terminus of an alpha helix. *Science* **257,** 947-951.

Lockhart, D. J., and Kim, P. S. (1993) Electrostatic screening of charge and dipole interactions with the helix backbone. *Science* **260,** 198-202.

Loladze, V. V., Ermolenko, D. N., and Makhatadze, G. I. (2002) Thermodynamic consequences of burial of polar and non-polar amino acid residues in the protein interior. *J. Mol. Biol*. **320,** 343-357.

London, E. (1992) Diphtheria toxin: Membrane interaction and membrane translocation. *Biochim. Biophys. Acta* **1113,** 25–51.

Luo, J-K., Hornby, A. T. J., Wallace, A. W., Chien, J., Armstrong, N. R., and Dirr, W. H. (2002). Impact of domain interchange on conformational stability and equilibrium folding of chimeric class μ gluthione transferases. *Protein Sci.* **11,** 2208-2217.

Luque, I., Mayorga, O. L., and Freire, E. (1996) Structure-based thermodynamic scale of α-helix propensities in amino acids. *Biochem.* **35,** 13681-13688.

Lyu, P. C., Liff, M. I., Marky, L. A., and Kallenbach, N. R. (1990) Side chain contributions to the stability of alpha-helical structure in peptides. *Science*. **250,** 669-673.

Lyu, P. C., Zhou, H. X., Jelveh, N., Wemmer, D. E., and Kallenbach, N. R. (1992) Position-dependent stabilising effects in α-helices: N-terminal capping in synthetic model peptides. *J. Am. Chem. Soc*. **114,** 6560-6562.

Lyu, P. C., Wemmer, D. E., Zhou, H. X., Pinker, R. J., and Kallenbach, N. R. (1993) Capping interactions in isolated α-helices: Position-dependent substitution effects and structure of a serine-capped peptide helix. *Biochem.* **32**, 421-425.

Makhatadze, G. I., and Privalov, P. L. (1994) Hydration effects in protein unfolding. *Biophys Chem.* **51(2-3),** 291–309.

Manceva, S. D., Pusztai-Carey, M., and Butko, P. (2004) Effect of pH and ionic strength on the cytolytic toxin Cyt1A: a fluorescence spectroscopy study. *Biochim. Biophys. Acta* **1699,** 123-130.

Matthew, J. B. (1985) Electrostatic effects in proteins. *Ann. Rev. Biophys. Biophys. Chem*. **14,** 387-417.

Mazzanti, M. (2002) Recombinant CLIC1 (NCC27) assembles in lipid bilayers via a pH-dependent two-state process to form chloride ion channels with identical characteristics to those observed in Chinese hamster ovary cells expressing CLIC1. *J. Biol. Chem.* **277,** 26003–26011.

McIntyre, S. (2007) Effect of the environment on the conformational stability of the chloride intracellular channel protein CLIC1. PhD thesis, University of Witwatersrand.

McPherson, A. (1999) *Crystallization of Biological Macromolecules*. Cold Spring Harbor Laboratory Press.

Menestrina, G., Forti, S., and Gambale, F. (1989) Interaction of tetanus toxin with lipid vesicles. Effects of pH, surface charge, and transmembrane potential on the kinetics of channel formation. *Biophys J*. **55,** 393-405.

Merutka, G., Lipton, W., Shalongo, W., Park, S. H., and Stellwagen, E. (1990). Effect of central-residue replacements on the helical stability of a monomeric peptide. *Biochem*. **29,** 7511-7515.

Minn, A.J., Velez, P., Schendel, S. L., Liang, H., Muchmore, S. W., Fesik, S. W., Fill, M., and Thompson, C. B. (1997) Bcl-xL forms an ion channel in synthetic lipid membranes. *Nature* **385,** 353-357.

Mugo, A., Gonzales-Manas, J. M., Lakey, J. H., Pattus, F., and Surewicz, W.K. (1993) pH-dependent stability and membrane interaction of the pore-forming domain of Colicin A. *J. Biol. Chem.* **268,** 1553-1557.

Munoz, V., and Serrano, L. (1994a) Elucidating the folding problem of a- helical peptides using empirical parameters, II. Helix macrodipole effects and rational modification of the helical content of natural peptides. *J. Mol. Biol*. 245:275-296.

Munoz, V., and Serrano, L. (1994b) Elucidating the folding problem of α-helical peptides using empirical parameters III: Temperature and pH dependence. *J. Mol. Biol.* **245,** 297-308.

Munoz, V., and Serrano, L. (1997). Development of the Multiple Sequence Approximation within the Agadir Model of a Helix Formation. Comparison with Zimm-Bragg and Lifson-Roig Formalisms. *Biopolymers* **41,** 495-509.

www.embl-heidelberg.de/Services/serrano/agadir/agadir-**start.html**

Munoz, V., Blanco, F. J., and Serrano, L. (1995) The hydrophobic-staple motif and a role for loop-residues in alpha-helix stability and protein folding. *Nat. Struct. Biol*. **2,** 380-385.

Myers, J.K., Pace, C.N., and Scholtz, J.M. (1995) Denaturant *m*-values and heat capacity changes: relation to changes in accessible surface areas of protein unfolding. *Protein Sci.* **4,** 2138-2148.

Nathaniel, C. (2007) Structural dynamics and membrane interaction of the chloride intracellular channel protein, CLIC1. PhD thesis, University of Witwatersrand.

Nishizawa, T., Nagao, T., Iwatsubo, T., Forte, J. G., and Urushidani, T. (2000) Molecular cloning and characterisation of a novel chloride intracellular channel-related protein, parchorin, expressed in water-secreting cells. *J. Biol. Chem*. **275,** 11164-11173.

Novarino, G., Fabrizi, C., Tonini, R., Denti, M. A., Malchiodi-Albedi, F., Lauro, G. M., Sacchetti, B., Paradisi, S., Ferroni, A., Curmi, P.M., Breit, S.N. and Mazzanti, M. (2004) Involvement of the intracellular ion channel CLIC1 in microglia-mediated b-amyloid-induced neurotoxicity. *The Journal of Neuroscience* **24,** 5322-5330.

Oakley, A. J. (2005) Glutathione transferases: new functions. *Curr. Opin. Struc.Biol*. **15,** 716-723.

O`Neil, K. T. and DeGrado, W. F. (1990) A thermodynamic scale for the helix-forming tendencies of the commonly occurring amino acids. *Science* **250,** 646-651.

Ogasahara, K., Matsushita, E., and Yutani, K. (1993) Further examination of the intermediate state in the denaturation of the tryptophan synthase α subunit: evidence that the equilibrium denaturation intermediate is a molten globule. *J. Biol. Chem.* **234,** 1197-1206.

Oh, K. J., Zhan, H., Cui, C., Hideg, K., Collier, R. J., and Hubbell, W. L. (1996) Organization of diphtheria toxin T domain in bilayers: a site-directed spin labeling study. *Science* **273(5276),** 810-812

Pace, C. N. (1986a) Determination and analysis of urea and guanidine hydrochloride denaturation curves. *Methods in Enzymology*. **131,** 266-280.

Pace, C. N. (1986b) in *Enzyme structure*, Part L (Hirs, C. H. W., Timasheff, S. N.., Eds.) pp 266-280, Academic Press, Inc.

Pace, C. N., Shirley, B. A., McNutt, M., Gajiwala, K. (1996) Forces contributing to the conformational stability of proteins. *FASEB J.* **10,** 75-83.

Pace, C.N., and Scholtz, J.M. (1997) *in Protein Structure: a practical approach* (Creighton, T.E. ed.) 2nd edition, pp 299-321, IRL Press, Oxford University Press, Oxford.

Padmanabhan, S., Marqusee, S., Ridgeway, T., Laue, T.M., and Baldwin, R. L. (1990) Relative helix-forming tendencies of nonpolar amino acids. *Nature*. **344,** 268-270.

Padmanabhan, S., and Baldwin, R. L. (1994a) Helix-stabilising interaction between Tyr and Leu or Val when the spacing is i, i+4. *J. Mol. Biol*. **241,** 706-713.

Padmanabhan, S., and Baldwin, R. L. (1994b) Test for helix-stabilising interactions between various side-chains in alanine-based peptides. *Protein Sci*. **3,** 1992-1997.

Pal, L., Chakrabarty, P., and Basu, G. (2003) Sequence and structure patterns in proteins from an analysis of the shortest helices: implications for helix nucleation. *J. Mol. Biol*. **326(1),** 273-91.

Parker, M.W., and Pattus, F. (1993) Rendering a membrane protein soluble in water: A common packing motif in bacterial protein toxins. *Trends Biochem. Sci.* **18,** 391–395.

Parker, M.W., Buckley, J.T., Postma, J.P., Tucker, A.D., Leonard, K., Pattus, F., and Tsernoglou, D. (1994) Structure of the *Aeromonas* toxin proaerolysin and the membrane-channel states. *Nature* **367,** 292**–**295.

Parker, M.W. and Feil, S.C. (2005) Pore-forming protein toxins: from structure to function. *Prog. Biophys. Mol. Biol.* 88:91–142.

Parker, M.W., Pattus, F., Tucker, A.D., and Tsernoglou, D. (1989) Structure of the membrane-pore-forming fragment of colicin A. *Nature* **337,** 93-96.

Pauling, L., Corey, R. B., and Branson, H. R. (1951) The structure of proteins: two hydrogen-bonded helical configurations of the polypeptide chain. *Proc. Natl. Acad. Sci.* **37,** 205-211.

Peitzsch, R. M., Eisenberg, M., Sharp, K. A., and McLaughlin, S. (1995) Calculations of the electrical potential adjacent to model phospholipids bilayers. *Biophys. J*. **68,** 729-738.

Perkins, S. J. (1986) Protein volumes and hydration effects. The calculations of partial specific volumes, neutron scattering matchpoints and 280-nm absorption coefficients for proteins and glycoproteins from amino acid sequences. *Eur. J. Biochem.* **157,** 169–180.

Petosa, C., Collier, R. J., Klimpel, K. R., Leppla, S. H., and Liddington, R.C. (1997) Crystal structure of the anthrax toxin protective antigen. *Nature* **385,** 833**–**838.

Pitt-Rivers, R., and Impiombato, F.S.A. (1968) The binding of sodium dodecyl sulfate to various proteins. *Biochem. J.* **109,** 825-830.

Popot, J. L., Gerchman, S. E., and Engelman, D. M. (1987) Refolding of bacteriorhodopsin in lipid bilayers. *J. Mol. Biol*. **198,** 655-676.

Powis, G., and Montfort, W. R. (2001) Properties and biological activities of thioredoxins. *Annu. Rev. Biophys. Biomol. Struct*. **30,** 421-55.

Prats, M., Teissie, J., and Tocanne, J. F. (1986) Lateral proton conduction at lipid-water interfaces and its implication for the chemiosmotic coupling hypothesis. *Nature* **322,** 756–758.

Presta, L. G., and Rose, G. D. (1988) Helix signals in proteins. *Science* **240,** 1632-1641.

Promdonkoy, B., and Ellar, D.J. (2003) Investigation of the pore-forming mechanism of a cytolytic d-endotoxin from *Bacillus thuringiensis. Biochem. J.* **374,** 255-259.

Qian, Z., Okuhara, D., Abe, M. K., and Rosner, M. R. (1999) Molecular cloning and characterisation of a mitogen-activated protein kinase-associated intracellular chloride channel. *J. Biol. Chem*. **274,** 1621-1627.

Ronnov-Jessen, L., Villadsen, R., Edwards, J. C., and Petersen, O.W. (2002) Differential expression of a chloride intracellular channel gene, CLIC4, in transforming growth factor-beta1-mediated conversion of fibroblasts to myofibroblasts. *Am. J. Pathol.* **161,** 471–480.

Ragone, R. (2001) Hydrogen-bonding classes in proteins and their contribution to the unfolding reaction. *Protein Sci*. **10,** 2075-2082.

Ratnaparkhi, G. S., and Varadarajan, R. (2000) Thermodynamic and structural studies of cavity formation in proteins suggest that loss of packing interactions rather than the hydrophobic effect dominates the observed energetics. *Biochem.* **39,** 12365-12374.

Reed, R., Holmes, D., Weyers, J., and Jones, A. (2003) Practical skills in biomolecular sciences (2nd Ed.), pp 131. Pearson Education Ltd., UK.

Reviakine, I., Bergsma-Schutter, W., and Brisson, A. (1998) Growth of Protein 2-D Crystals on Supported Planar Lipid Bilayers Imaged in Situ by AFM. *J. Struct. Biol.* **121,** 356-361.

Reynolds, J.A., and Tanford, C. (1970) Binding of dodecyl sulfate to proteins at high binding ratios. Possible implications for the state of proteins in biological membranes. *Proc. Natl. Acad. Sci.* **66,** 1002-1007.

Richardson, J. S. (1981) The anatomy and taxonomy of protein structure. *Adv. Prot. Chem.* **34,** 168-339.

Richardson, J. S., and Richardson, D. C. (1988) Amino acid preferences for specific locations at the ends of a helices. *Science* **240,** 1648–1652.

Rocha, J. C., Cheng, C., Liu, W., Kishi, S., Das, S., Cook, E. H., Sandlund, J. T., Rubnitz, J., Ribeiro, R., and Campana, D. (2005) Pharmacogenetics of outcome in children with acute lymphoblastic leukemia. *Blood* **105,** 4752-4758.

Roder, H., Elöve, G. A., and Shastry, M. C. R. (2000) *in Mechanism of Protein Folding*. (2nd ed.) (Pain, R. H., ed) pp:65-104, Oxford University Press, Great Britain.

Rønnov-Jessen, L., Villadsen, R., Edwards, J. C., and Petersen, O. W. (2002) Differential expression of a chloride intracellular channel gene, CLIC4, in transforming growth factor-beta1-mediated conversion of fibroblasts to myofibroblasts. *Am. J. Pathol*. **161(2),** 471-480.

Rossjohn, J., Polekhina, G., Feil, S. C., Allocati, N., Masulli, M., Di Ilio, C., and Parker, M.W. (1998) A mixed disulphide bond in bacterial glutathione transferase: functional and evolutionary implications. *Structure* **6:**721-734.

Royer, C. A. (1995) in *Methods in Molecular Biology*, Vol:40 *Protein Stability and Folding*: *Theory and Practice* (Shirley, B. A., ed) pp 65-89, Humana Press Inc., Totowa, NJ.

Royer, C. A., Mann, C. J., and Matthews, R. (1993) Resolution of the fluorescence equilibrium unfolding profile of trp aporepressor using single tryptophan mutants. *Protein Sci.* **2,** 1844-1852.

Russ, W. P., and Engelman, D. M. (2000) The GxxxG motif: a framework for transmembrane helix-helix association. *J. Mol. Biol*. **296,** 911-919.

Saito, M., Korsmeyer, S.J., and Schlesinger, P.H. (2000) BAX-dependent transport of cytochrome *c* reconstituted in pure liposomes. *Nat. Cell Biol*. **2,** 553-555.

Sali, D., Bycroft, M., and Fersht, A. R. (1991) Surface electrostatic interactions contribute little to stability of Barnase. *J. Mol. Biol*. **220,** 779-788.

Sal-Man, N., Gerber, D., Bloch, I., and Shai, Y. (2007) Specificity in transmembrane helix-helix interaction mediated by aromatic residues. *J. Biol. Chem*. **282,** 19753-19761.

Sambrook, J., Fritsch, E.F., and Maniatis, T. (1989) Molecular cloning: A laboratory manual (2^{nd} ed.), pp 1.25-1.28. Cold Spring Harbor Laboratory Press, Cold Spring Harbor, New York.

Schellman, C. (1980) *The α_L conformation at the ends of helices*. In Protein Folding (ed. R. Jaenicke), pp. 53–61. North-Holland Biomedical Press, Elsevier, Amsterdam.

Schendel, S.L., Montal, M., and Reed, J.C. (1997) Bcl-2 family proteins as ion channels. *Cell Death Differ*. **5,** 372–380.

Schlesinger, P. H., Blair, H. C., Teitelbaum, S. L., and Edwards, J.C. (1997) Characterisation of the osteoclast ruffled border chloride channel and its role in bone resorption. *J. Biol. Chem.* **272,** 18636-18643.

Schneider, D., and Engelman, D. M. (2004) Motifs of two small residues can assist but are not sufficient to mediate transmembrane helix interactions. *J. Mol. Biol.* **343,** 799-804.

Scholtz, J. M., Marqusee, S., Baldwin, R. L., York, E. J., Stewart, J. M., Santoro, M., and Bolen, D. W. (1991). Calorimetric determination of the enthalpy change for the alpha-helix to coil transition of an alanine peptide in water. *Proc. Natl. Acad. Sci.* **88,** 2854–2858.

Scholtz, J. M., Quian, H., Robbins, V. H., and Baldwin, R. L. (1993) The energetics of ion-pair and hydrogen-bonding interactions in a helical peptide. *Biochem.***32,** 9668-9676.

Seale, J. W., Srinivasan, R. and Rose, G. D. (1994) Sequence determinants of the capping box, a stabilising motif at the N-termini of α-helices. *Protein Sci*. **3,** 1741-1745.

Serrano, L., and Fersht, A. R. (1989) Capping and α-helix stability. *Nature* **342,** 296-299.

Serrano, L., Neira, J. L., Sancho, J., and Fersht, A. R. (1992a): Effect of alanine versus glycine in α-helices on protein stability. *Nature* **356,** 453-455.

Serrano, L., Sancho, J., Hirshberg, J. M., and Fersht, A. R. (1992b) α-helix stability in proteins. I. Empirical correlations concerning substitution of side chains at the N- and C-caps and the replacement of alanine by glicine or serine at solvent-exposed surfaces. *J. Mol. Biol.* **227,** 544-549.

Senes, A., Gerstein, M., and Engelman, D. M. (2000) Statistical analysis of amino acid patterns in transmembrane helices: the GxxxG motif occurs frequently and in association with beta-branched residues at neighboring positions. *J. Mol. Biol*. **296,** 921-936.

Senes, A., Belandia, I. U., and Engelman, D. M. (2001) The Cα—H···O hydrogen bond: A determinant of stability and specificity in transmembrane helix interactions. *PNAS* **98,** 9056-9061.

Shanks, R. A., Larocca, M. C., Berryman, M., Edwards, J. C., Urushidani, T., Navarre, J., and Goldenring, J. R. (2002) *J. Biol. Chem*. **277,** 40973–40980.

Sheehan, D., Meade, G., Foley, V. M., and Dowd, C. A. (2001). Structure, function and evolution of glutathione transferases: implications for classification of non-mammalian members of an ancient enzyme superfamily. *Biochem. J*. **360,** 1–16.

Shimizu, S., Narita, M., and Tsujimoto, Y. (1999) Bcl-2 family proteins regulate the release of apoptogenic cytochrome c by the mitochondrial channel VDAC. *Nature* **399(6735),** 483-7.

Shin, Y. K., Levinthal, C., Levinthal, F., and Hubbell WL. (1993) Colicin E1 binding to membranes: time-resolved studies of spin-labeled mutants. *Science* **259(5097),** 960-963.

Shirley, B. A. (1995)) in *Methods in Molecular Biology*, Vol:40 *Protein Stability and Folding*: *Theory and Practice* (Shirley, B. A., ed) pp 177-190, Humana Press Inc., Totowa, NJ.

Shoemaker, K. R., Kim, P. S., Brems, D. N., Marqusee, S., York, E. J., and Chaiken, I. M. (1985) Nature of the charged-group effect on the stability of the C-peptide helix. *Proc. Natl. Acad. Sci*. **82,** 2349-2353.

Shoemaker, K. R., Kim, P. S., York, E. J., Steward, J. M., and Baldwin, R. L. (1987) Tests of the helix dipole model for stabilization of a-helices. *Nature* **326,** 563-567.

Shorning, B. Y., Wilson, D .B., Meehan, R.R., and Ashley, R. H. (2003) Molecular cloning and developmental expression of two Chloride Intracellular Channel (CLIC) genes in Xenopus laevis. *Dev. Genes Evol.* **213,** 514-514.

Singh, H., and Ashley, R. H. (2006) Redox regulation of CLIC1 by cysteine residue associated with the putative channel pore. *Biophys. J.* **90,** 1628-1638.

Smith, D. B., and Johnson, K. S. (1988) Single-step purification of polypeptides expressed in *Escherichia coli* as fusions with glutathione S-transferase. *Gene* **67,** 31-40.

Sokolov, Y., Mailliard, W. S., Tranngo, N., Isas, M., Luecke, H., Haigler, H. T., and Hall, J. E.(2000) Annexins V and Xii Alter the Properties of Planar Lipid Bilayers Seen by Conductance Probes. *J. Gen. Physiol.* **115,** 571-582.

Song, L., Hobaugh, M. R., Shustak, C., Cheley, S., Bayley, H., and Gouaux, J. E. (1996) Structure of staphylococcal α-hemolysin, a heptameric transmembrane pore. *Science* **274,** 1859–1866.

Soulages, J. L. (1998) Chemical denaturation: Potential impact of undetected intermediates in the free energy of unfolding and *m*-values obtained from a two-state assumption. *Biophys. J.* **75,** 484-492.

Stellwagen, E., Park, S., Shalongo, W., and Jain, A. (1992) The contribution of residue ion pairs to the helical stability of a model peptide. *Biopolymers* **32,** 1193-l 200.

Stoychev, S. H., Nathaniel, C., Fanucchi, S., Brock, M., Li, S., Asmus, K., Virgil, L. W. Jr., and Dirr, H. W. (2009) Structural Dynamics of Soluble Chloride Intracellular Channel Protein CLIC1 Examined by Amide Hydrogen-Deuterium Exchange Mass Spectrometry. *Biochem.* **48,** 8413-8421.

Stoychev, S. (2008) The role of the domain interface in the stability, folding and function of CLIC1. PhD thesis, University of Witwatersrand.

Strange, K., Emma, F., and Jackson, P. S. (1996) Cellular and molecular physiology of volume-sensitive anion channels. *Am. J. Physiol*. **270,** C711-C730.

Stryer, L. (1968) Fluorescence Spectroscopy of Proteins. *Science* **162,** 526-533.

Suh, K. S., Mutoh, M., Nagashima, K., Fernandez-Salas, E., Edwards, L. E., Hayes, D. D., Crutchley, J. M., Marin, K. G., Dumont, R.A., Levy, J. M., Cheng, C., Garfield, S., and Yuspa, S.H. (2004) The organellular chloride channel protein CLIC4/mtCLIC translocates to the nucleus in response to cellular stress and accelerates apoptosis. J. *Biol. Chem*. **279,** 4632–4641.

Suh, K. S., Mutoh, M., Gerdes, M., and Yuspa, S. H. (2005) CLIC4, an intracellular chloride channel protein, is a novel molecular target for cancer therapy. *J. Investig. Dermatol. Symp. Proc*. **10,** 105–109.

Swietnicki, W., Peterson, R., Gambetti, P., and Surewicz, W. K. (1997) pHdependent stability and conformation of the recombinant human prion protein PrP (90-231). *J. Biol. Chem.* **272,** 27517-27520.

Takanashi, M., Morimoto, A., Yagi, T., Kuriyama, K., Kano, G., Imamura, T., Hibi, S., Todo, S., and Imashuku, S. (2003) Impact of glutathione S-transferase gene deletion on early relapse in childhood B-precursor acute lymphoblastic leukemia. *Haematologica* **88,** 1238-1244.

Takano, K., Tsuchimori, K., Yamagata, Y., and Yutani, K. (2000) Contribution of salt bridges near the surface of a protein to the conformational stability. *Biochem.* **39,** 12375-12381.

Tanford, C. (1980) *The hydrophobic effect: Formation of micelles and biological membranes*. 2nd. Ed. John Wiley& Sons Inc., New York pages:186-187.

Tejuca, M., Dalla Serra, M., Ferreras, M., Lanio, M. E., and Menestrina, G. (1996) Mechanism of membrane permeabilisation of sticholysin I, a cytolysin isolated from the venom of the sea anemone *Stichodactyla helianthus. J. Membr. Biol.* **183,** 125-135.

Thompson, L. C., Walters, J., Burke, J., Parsons, J. F., Armstrong, R. N., and Dirr, H. W. (2006) Double mutation at the subunit interface of glutathione transferase rGSTM1-1 results in a stable, folded monomer. *Biochem.* **45,** 2267-2273.

Thuduppathy, G.R., and Hill, R.B. (2005) Acid destabilisation of the solution conformation of Bcl-XL does not drive its pH-dependent insertion into membranes. *Protein Sci.* **15,** 1-10.

Thuduppathy, G. R., Craig, J. W., Kholodenko, V., Schon, A., and Hill, B. (2006) Evidence that membrane insertion of the cytosolic domain of Bcl-XL is governed by an electrostatic mechanism. *J. Mol. Biol.* **359,** 1045-1058

Tilley, S. J., and Saibil, H. R. (2006) The mechanism of pore formation by bacterial toxins. *Curr. Opin. Struct. Biol*. **16,** 230-236.

Tonini, R., Ferroni, A., Valenzuela, S. M., Warton, K., Campbell, T. J., Breit, S. N., and Mazzanti, M. (2000) Functional characterisation of the NCC27 nuclear protein in stable transfected CHO-K1 cells. *FASEB J.* **14,** 1171-1178.

Torry, M. C., and Merrill, A. R. (1999) Adventures in membrane protein topology. A study of the membrane bound state of colicin E1. *J. Biol. Chem.* **274,** 24539-24549.

Tulk, B.M., and Edwards, J.C. (1998) NCC27, a homologue of intracellular chloride channel p64, is expressed in brush border of renal proximal tubule. *Am. J. Physiol*. **274,** F1140-F1149.

Tung, J.J., Hobert, O., Berryman, M., and Kitajewski, J. (2009) Chloride intracellular channel 4 is involved in endothelial proliferation and morphogenesis in vitro. *Angiogenesis*. **12,** 209–220.

Tweten, R. K., Parker, M. W. and Johnson, A. E. (2001) The cholesterol-dependent cytolysins. In: Pore-Forming Toxins (Ed. van der Goot, F.G.), pp. 1–14. Springer, Heidelberg, Germany.

Ulrih, N.P., Anderluh, G., Macek, P., and Chalikian, T.V. (2004) Salt-induced oligomerisation of partially folded intermediates of equinatoxin II. *Biochem*. **43,** 9536-9545

Valenzuela, S. M., Martin, D. K., Por, S. B., Robbin, J. M., Warton, K., Bootcov, M. R., Schofield, P. R., Campbell, T. J., and Breit, S. N. (1996). Molecular cloning and expression of a chloride ion channel of cell nuclei. *J. Biol. Chem*. **272,** 12575-12582.

Valenzuela, S. M., Mazzanti, M., Tonini, R., Qui, M. R., Warton, K., Musgrove, E. A., Campbell, T. J., and Breit, S. N. (2000) The nuclear chloride ion channel NCC27 is involved in regulation of the cell cycle. *J. Physiol*. **529,** 541-552.

Van der Goot, F. G., Gonza´lez-Mana˜s, J. M., Lakey, J. H., and Pattus, F. (1991) A 'molten-globule′ membrane-insertion intermediate of the pore-forming domain of colicin A. *Nature* **354,** 408–410.

Vander Heiden, M. G., Li, X. X., Gottleib, E., Hill, R. B., Thompson, C. B., and Colombini, M. (2001) Bcl-xL promotes the open configuration of the voltage-dependent anion channel and metabolite passage through the outer mitochondrial membrane.*J Biol Chem*. **276(22),** 19414-19419.

Viguera, A. R., and Serrano, L. (1995) Side-chain interactions between sulphur containing amino acids and phenylalanine, in α-helices. *Biochem.* **34,** 8771-8779.

Wallace, A. L., Burke, J., and Dirr, W. H. (2000) Domain-domain interface packing at conserved Trp-20 in class α glutathione transferase impacts on protein stability. *Biochim. Biophys. Acta* **1478,** 325-332.

Warton, K., Tonini, R., Fairlie, W. D., Mathews, J. M., Valenzuela, S. M., Qiu, M. R., Wu, W. M., Pankhurst, S., Bauskin, A. R., Harrop, S. J., Campbell, T. J., Curmi, P. M. G., Breit, S. N., and Mazzanti, M. (2002) Recombinant CLIC1 (NCC27) assembles in lipid bilayers via a pH-dependent two-state process to form chloride ion channels with identical

characteristics to those observed in Chinese hamster ovary cells expressing CLIC1. *J. Biol. Chem.* **277,** 26003-26011.

Wei, C., Yang, J., Zhu, J., Zhang, X., Leng, W., Wang, J., Xue, Y., Sun, L., Li, W., Wang, J. and Jin, Q. (2006) Comprehensive proteomic analysis of Shigella flexneri 2a membrane proteins. *J Proteome Res*. **5(8),** 1860-5.

White, S. H., and Wimley, W. C. (1994) Peptides in lipid bilayers: Structural and thermodynamic basis for partitioning and folding. *Curr. Opin. Struct. Biol*. **24,** 113-117.

White, S. H., and Wimley, W. C. (1999) Membrane protein folding and stability: physical principles. *Annu. Rev. Biophys. Biomol. Struct*. **28,** 319-365.

Whitten, S. T., Wooll, J. O., Razeghifard, R., Garcia-Moreno, E., and Hilser, V.J. (2001) The origin of pH-dependent changes in *m*-values for the denaturantinduced unfolding of proteins. *J. Mol. Biol.* **309,** 1165-1175.

Wilce, M. C. J., and Parker, M. W. (1994). Structure and function of glutathione Stransferases. *Biochim. Biophys. Acta.* **1205,** 1-18.

Wilson, K., and Walker, J. (2005) *Principles and techniques of biochemistry and molecular biology* (6^{th} ed.). Pp 451, 524, 526, 535, 571, 579, 581-582. Cambridge University Press, Cambridge.

Wilson, K., and Walker, J. (2000) *Principles and techniques of practical biochemistry*. (5^{th} Ed.) 459-465, 588-607, 656-661, 665-672, Cambridge university press, UK.

Woody, R. M. (1995) Circular dichroism. *Meth. Enzymol*. **246,** 34-71.

Woody, R.W., and Dunker, K. 1996. Aromatic and cystine sidechain circular dichroism in proteins. In *Circular dichroism and the conformational analysis of macromolecules* (ed G.D. Fasman), pp. 109–157. Plenum Press, New York, NY

Wu, L. C., and Kim, P. S. (1998) A specific hydrophobic core in the α-lactalbumin molten globule. *J. Mol. Biol*. **280,** 175-182.

Xia, B., Vlamis-Gardikas, A., Holmgren, A., Write, P. E., and Dyson, J. (2001) Solution structure of *Escherichia coli* glutaredoxin2 shows similarity to mammalian glutathione S-transferases. *J. Mol. Biol.* **310**, 907-918

Zakharov, S. D., and Cramer, W. A. (2002) Colicin crystal structures: Pathways and mechanisms for colicin insertion into membranes. *Biochim. Biophys. Acta* **1565,** 333–346.

Zakharov, S.D., Katova, E. A., Antonenko, Y. N., and Cromer, W. A. (2004) On the role of lipid in colicin pore formation. Biochim. Biophys. Acta **1666,** 239-249.

Zhou, H. X., Kay, C. M., and Hodges, R. S. (1994) The role of interhelical ionic interactions in controlling protein folding and stability. *J. Mol. Biol*. **237,** 500-512.

Zimm, B. H., and Bragg, J. K. (1959) Theory of the phase transition between helix and random coil in polypeptide chains. *J. Chem. Phys*. **31,** 526-535.

Zitzewitz, J. A., Bilsel, O., Luo, J., Jones, B. E., and Matthews, C. R. (1995) Probing the folding mechanism of a leucine zipper peptide by stopped flow circular dichroism spectroscopy. *Biochem.* **34(39),** 12812-12819.

Zhou, H. X., Kay, C. M., and Hodges, R. S. (1994) The role of interhelical ionic interactions in controlling protein folding and stability. *J. Mol. Biol*. **237,** 500-512.

Zhukovsky, E. A., Mulkerrin, M. G., and Presta, L. G. (1994) Contribution to global protein stabilization of the N-capping box in human growth hormone. *Biochem.* **33,** 9856–9864.